Flight mechanics
&
Aerodynamic design

Last updated: May 26, 2026

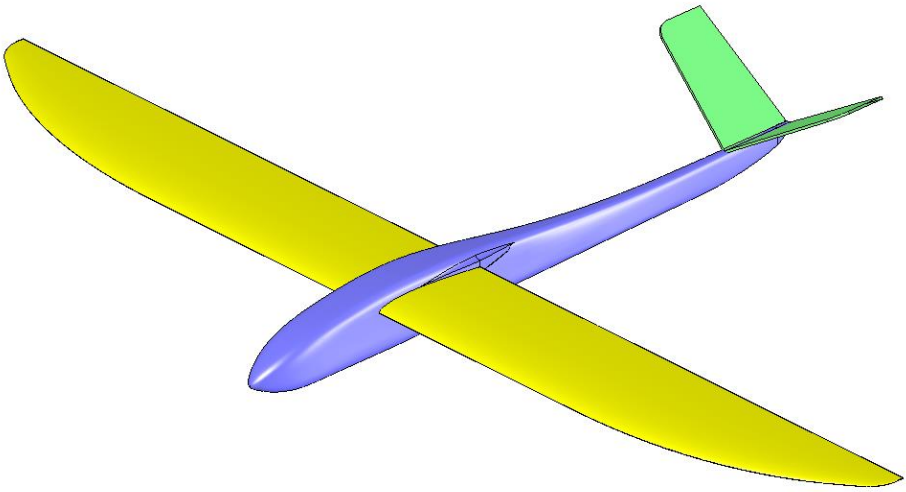

Franck Aguerre

My sincere gratitude to:

- *My wife Pascale, both chief proofreader and moral support, who brilliantly fulfilled these two difficult roles.*
- *Laurent Michelet (RCM and RC Pilot magazines), the French Federation of Aeromodelling and the publisher Isofac, who believed in this project.*
- *All of them, in particular Serge Barth, Paul Bizard, Jean-Luc Bolteau, Jean Champenois, Raphaël Gougnot, Emmanuel de Margerie, Thierry Platon, Marco Ricci, Guillaume Rouby, Matthieu Scherrer, Martin Simons, and many others, who contributed, directly through the time spent in our discussions or indirectly through their technical publications, to this work.*
- *All the people around me and the readers of previous editions who, through their questions or suggestions, allowed me to approach new points of view, which ultimately benefited this work.*

This book is primarily intended for understanding flight and designing flying model aircraft. That being said, the formulas and concepts used are mostly derived from full-size aviation, with some restrictions specific to the model-making field; therefore, it is perfectly feasible to use it for designing a light aircraft. In all cases, the designer is solely responsible for their design and technical choices. The use of this manual and its contents cannot, under any circumstances, engage the author's liability.

Table of Contents

Flight mechanics & aerodynamic design

Who hasn't dreamed of designing their own model airplane? Every modeler has probably thought about it at some point, but few dare to try due to a lack of sufficient knowledge in aerodynamics; or, more frequently, some have done so by reproducing tried-and-tested designs, without the necessary understanding to decipher them. Certainly, there's no shortage of treatises on flight mechanics… but they most often focus solely on mathematical formulas, hopelessly opaque to the average person, at the expense of explanations. Conversely, some so-called popular science publications don't go beyond the stage of overly empirical recipes and, worse, spread and perpetuate misconceptions. Between these two extremes, there's not much to choose from.

However, aerodynamics is not as complex as it seems; all the physical phenomena involved can be explained very pragmatically and often simply by using common sense. Similarly, even though the underlying theoretical formulations are sometimes very complex (Navier-Stokes equations, thin airfoil theory, lifting-line theory, etc.), many of these phenomena can be accurately described by simple results.

The entire aim of this book is precisely to make the fundamentals of flight mechanics accessible, so that you can then carry out your designs simply and coherently, with the assurance of success. Or, failing that, to simply be able to tune or improve an existing model with full knowledge of the facts.

It will not be possible, however, to dispense with the formula sheet, sometimes accompanied by demonstrations intended to help those who wish to better "juggle" the different concepts. Rest assured, mastering these concepts is by no means essential for a proper understanding of this work. Indeed, several levels of reading are offered, including, alongside the formula sheet, written explanations, illustrated examples, and a method of graphical analysis. The only essential tools will therefore be a sheet of paper, a ruler, and a pencil, than a simple calculator. Not forgetting a little patience is needed to take the time to properly assimilate, step by step, all the concepts discussed here.

1. Preface

Before delving into the heart of the matter, a brief reminder might be helpful. Like all applied sciences, aerodynamics and flight mechanics do not claim to deliver exact results. Airflow around an aircraft can be so complex that it would be illusory to try to understand it in its entirety, even with infinite computing power and even if, taken individually, each phenomenon involved is generally very well described and theorized. Their study therefore relies on modeling built on simplifying assumptions, but above all, without losing sight of the essentials in order to guarantee a correct representation of reality—the very foundation of any scientific and technical endeavor.

At our level, far removed from the immense technical and scientific resources available to full-scale aeronautics, simplifications are therefore inevitable, and this imperative of representativeness takes on even more crucial importance. Fortunately for us, supercomputers have not always existed, and theorists of the pre-digital era had to manage without them, achieving quite extraordinary results despite very limited resources. Theories such as those of thin airfoils and the lifting line, dating from the golden age of the early 20th century (Prandtl, Munk, Von Karman, Joukovski, etc.), proceed from this principle by decomposing the aircraft into simple and easily characterized elements: airfoil, chord, surface area, aspect ratio, lever arm, etc. With a few precautions related to their domain of validity, they allow us to obtain perfectly satisfactory results with relatively affordable calculations, and they will therefore be used extensively here.

Since the formulas and associated demonstrations are widely available, both in print and online, this book does not aim to list them exhaustively, even though it is already relatively comprehensive. The approach is rather to focus primarily on providing the most accessible and clear explanations possible, and then to develop a simple, effective, and above all, coherent methodology. The important thing is not to master all the equations of flight—there are very powerful tools for that—but rather to acquire a global understanding of the main mechanisms of flight and to develop a critical perspective on the data and results used. Similarly, while it will not be possible to study every slightly exotic aerodynamic configuration in minute detail, the keys provided here will allow you to understand them with sufficient perspective. To this end, we will approach things on three levels: first, a general overview of the mechanics of flight, then a detailed examination of each element, and finally, specific details on certain points. The formulas follow the same logic.

Another distinction is also necessary: designing a model and drawing up its plans are two very different processes. The first defines an overall architecture, the second makes it manufacturable. This book will therefore tell you nothing about the detailed drawing and manufacturing of an aircraft. But, in my opinion, that's not the most important point; an experienced builder can easily manage with a rough sketch to successfully complete a model, whereas a sloppy aerodynamic design can eliminate any chance of a satisfactory result from the outset.

Last but not least: in aerodynamics, the real challenge lies not in the pursuit of pure performance, but in achieving optimal flight characteristics. Sound and linear behavior, tight and precise trajectories, well-decoupled control axes, and so on, are far more important than achieving a few percent reduction in drag. To paraphrase a well-known saying, without flight characteristics, performance is nothing.

As this photo reveals (Copyright Thermal Soaring, Burkhard Martens, Edoceo Editions), many aerodynamic phenomena are easily observable in everyday life. Simply open your eyes, for example, by observing what is happening on the surface of a stream or even a simple bathtub. Here, we can observe the Coanda effect, the boundary layer, and the laminar/turbulent transition.

2. Hey, how does it fly?

2.1 A little vocabulary

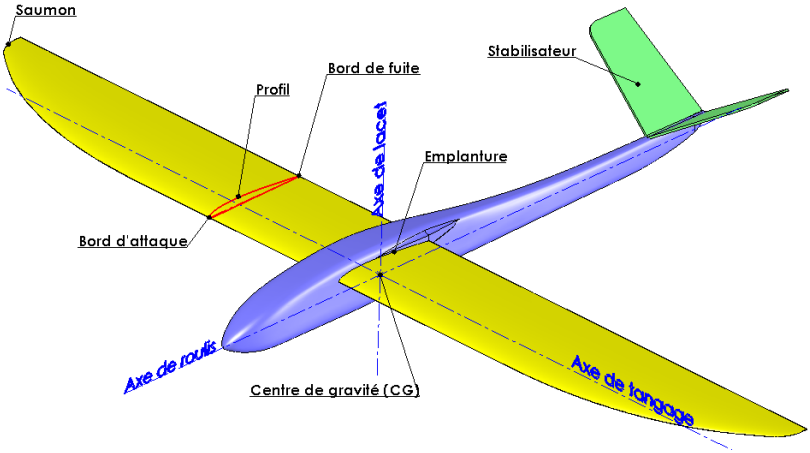

Fig. 01

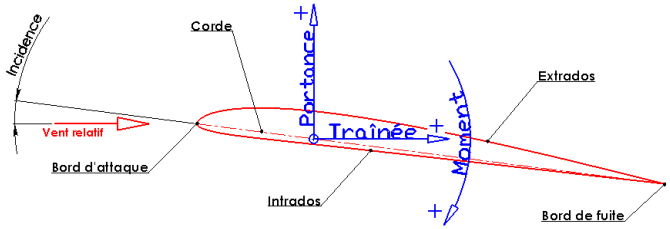

Fig. 02

- Aerodynamics: the science of flows, aiming to define and quantify the forces involved.
- Flight mechanics: the science of piloting the trajectory, using different lift forces.
- Roll (X), pitch (Y) and yaw (Z) axes: controlled respectively by the "aileron", "depth" and "rudder" functions.
- Angle of attack (α, alpha): the angle of attack of a surface or airfoil relative to the wind direction of the air mass. The angle is measured with respect to the chord (the line passing through the leading and trailing edges). By convention, this angle is positive when the leading edge is higher than the trailing edge and negative otherwise.
- Pitch (or trim): the angle between the fuselage's median axis and the horizontal. Unlike the angle of attack, which is difficult to judge, it is the angle most directly perceived by model aircraft pilots.

- Slope: angle between the direction of flight and the horizontal.
- Angle of attack: angle between a reference axis (usually the mid-axis of the fuselage) and the chord of a wing or horizontal tail.
- Lift: the force that opposes the weight of the model and/or its inertia, characterized by the lift coefficient (Cl). By definition, it is perpendicular to the aerodynamic flow (= direction of flight in the air mass), along the Z-axis.
- Drag: the force that opposes the forward motion of the model, characterized by the drag coefficient (Cd). By definition, it acts in the direction of the aerodynamic flow (opposite to the direction of flight), along the X-axis.
- Moment: rotational force due to the action of a force on a lever arm. In the case of an aircraft, it is characterized by the moment coefficient (Cm) and results from the airflow around the airfoil. It can be nose-down (negative moment) or nose-up (positive moment).
- Couple: special case of a moment generated by two identical lever arm forces but in opposite directions (pure moment, without resultant force).
- Neutral point: point of an aerodynamic element (airfoil, wing, fuselage, model) around which its moment is constant and independent of the angle of attack.
- Stability: ability to naturally resume a normal flight path after a disturbance (air turbulence or pilot command).
- Equilibrium: a situation where all forces and moments cancel each other out.
- Center of gravity: the point where all the masses are balanced and where the force of gravity is concentrated. It is also the instantaneous center of rotation of the aircraft. Its placement determines flight stability, primarily around the pitch axis, and can be adjusted by moving certain onboard masses (battery, receiver, etc.) or by adding mass (lead) to the front or rear ends.
- Aspect ratio (λ, lambda): value quantifying the importance of the wingspan compared to the wing chords.
- Polar: curve representing the evolution of an aerodynamic vector that varies according to a parameter.
- Eiffel polar: graph of Cl/Cd, in fact Cd is a function of Cl although Cd is on the x-axis, the angle of attack being the parameter. By extension, all graphs of aerodynamic characteristics are called "polar".

Not much more is needed to describe the basic principles of flight, with a brief reminder, almost self-evident: the laws of flight mechanics and aerodynamics apply regardless of the aircraft's design: glider, airplane, canard, jet, biplane, flying wing, flying saucer, etc., all are rigid and heavy bodies moving through a fluid (air), which provides lift and, in some cases, propulsion. Unfortunately for our hobby, an additional difficulty arises due to the scale effect, further reducing the margins of error: the smaller the aircraft, the more challenging the flow is to control. This is all thanks to a certain Mr. Reynolds… and especially to the viscosity of air.

2.2 Origin of lift

Overall, the principle of flight is simple: on one hand, energy (engine, potential energy (altitude), or thermodynamic energy (lift)) is supplied to propel the aircraft forward; on the other hand, the resulting displacement generates a lift force that balances the aircraft's weight. This is elementary so far, but things become more complex as soon as we try to characterize this lift force.

First of all, let's dispel a myth: in a conventional aircraft, it is not only the wing that generates lift, even if it is the main contributor, but the entire aircraft, and this varies according to the different phases of flight.

Furthermore, the traditionally accepted explanation of lift, based solely on the geometric flow of air around the airfoil (greater distance to travel to follow the upper surface than the lower surface, etc.), falls apart under even the simplest visual observation. Consider, for example, an indoor aerobatic model whose airfoil is essentially a flat plate devoid of any curve, or a transition aircraft with an asymmetrical airfoil that nevertheless performs very well inverted flight. There is, therefore, something else, something far more fundamental: the wing's angle of attack, as lift is generated proportionally to the angle of attack (for a given airspeed and wing area).

Yes, but how? Here too, it's very simple and full of basic common sense: the greater the angle of attack, within the limit of the stall angle of attack, the more the wing deviates and therefore accelerates the mass of air circulating around the airfoil (fig. 03).

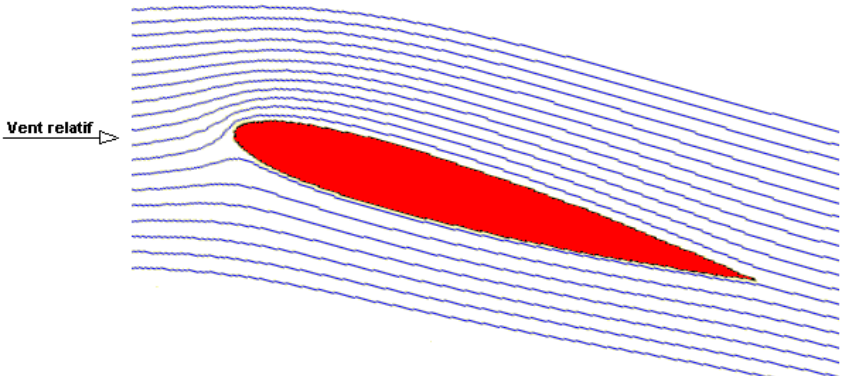

Fig. 03

From a global perspective, Newton's third law is sufficient to describe the principle: in reaction to the momentum of the air mass deflected in one direction, the wing experiences a force in the opposite direction that lifts the aircraft. However, because it is impossible to quantify this deflected air mass a priori, this law does not allow us to go further, unlike the local application (along the airfoil,

by breaking it down into small elements studied step by step) of Bernoulli's theorem, which defines the relationship between the velocity of a fluid, here around the airfoil, and its static pressure (a quick reminder: the "." symbol represents the "multiplication" operator):

$$P + \frac{1}{2}.\rho.V^2 = Cste$$

With: $\rho = 1{,}225\, kg / m^3$ the density of the air (at sea level and 15°C), V the relative wind speed (in m/s), P the static pressure (in Pa).

The term $\rho.V^2/2$ is called the dynamic pressure (q) of the fluid, in this case air, and represents its kinetic energy. In the case of an aircraft, the value of Cste (constant), also called P0 at sea level, is the ambient atmospheric pressure.

The introduction of Bernoulli's theorem does not, however, validate the pseudo-theory of "equal transition times" (which claims that air separated at the leading edge rejoins at the trailing edge). Quite the contrary, in fact, because it is precisely because the air circulates independently between the lower and upper surfaces (by what miracle would air molecules separated at the leading edge and following different paths arrive simultaneously at the trailing edge?) that Bernoulli's theorem allows us to quantify the aerodynamic behavior of the airfoil.

Bernoulli's theorem is actually applied along the entire airfoil, by locally studying (the airfoil being discretized into a sufficient number of points) the pressure at each point. The set of points gives the pressure field (in the literal sense of the term) generated by the air circulation around the airfoil (fig. 04).

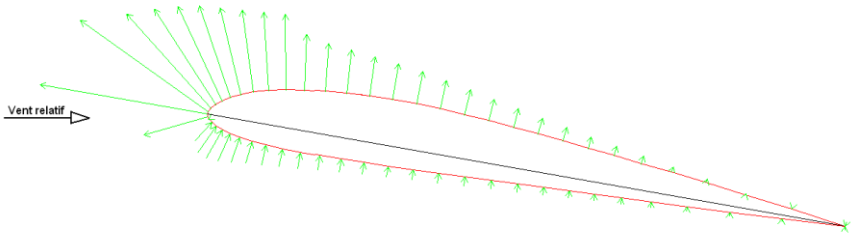

Fig. 04

This pressure field exhibits, relative to ambient pressure, areas of low pressure (arrows pointing away from the airfoil) and areas of high pressure (arrows pointing towards the airfoil), with the difference proportional to the arrow length. It can be observed that the highest levels of both low and high pressure are concentrated at the leading edge, as this is the area where the air undergoes the greatest deflection and therefore flows fastest.

Introducing the concept of a pressure field also helps us understand that the airfoil's influence on the air mass is not limited to the immediate vicinity of the wing. Indeed, if a certain area is under low or high pressure, nearby areas are affected: the height of air deflected by the airfoil is therefore much greater than the thickness of the airfoil itself. This is particularly visible in Fig. 03, where the narrowing of the airflow is clearly visible well above the leading edge. This deflection does not stop at the trailing edge of the wing or airfoil, but extends well beyond it downstream. As we will see in detail later, this influences the operation of the horizontal tail, which is subjected to this deflection, known as wake deflection (see §2.14.3).

Integrating all these pressure values around the airfoil's periphery yields a force, called the aerodynamic resultant (R), whose magnitude, direction, and point of application (called the center of pressure, CP) vary according to the airfoil's geometry, angle of attack, and airspeed. As such, this force is therefore completely impractical to use, unlike its decomposition into elementary forces. This decomposition is carried out using the reference frame (also called the coordinate system) formed by the direction of flight and its perpendicular (Fig. 5).

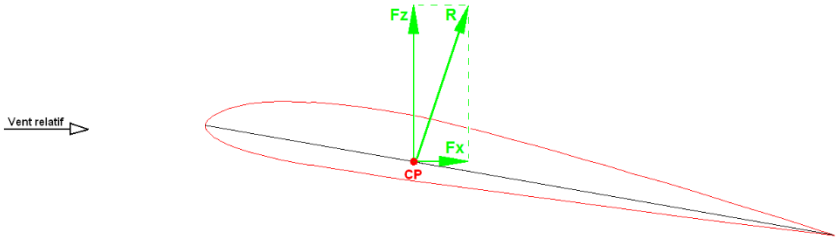

Fig. 05

This results in drag (Fx) and lift (Fz) forces, respectively parallel and perpendicular to the direction of flight. Their point of application is always the center of pressure (CP), whose position varies depending on the angle of attack (it can even be located outside the airfoil, see formula in §2.13), which makes this concept very difficult to grasp. So much so, in fact, that it has largely contributed to making flight mechanics almost incomprehensible to the general public, particularly regarding balance and longitudinal stability (center of gravity).

This difficulty is circumvented thanks to a final decomposition (fig. 06), the principle of which stems from two fundamental observations:

- In the specific case of symmetrical airfoils, the position of the center of pressure (CP) is fixed and located precisely at 25% of the chord. This singular point, called the apex, is in fact common to all airfoils. Its calculation is too complex to discuss here, but it can be observed that its position is visually consistent with the pressure distribution around the airfoil, which is noticeably denser around the leading edge.
- For other airfoils, the distance between the CP and the neutral point is inversely proportional to the lift.

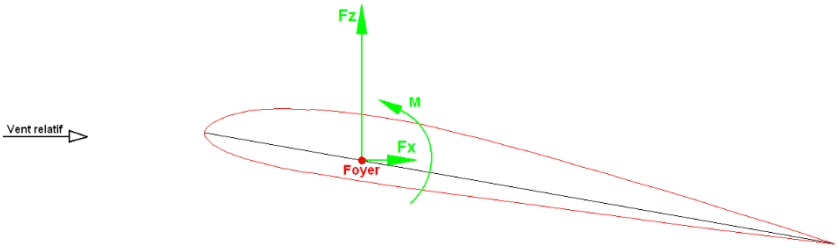

Fig. 06

Consequently, if we consider the lift at the apex, a pitching rotational force appears (equal to the product of the lift and the distance between the center of pressure (CP) and the apex), called the moment. Its key advantage is that, for a given flow velocity, it is constant and therefore independent of the angle of attack (subject to certain limitations, see §4.3.6). Even better, this moment is described by a constant coefficient (see §2.3), regardless of the flow velocity. Only the value (zero if the airfoil is symmetrical) and the sign (negative if the CP is located behind the apex, positive otherwise) of this coefficient are specific to each airfoil (primarily its camber, see §4.3.2). However, the apex is always located at 25% of the chord, regardless of the airfoil.

Certainly, one might object, but what about when the lift is zero? In fact, it is always the same and therefore not necessarily zero… To understand this apparent paradox, it suffices to decompose the integration of the pressure field around the airfoil between the upper and lower surfaces (fig. 07):

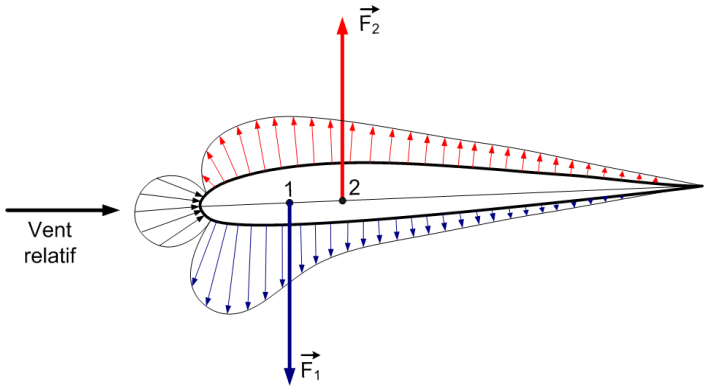

Fig. 07

We then observe that if the two "half-lift forces" can cancel each other out (F2 = -F1), then the lift can be zero (Fz = F1 + F2 = 0) without the moment of these forces around the apex being zero. In this particular case, the resulting moment is then called a couple (or pure moment), because the resultant of the lift forces is zero.

To summarize these fundamental points, the effects of the flow around the airfoil and, by extension, of the wing (or any wing shape) are described in a particularly simple and easy-to-use way:

- A fixed reference frame: origin = neutral point at 25% of the chord, X axis = direction of flight, Z axis = perpendicular to X.
- A drag force, along the X axis.
- A lift force, along the Z axis, proportional to the angle of attack.
- A moment independent of the angle of attack and described by a constant coefficient.

NOTE

- This particularly remarkable result was identified by Max Munk, one of the historical fathers of aerodynamics, and formulated mathematically in his linear theory of thin airfoils. We will be using this theory almost unconsciously throughout this book, as it remains perfectly suited to describing the operation of our small aircraft.
- Incidentally, these elements also allow us to understand the de facto mechanical dimensioning of a wing structure, particularly the positioning of the spar at the first quarter of the chord and the sheeting of this first quarter, where the majority of the pressure field is concentrated. We might also question whether the airfoil is maintained in this area in the case of an open structure simply covered with fabric. However, it's a step too quickly to conclude that this type of design is aerodynamically unsuitable, as it's not certain that the modification of the fabric-covered airfoil under the effect of the pressure field is necessarily negative. This warrants further investigation rather than premature dismissal.

2.3 Quantification of lift

The previous paragraph was addressed by emphasizing that everything in an aircraft can be a source of lift. Indeed, a significant wing angle of attack (measured relative to the relative wind, in other words the direction of flight within the air mass) that occurs during low-speed phases, tight turns, or loops will de facto result in a high angle of attack of the fuselage and horizontal tail, which will therefore also be sources of lift (fig. 08).

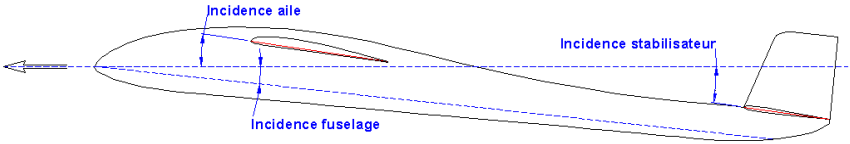

Fig. 08

Similarly, during phases of low wing lift (Fig. 9), the fuselage or horizontal tail will provide little lift, or even generate downward lift depending on their geometric configuration. The effect of the angle of attack also explains quite naturally why an aircraft can fly at different speeds: up to a certain limit (stall), a high angle of attack compensates for a reduced airspeed to keep the aircraft airborne, while at high speeds the angle of attack is low.

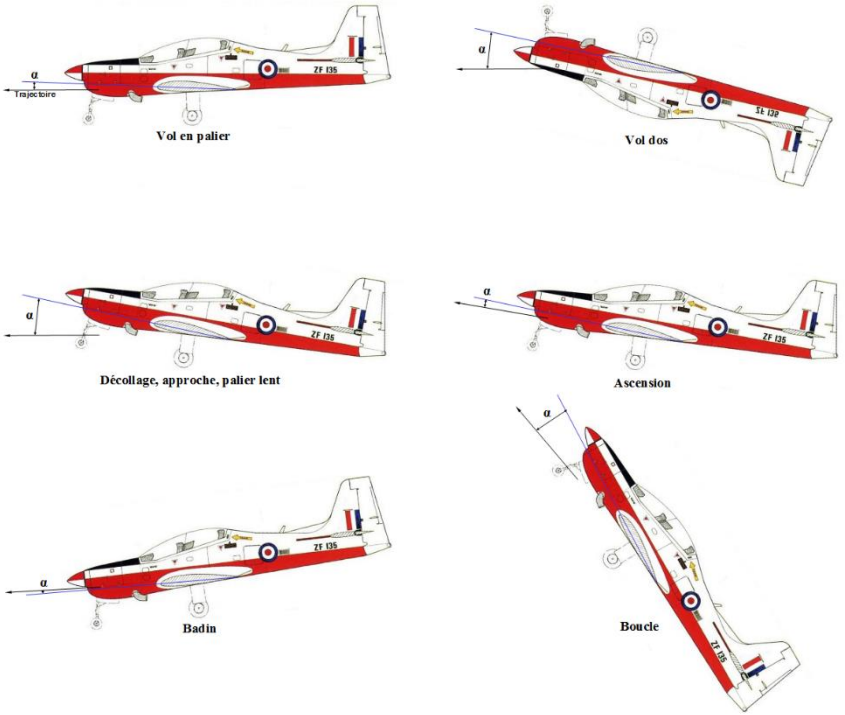

Fig. 09: Wing angle of attack, pitch and bank angle at different phases of flight

If lift is directly proportional to the angle of attack (α), the latter is not particularly practical to use because of the zero lift angle of attack of any element (denoted α0 or Alpha0), particularly of the wing airfoil (fig. 10).

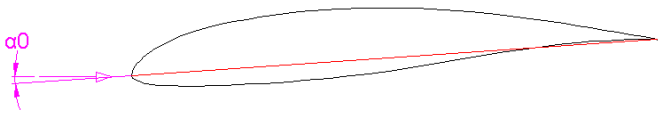

Fig. 10

For the latter, this angle of attack at which the lift is zero will generally from about -4° (airfoil "hollow") to +1° (airfoil "self-stabilizing") via 0° (airfoil "symmetrical" or "plank"), which represents a non-negligible value because it is of the same order of magnitude as the angles of attack commonly encountered during flight (around +/- 10°).

Characterizing the lift therefore requires using not only the geometric angle of attack (α) but the relative angle of attack (α- α0).

Instead of this relative angle of attack, we will prefer the concept of lift coefficient (Cl):

$$Cz = 2\pi.(\alpha - \alpha 0)$$

With angles in degrees instead of radians, this relationship becomes:

$$Cz = 0{,}11.(\alpha - \alpha 0) \text{ Or } Cz = (\alpha - \alpha 0)/9{,}1$$

This relationship is given by the theory of thin airfoils and represents reality very well regardless of the airfoil insofar as it works correctly (that is to say that it is not stalled and compatible with the Reynolds numbers to which it is subjected, see below) and where said airfoil really resembles a airfoil, which of course includes "plank" airfoils, and not a "potato".

Subject to these reservations, the theory of thin airfoils reveals a particularly striking fact: whatever the airfoil, the proportionality between angle of attack and lift (=dCl/d α, i.e. the slope of the curve Cl(α)) is always the same: the curve Cl(α) is in fact a straight line, hence the qualification "linear" of this theory.

The use of lift coefficient (Cl), while perhaps less intuitive than that of angle of attack, offers a decisive advantage: it allows for the immediate calculation of lift force, independent of the airfoil. This calculation is based on the dynamic pressure (q) and the surface area (S) of the load-bearing element under consideration, and finally allows us to write the well-known equation for lift force:

$$Fz = q.S.Cz = \frac{1}{2}.\rho.V^2.S.Cz$$

The result is expressed in N (newtons, 10 N ≈= 1 kgf, to put it simply). Since the wing is by nature the reference lifting surface (the one that provides the majority

of the lift), S is generally the wing area when referring to the complete aircraft. We will see later (§ 4.8) how to also take into account the lift of the horizontal tail in the flight equations.

NOTE

- This relationship highlights that lift is not intrinsic to the airfoil, or by extension to the wing, but is instead imposed upon it by flight conditions: speed and lift coefficient (via the angle of attack), all determined by the pilot through the elevator and throttle controls. To use a car analogy: it is not the tire (⇔airfoil or wing) that generates the forces (⇔lift) during a turn (⇔flight conditions); it is simply the conduit, via the steering angle (angle of ⇔attack) imposed by the steering wheel (⇔elevator control) within the limits of the airfoil's grip capacity (⇔maximum lift allowed by the airfoil before stalling).
- Unlike drag, lift is therefore not a parameter that can be manipulated in aircraft design. Except indirectly, through mass. For example, in level flight (= flight at a constant altitude), lift is exactly equal to the weight (= mg, where m is mass and g is the acceleration due to gravity) of the aircraft: for a given flight speed, changing the mass therefore changes the lift coefficient proportionally, whereas changing the airfoil makes absolutely no difference in this respect.
- At our scales, the maximum lift coefficient (Cl) supported by a airfoil before stall is approximately 1 to 1.5 in normal flight and -0.5 to -1 in inverted flight.

2.4 What about the airfoil?

And what about the airfoil, or more precisely its shape, in all of this? Its role, secondary to that of the angle of attack, is to facilitate airflow… Nothing more, even though it's already important. The airfoil shape notably influences drag as well as the stall angle of attack (around 10 to 15° in model aircraft), the angle of attack at which the airflow can no longer follow the upper surface of the wing: the flow becomes turbulent and/or separates from the airfoil, and lift collapses. Under certain conditions, the difference in stall angle of attack between a well-suited airfoil and one that is not at all suitable can be as much as double. This phenomenon is linked to the viscosity of air, which tends to make the air adhere to the surface of the airfoil (Coanda effect). This results in a transition zone, called the boundary layer, between the air at its "normal" speed as it flows around the airfoil and the air closest to the airfoil, at zero speed. This boundary layer, thin and smooth in normal (laminar or semi-turbulent) flow, can become thick and turbulent (locally, the flow can even reverse) when the air can no longer follow the airfoil's contour, which consequently malfunctions. The boundary layer then separates (Fig. 11), a process that occurs more easily when the flow is at low speed, the wing chord is small, or the curvature is pronounced. This is where the Reynolds number comes into play.

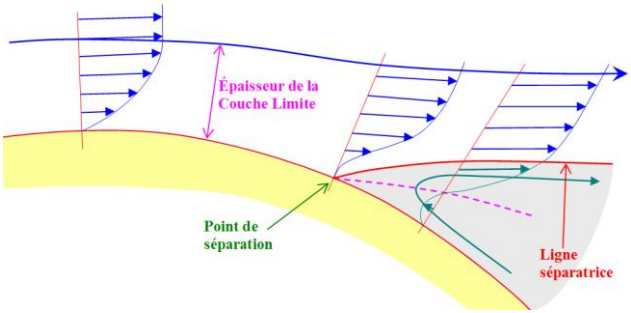

Fig. 11, evolution of the boundary layer (copyright Wikipedia - Bernard de GoMars)

2.5 Reynolds number

This is one of the fundamental principles of aerodynamics, allowing us to understand airflow by combining the airfoil chord and the flight speed into a single number. In practical terms, this number indicates that an airfoil with a 100mm chord traveling at 50 km/h will behave in exactly the same way (drag, lift, etc.) as the same airfoil with a 50mm chord flying twice as fast. The Reynolds number (Re) is calculated as follows:

$$\mathrm{Re} = \frac{C.V}{\nu}$$

With: ν = kinematic viscosity of the fluid (air: approximately 1.47 x 10E-5 m²/s at 15°C), C = chord (m) and V = velocity of the airfoil in air (m/s)

Or, to simplify: $\mathrm{Re} \approx 68.C.V$ with C in mm and V in m/s.

Typical Re values in scale models range from approximately 15 000 (micro-model horizontal tail) at 3 000 000 (turbine jet wing). Regardless of the aircraft, it should also be noted that the slower it is, the higher the angle of attack must be (to provide the necessary lift) and the less effectively the airfoil functions (low drag coefficient), which doubly increases the risk of stalling…

The Reynolds number (Re) below which the airfoil no longer functions correctly is called the critical Reynolds number (see §4.3.6), and depends primarily on the airfoil thickness and its position. The thicker the airfoil and/or the further back the airfoil is located, the higher the critical Reynolds number will be; this is, in fact, one of the main causes of failure with very small aircraft.

2.6 Drag and drag coefficient

Drag is the force resisting the forward motion of an aircraft. Since lift results from forward motion, which drag opposes, it's clear that the true guarantee of good performance is reduced drag, not high lift as is often assumed. In short, the engine or updraft provides the energy, drag dissipates it… Therefore, minimizing drag is highly advantageous, either to achieve higher speeds with a given power output or to reduce the power required for the same airspeed.

The origin of drag is often attributed solely to the airfoil, but things are far from that simple. Generally speaking, drag is generated by the airflow around the aircraft, by friction (air adhesion to the surfaces, typically a large part of airfoil drag), and by separation (parasitic vortices around the wingtip, which cause induced drag, or downstream of an overly abrupt shape: unfaired wheel, abruptly cut rear fuselage, protruding control surfaces, etc.). These two components are respectively referred to as viscous drag and pressure drag.

Like lift, drag is quantified in relation to a drag coefficient (Cd), with a perfectly similar equation:

$$Fx = \frac{1}{2}.\rho.V^2.S.Cx$$

Since the overall drag coefficient (Cd) of an aircraft cannot be determined directly, the overall drag is calculated by adding the individual drag of each characteristic element: wing, horizontal tail, fuselage, but also other ancillary elements such as landing gear, struts, an external tank or simply protruding control surfaces.

To complicate matters, each of the drag coefficients (Cd) associated with these elements evolves differently (Fig. 12) depending on the flight phase (angle of attack and speed) and the aerodynamic quality of the element. This is represented by a 3D surface whose equation is of the form Cd = f(Re,Cl), which we will discuss in detail in §4.8.

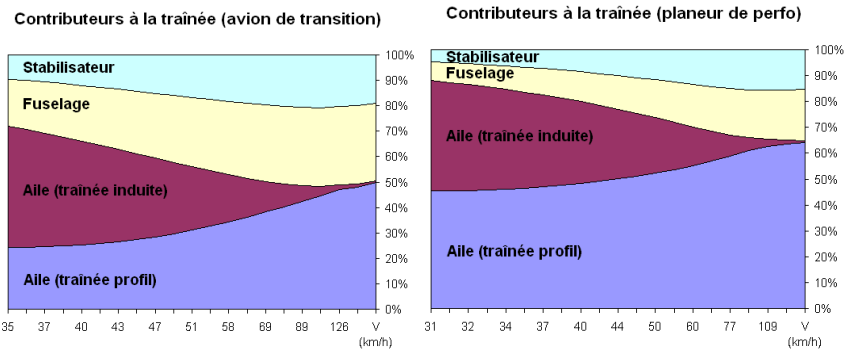

Fig. 12, distribution of the main drags of two models with equivalent surfaces. The differences are significant and clearly show that it is not only the airfoil that can be worked on to reduce drag.

2.7 Induced drag

Figure 12 illustrates the concept of induced drag, which represents a significant portion of the total drag and is added to the airfoil drag. This drag, which affects both the wing and the horizontal tail, results from an airflow around the wingtip from the lower surface (under pressure) to the upper surface (under pressure), resulting in the well-known wingtip vortex (Figure 13).

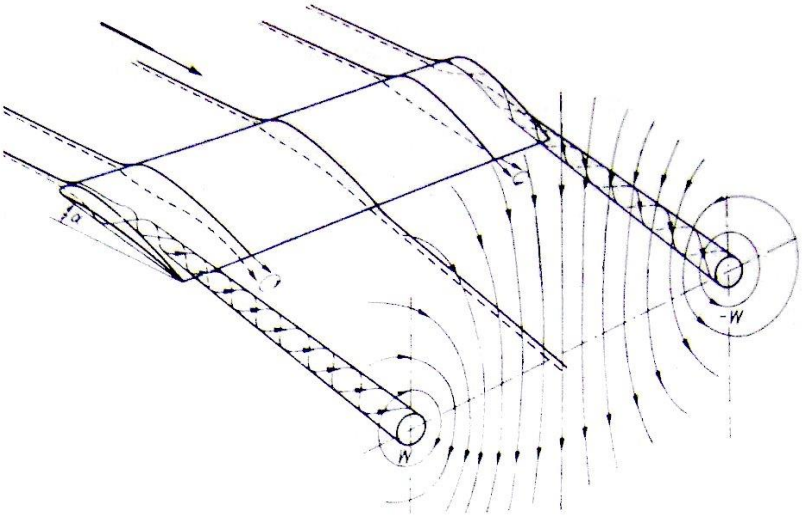

Fig. 13

From being almost negligible at low lift, induced drag can be of the same order of magnitude as the airfoil drag at high lift, or even greater in the case of a low aspect ratio. It is proportional to the lift (specifically to its square, see §4.2.3): the greater the lift, the greater the pressure difference between the lower and upper surfaces, and therefore the more airflow develops at the wingtip. This flow modifies the aerodynamic angle of attack of the chords near the wingtip. This is called the induced angle, which directs the local lift slightly aft (while the lift is vertical). The projection of this local lift onto the horizontal axis results in a rearward force, which is the induced drag. Consequently, the effective lift (directed along the vertical axis) is reduced; we will see the details later (see §2.14.1).

This is an opportunity to introduce the concept of aspect ratio, which reflects the relative size of the wingspan compared to the chord (or surface area, which amounts to the same thing). For example, a high-aspect-ratio wing, typically used in gliders, has a large wingspan and proportionally small chords. The physical role of aspect ratio is very simple: the greater the aspect ratio, the weaker the effects of airflow from the lower surface to the upper surface at the wingtip, because they affect a proportionally smaller area of the wing. This is a particularly important element of flight mechanics because it primarily determines the behavior of a wing, much more so than its airfoil.

The aspect ratio λ(Greek letter "lambda"), is defined by the following formula :

$$\lambda = \frac{E^2}{S}$$

Where: E is the wingspan and S is the wing area

Induced drag is also affected by the shape of the wing because the latter conditions the distribution of lift (see §2.14.1 and § 5.6), therefore ultimately the flow at the wingtip, the ideal being to obtain an elliptical distribution of lift (see the Spitfire, but also all modern performance gliders).

Similarly, the model's behavior is also influenced by the distribution of lift coefficient (which differs from that of lift due to the surface area distribution, but the calculation method is fundamentally the same). A rectangular wing, typical of entry-level aircraft, will be less efficient than an elliptical wing but will exhibit more predictable stall behavior because the stall will initiate at the wing root (highest local lift coefficient) and then progress gradually towards the wingtip (lowest local lift coefficient). Conversely, the induced angle of the elliptical wing, and therefore the local lift coefficient, being constant over the entire wingspan, its stall will be uniform and thus potentially abrupt (see § 5.6).

2.8 Additional drags

For the fuselage, drag is broken down into wetted surface drag (viscous drag) and bypass drag (pressure drag when subjected to an angle of attack). Determining these is complex and requires the use of a 3D CFD (Computational Fluid Dynamics) code or, failing that, approximate analytical equations that take into account the main dimensions (see §4.8.3).

Next comes the drag of accessories (landing gear, struts, controls, etc.), which can represent a very significant portion of an aircraft's total drag. This type of drag, known as tail drag because it's linked to the low pressure created in the turbulent wake of an obstacle, is primarily a matter of frontal area. Hence, for example, the use of small, narrow wheels on FAI 40 racers or fully integrated control surfaces on competition gliders.

Fairing these accessories generally offers a fairly moderate gain (Fig. 14) unless a particularly tapered fairing is used, tapering towards the trailing edge, like an airfoil. In that case, the flow becomes much more laminar and the drag is then more of the viscous type.

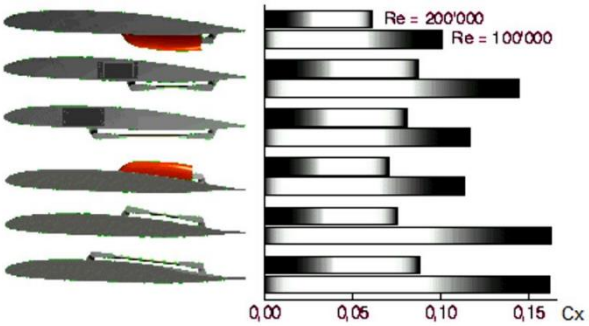

Fig. 14, study by Martin Hepperle

To be exhaustive, we must also add a component called interaction drag, which characterizes the drag at the junctions between the different elements that make up the aircraft (wing fairing, for example). This drag varies depending on the quality of the design and the phase of flight, but it can be considered to represent on average 10% of the aircraft's total drag.

2.9 One moment, please!

The pitching moment, or "rotational force in pitch," primarily concerns the airfoil, but also the various elements of the aircraft. It can be broken down into two variants.

First, there is the airfoil moment, also called torque, which results from the transfer of the lift force at the aerodynamic center. This moment is directly dependent on the airfoil shape (particularly its camber), both in magnitude and direction. Typically, a conventional aircraft airfoil will exhibit a negative moment (a force causing a tendency to pitch down), while a flying wing airfoil, incorrectly called self-stabilizing (see 2.12), will exhibit a positive moment (a tendency to pitch up). A symmetrical airfoil or a plank airfoil, generally used on a horizontal tail, exhibits a zero moment.

The airfoil moment is governed by the same type of equation as drag and lift, based on the moment coefficient (Cm) and the airfoil chord (C):

$$M_{profil} = \frac{1}{2}.\rho.V^2.S.C.Cm_p$$

As mentioned earlier, this moment is normally (the meaning of this caveat is detailed in 4.3.5) independent of the angle of attack. It is characterized by the moment coefficient, denoted Cm (or Cm_p, to distinguish it from the overall moment of the aircraft), or in some publications Cm0.25 to recall its origin (transposition of the lift at the aerodynamic center at 25% of the chord). The designation Cm0 is also found, which is the value of Cm at any point on the chord for Cl=0. This value is, in the general case, a constant, independent of the angle of attack and the speed, and it is this value that we will use subsequently.

Next, we find the moment generated by the lift force, which is the product of this force and its lever arm (distance between the apex and the point considered, typically the center of gravity). This moment is therefore proportional to the angle of attack, and is written (BL = lever arm, positive when the apex is located downstream of the point considered):

$$M_{portance} = -Fz.BL$$

At the level of the complete aircraft, its overall moment is the sum of the airfoil moments and lift moments (note the signs, see §2.12) of each element (wing, horizontal tail, fuselage) around the center of gravity. Stabilized straight flight is therefore achieved by the equilibrium of these moments, that is to say, a zero overall moment, or:

$$M_{avion} = \sum M_{profil} + \sum M_{portance} = 0$$

The stability of the aircraft, characterized by its resistance to a change in angle of attack, meaning that its moment varies inversely with the angle of attack, is therefore described by the following equation (note for those less mathematically inclined: it simply indicates that the slope of the aircraft moment curve [as a function of the angle of attack] is negative, i.e., that this curve is decreasing):

$$\frac{dM_{avion}}{d\alpha} < 0$$

2.10 Finally, let's talk of CG… and weather vanes

We are now able to address one of the most important parameters of flight quality, the center of gravity (CG), the adjustment of which (called "centering") determines pitch stability (= ability to naturally maintain a defined trajectory).

First, let's remember that "centering an aircraft" (or "adjusting the center of gravity") involves positioning its center of mass, for example by moving a battery or adding lead to the nose or tail, until it reaches a point that allows for safe flight. This is far from trivial; experience shows, for example, that an aircraft with its center of gravity too far aft has a significantly reduced lifespan.

Like lift, this issue is rather poorly understood, especially in France where numerous publications have perpetuated a certain ambiguity. Who hasn't read that one airfoil should be centered at 29% of the chord, another at 37%, and so on? And then there's the sacrosanct rule of one-third of the chord (which one, by the way?) which is simply invoked as an absolute truth.

To move beyond this heated debate and towards a more reasoned approach, nothing beats a little observation. Let's revisit the examples of the indoor aircraft lacking a "true" airfoil and the transition aircraft in inverted flight: in the first case, it's difficult to link the center of gravity to any airfoil, while in the second case, the center of gravity would need to be changed once in inverted flight, since the airfoil is radically inverted! In this configuration, the inverted airfoil is even highly self-stabilizing. Similarly, what about the substantial airfoil modification caused by deflecting a camber flap? Let's also consider a canard or a Flying Flea, whose center of gravity is not at all in the "usual" position and is located respectively towards the leading edge or the trailing edge, even though its wing and airfoil can be virtually identical to those of conventional aircraft. Finally, let's discuss the center of gravity of flying wings, which everyone knows is around 20% (this time completely ignoring the question of the airfoil), and let's not forget certain models where in-flight adjustments (the only ones that make sense!) lead to a center of gravity of 55%...
These few examples thus seem to refute any relationship between center of gravity and airfoil, and instead point towards a link with the aerodynamic design

(canard, Pou du Ciel, flying wing, etc.). However, very serious publications, such as the excellent "Aerodynamics Made Easy" by Marcel Chabonat, rely solely on the airfoil to determine the center of gravity. But when one carefully reads the method used, which is dedicated to the very specific context of free flight, it becomes clear that the center of gravity is fixed a priori for a precise criterion (neutral horizontal tail, to minimize drag, at maximum lift-to-drag ratio), which—at this stage—effectively only involves the airfoil.

Yes, but then what? The answer isn't far off: if we continue reading these works, we discover that they detail how to verify that the aircraft thus designed is sufficiently stable, using the same calculation of moment variations discussed earlier. And this calculation is not limited to the wing at all, but involves the horizontal tail (in particular its surface area and its lever arm with the wing), which serves as an adjustment variable to obtain sufficient stability (which, incidentally, has a significant impact on its drag, and therefore can even exceed the minimum drag criterion used as the basis for this method, to which we will later prefer a more decoupled approach). In other words, when it comes to stability (as indeed to all its parameters in general…), an aircraft is by no means reducible to its wing or its airfoil.

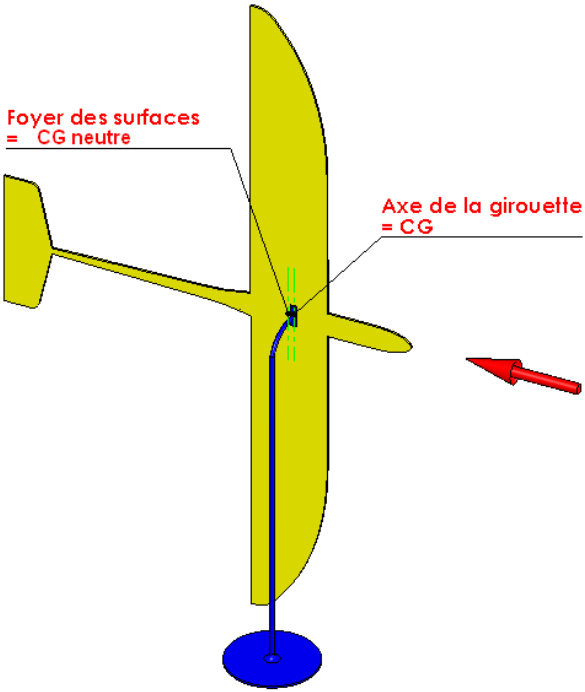

Fig. 15, flat weather vane representing pitch stability

Therefore, understanding centering requires a more holistic view of the aircraft, which involves recalling a fundamental definition of rigid body mechanics: an aircraft, regardless of its design, airfoil(s), etc., is defined as a pseudo-isolated rigid body moving through the air, its instantaneous center of rotation being its center of gravity. This can be translated into very simple terms: an aircraft is a weather vane pivoting around its center of gravity (Fig. 15).

As almost everyone has experienced, the positioning of a weathervane's axis determines its stability in the wind. If placed too far forward, the weathervane follows the wind particularly well (it is very stable), with the slightest angular deviation generating a restoring force (a moment around the pivot point) that increases with the angle. Conversely, if placed too far back, the weathervane flaps in the wind or even reverses abruptly, as the restoring force is in the same direction as the disturbance, exacerbating it (it is unstable). Between these two extremes, there is a point, called the apex, where the weathervane has no preferred position relative to the wind (it is neutral).

In other words, a wind vane whose hinge (= CG) is positioned at the apex does not exert a restoring moment when its angle of attack relative to the wind changes ($dCm/d\ \alpha = 0$, see §2.9). To ensure stable behavior, it is therefore sufficient to position the center of gravity in front of the apex, which by nature corresponds to the neutral center of gravity (used, for example, on high-performance or aerobatic aircraft).

The center of gravity, and consequently the center of gravity, is therefore simply a matter of surface area distribution (Fig. 16). The more surface area there is behind the wing, or the further this surface is located behind the wing, the further the center of gravity will be behind the usual values, and vice versa. Hence, for example, the very particular centers of gravity of a classic aircraft (large horizontal tail with a long lever arm relative to the wing) or a canard (horizontal tail and fuselage in front of the wing).

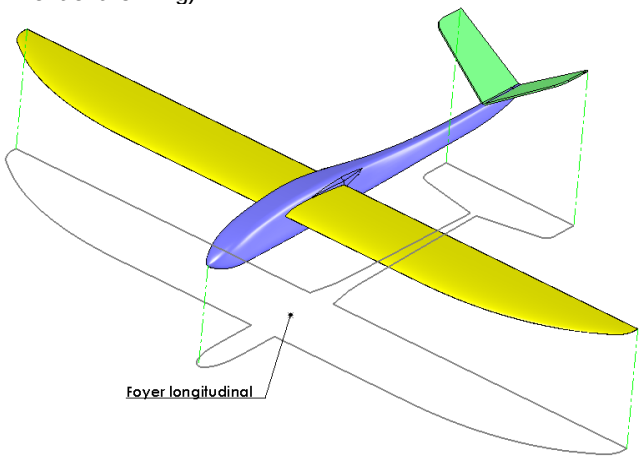

Fig. 16, projection of active surfaces longitudinally

The concept of a center of gravity applies equally to a complete aircraft as to a wing or airfoil. The principle is exactly the same in all cases: it is the geometric point where the element in question behaves like a neutral wind vane. Since an aircraft is an assembly of different lifting elements (wings, horizontal tail, fuselage), its center of gravity can therefore be determined by characterizing the centers of gravity of these elements separately. However, we saw earlier that the center of gravity of a single airfoil does not depend on its shape, but solely on its chord. Thin-walled airfoil theory shows that it is located at 25% of this chord (see §2.2). As the center of gravity of an airfoil is a purely geometric concept, the same is true for the centers of gravity of the elements composing the aircraft. These are located at 25% of the mean chord (a virtual chord representing aerodynamic behavior; we will see later how to calculate it, see §4.2.1) of any lifting element. The global center of gravity of the aircraft is therefore, by extension, a fixed point which depends only on the geometry of the aircraft, and not on its airfoil(s), whatever they may be, as we had already noted above.

NOTE

- The calculation of the aircraft's center of gravity, and therefore of the CG, is reduced to the mean chord of the wing (reference lifting element) hence, perhaps, the establishment in the collective unconscious of an [unfounded] relationship between center of gravity and wing airfoil.
- The concept of neutral point also relates to the yaw axis. In the general case, since the lateral surfaces are more concentrated towards the rear (vertical tail) than the longitudinal surfaces, the lateral neutral point is therefore naturally behind the longitudinal neutral point, hence the fact that it is of little concern.

2.11 Taming the concept of neutral point

The concept of neutral point at the basis of the stability problem can be illustrated in a minimalist way by a rectangular flat plate (Cm0 = 0) placed at an angle of attack in the relative wind (fig. 17), its pivot materializing the CG and F being the neutral point of the airfoil at 25% of its chord.

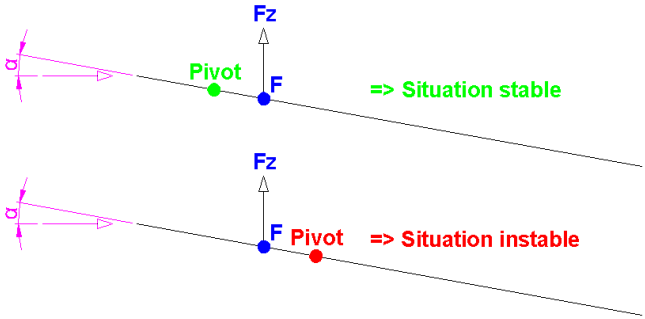

Fig. 17, incident plate in the flow (side view)

If the pivot point is located in front of the aerodynamic center (at 25% of the chord), the lift force (Fz) generated by the angle of attack tends to counteract it: the system is stable. Conversely, if the pivot point is located behind the aerodynamic center, the lift force "carries" the airfoil: the system is unstable. And if the pivot point is located at the aerodynamic center, the wing has no preferred angle of attack: the system is neutral, which clearly demonstrates that the lift force is applied at the aerodynamic center.

This example of the flat plate can be implemented in a small experiment that is very easy to reproduce (fig. 18):

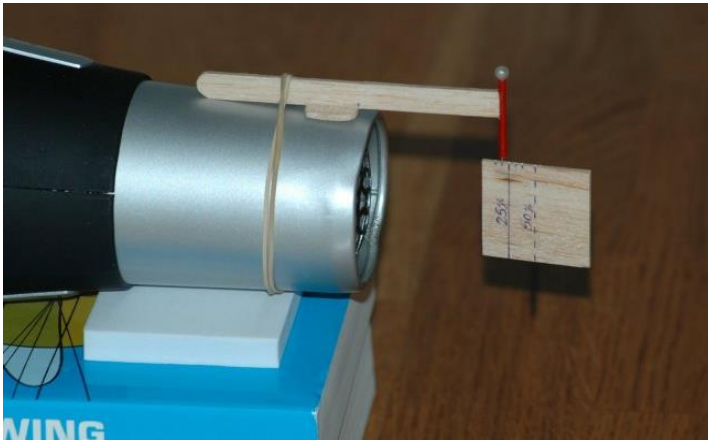

Fig. 18, highlighting the neutral point

Take a square of lightweight balsa wood approximately 32 x 32 mm (to ensure round dimensions) and 2 mm thick. Insert a rotating pin into a piece of plastic tubing, which is itself glued to a support. Start 4 mm from one edge, which we'll call the leading edge, and then move back every 2 mm. Each time, expose this improvised wing to the wind from a hairdryer and observe what happens when you destabilize it using a small rod (more practical and much less intrusive than using your hands).

Guaranteed effect: with a little care, you'll notice that the behavior changes radically on either side of the 25% chord position (8 mm from the leading edge). In front of this position, the wind vane aligns perfectly with the airflow from the hairdryer and returns to this alignment after adjusting its angle of attack using the rod. Behind this position, the wind vane no longer aligns with the wind and may even begin to oscillate or rotate if the joint is moved further back. We have therefore identified the center of gravity of this improvised wing, as well as that of the airfoil, since the chord length remains constant.
Within the instability range, and as long as the hinge is not too far from the apex, another phenomenon is also easily detectable: stalling. Indeed, the wind vane is

only truly unstable within a range of approximately +/-10° around zero angle of attack and stabilizes once either of these two angles of attack is reached. In fact, on the stalled airfoil, the strong low-pressure area of the first quarter of the upper surface collapses, which generates a moment opposing the increase in angle of attack.

Another rather instructive point: despite the particularly low Reynolds number encountered here (approximately 7 m/s and 32 mm chord => Re ≈ 15 000), the rustic airfoil used works rather well, we will see why in §4.4.8.

2.12 Stability and balance, two different concepts

The problem can be made more complex (fig. 19) by equipping the flat plate with a cambered airfoil with a non-zero moment, which amounts to studying a straight flying wing.

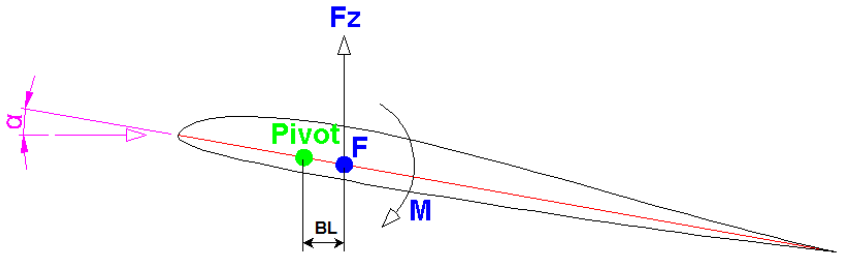

Fig. 19

Observation shows that, compared to a flat plate, the behavior remains unchanged from a stability standpoint, with lift always applied at 25% of the chord. Only the angle of attack changes, at which the airfoil naturally positions itself (that is, in the absence of pilot input or external disturbance): from zero for a flat airfoil, it takes on a certain value that depends on the airfoil's shape. This angle of attack is the one at which the lift moment balances the airfoil moment, and is calculated by expressing the equilibrium of moments around the pivot axis.

According to the relationship seen in §2.9, the equilibrium around the CG (with BL = lever arm between the neutral point F and the pivot axis, p the airfoil) is written:

$$M_{avion} = M_p - Fz.BL = 0$$

Therefore, expanding (with C = chord and Cm = overall moment of the aircraft) :

$$\frac{1}{2}.\rho.S.C.Cm.V^2 = \frac{1}{2}.\rho.S.C.Cm_p.V^2 - \frac{1}{2}.\rho.S.0{,}11.(\alpha - \alpha 0).V^2.BL = 0$$

Therefore, simplifying by 1/2ρV²:

$$C.Cm = C.Cm_p - 0{,}11.(\alpha - \alpha 0).BL = 0$$

Consider the following equilibrium equation:

$$\alpha = 9{,}1.\frac{C}{BL}.Cm_p + \alpha 0 \qquad (\text{Or : } Cz = \frac{C.Cm_p}{BL})$$

And its derivative, describing stability:

$$\frac{dCm}{d\alpha} = -0{,}11.\frac{BL}{C} \qquad (\text{Or : } \frac{dCm}{dCz} = -\frac{BL}{C})$$

These equations, which characterize the equilibrium and longitudinal stability of a flying wing, are highly instructive:

- For flight to be stable, the lift moment must increase inversely with the angle of attack (dCm/dα or dCm/dCl < 0), so as to counteract the change in angle of attack. The only necessary and sufficient condition to satisfy this requirement is that BL be positive. As we will see later, the term BL/C is in fact the aircraft's static margin, that is, its stability rate. If further confirmation were needed, the airfoil therefore has no influence on flight stability.
- By noting that, in the stability equation, the term 0.11 is in fact dCl/dα, the principle of stability becomes evident: when the angle of attack increases, Cl increases, generating (if BL > 0) a restoring moment opposing the variation in angle of attack, a moment that is therefore identical regardless of the airfoil.
- However, the airfoil has a predominant influence on the equilibrium angle of attack: the lift coefficient (Cl) of flight (= 0.11(α-α0)) can only be positive if the lift coefficient (Cm) is positive, which is therefore the key characteristic of a flying wing airfoil. The term "self-stabilizing" for such an airfoil is consequently inappropriate because of the ambiguity it creates regarding the concept of stability; referring to a "self-balancing" airfoil would be much more suitable.
- If we introduce the fact that Cm_p is strongly modified by the deflection of the trailing edge control (aileron), then the piloting of a flying wing becomes obvious to understand, since the equilibrium equation shows that the angle of attack α of the airfoil is linearly a function of Cm_p, itself controlled by the elevator or aileron control (or trim).

NOTE
Therefore, be careful not to confuse stability and equilibrium: stability is the ability to naturally return to a state of equilibrium, where all forces or moments cancel each other out. To fly, an aircraft must therefore be both stable and balanced, which in practical terms means being "well centered" and "well trimmed," the latter concept referring to the adjustment of the elevator trim and/or the angle of attack of the horizontal tail relative to the wing.

2.13 Complete aircraft

Having grasped the principle of the center of pressure, and then detailed it on a straight flying wing, we can begin to understand it a little better on a tailplane. As a reminder, it is the point around which a change in angle of attack (or lift) does not generate a change in overall moment (dCm/dα = 0).

The neutral point of the model is therefore determined by studying, on the complete device, the variation of the balance of moments around the center of gravity during a pitch disturbance (here in nose-up, but it works exactly the same way in nose-down… it is the famous nose-down test, precisely).

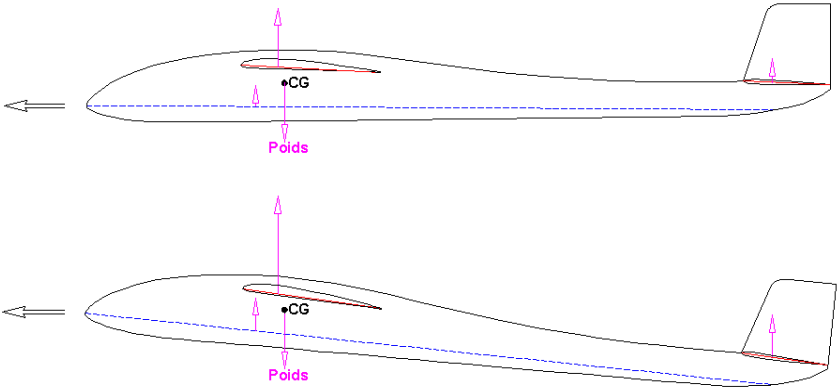

Fig. 20, evolution of the different lift forces during a pitch-up increment from an equilibrium situation

The lift forces of the wing, horizontal tail, and fuselage increase proportionally to the angle of attack, each in a different way depending on the respective efficiency of the element considered (a concept detailed below). Since the resulting moments are the products of the lift forces and the distances between their respective points of application (foci) and the center of gravity, the result of a change in angle of attack can be qualitatively determined by simple logic:

- In simple terms: all focal points located in front of the center of gravity (CG) produce a destabilizing moment that tends to amplify the change in angle of

attack, while focal points behind the CG produce a stabilizing moment that opposes it. In this example, the fuselage and wing are therefore destabilizing, while the horizontal tail is aptly named.

- If the center of gravity (CG) is positioned towards the front of the aircraft, for example directly above the wing's apex: the wing's apex lever arm is zero, the fuselage apex lever arm is very small, while the horizontal tail's lever arm is significant. The overall moment resulting from the increase in angle of attack is then nose-down and opposes the change in angle of attack. The aircraft therefore tends to return to its initial trajectory and is stable.
- If the center of gravity (CG) is positioned towards the rear of the aircraft, for example, directly over the wing's trailing edge, the leverage arms of the wing and fuselage apexes are significant, while that of the horizontal tail apex is reduced. The overall moment, resulting from the increased angle of attack, is nose-up and amplifies the change in angle of attack, making the aircraft unstable.
- Between these two positions giving opposite behaviors in terms of stability, there is therefore inevitably a position giving a neutral behavior, that is to say without variation of global moment after the variation of angle of attack: this is the neutral point of the device.

The wing airfoil moment, given by its moment coefficient Cm0, is not shown. As seen above, since it is a constant when the airfoil is functioning correctly, it does not vary with the angle of attack and therefore does not contribute to the righting moment. In balanced flight, the airfoil moment is simply compensated statically by a lift correction (and therefore angle of attack) of the horizontal tail (we will see this in the adjustments chapter).

This confirms that the airfoil does not play a role in the centering problem, a result which would not have been trivial to understand by using the concept of the center of pressure instead of that of the neutral point, even though these are two strictly equivalent models.

Approached formally, this problem is paradoxically easier to grasp, regardless of the concept used, whether it be the center of pressure or the center of buoyancy (which only adds a step to the reasoning). Here is a simplified demonstration of the wing + horizontal tail center of pressure (the fuselage will be addressed later) using the center of buoyancy (CP).

To do this, let's write the equation for the equilibrium of moments around the CG:

$$M_{aile} + M_{stab} = 0$$

In other words, expanding on this:

$$\frac{1}{2}.\rho.V^2.S_a.Cz_a.(xCP_a - xCG).C_a + \frac{1}{2}.\rho.V^2.S_s Cz_s.BL_s = 0$$

With :

BLs the longitudinal lever arm of the horizontal tail.
That's the wing chord (rectangular for this simplified example).
XCp and xCG are the positions of CP and CG, as a percentage of the chord.

Since the position of the center of pressure on the wing's mean chord is:

$$xCP_a = 25\% - \frac{Cm0}{Cz_a}$$

We obtain the equation defining the equilibrium around the CG, by simplifying by 1/2ρV²:

$$S_a.Cz_a.(25\% - xCG).C_a - S_a.Cm0.C_a + S_s.Cz_s.BL_s = 0$$

This expression could have been found more directly by using the concepts of lift at the center of pressure and airfoil moment. It can be noted that it allows us to determine the horizontal tail lift coefficient (Cl), and therefore its setting (provided the wake deflection angle is known, see §2.14.3) to achieve equilibrium at the considered wing lift coefficient. It is also observed that the horizontal tail setting depends on the airfoil's center of gravity (Cm0) and the center of gravity.

Let's replace the center of gravity with the neutral point and differentiate the equilibrium equation with respect to the angle of attack, so as to describe the neutrality condition:

$$(25\% - xF).S_a.C_a.dCz_a/d\alpha + S_s.BL_s.dCz_s/d\alpha = 0$$

From this, we can deduce the position of the center of gravity of the wing + horizontal tail assembly, as a percentage of the mean chord of the wing:

$$xF = 25\% + \frac{S_s.BL_s}{S_a.C_a}.\frac{dCz_s}{dCz_a}$$

This expression comprises three distinct terms:

- The position of the wing's focal point: 25%.
- The stab volume (see § 4.4.3), negative in the case of a duck.
- The lift efficiency of the horizontal tail relative to that of the wing (see below).

Using the concept of center of pressure does not change the fact that the position of the CG is purely geometric and does not depend on the wing airfoil. For the sake of intellectual honesty, it should be emphasized that the term BLs is not exactly the same depending on whether one considers the aerodynamic center or the CG; this will be discussed in detail later.

NOTE

- The formalism developed in §2.12 for the flying wing applies strictly to the complete aircraft and its center of gravity. We then find an overall lift (composed primarily of the lift of the wings and the horizontal tail) applied to the overall center of gravity and an overall moment (composed of the wing and fuselage moments, plus the lift moment of the horizontal tail). The advantage of this formalism, which is found in many flight mechanics textbooks, is that it explains stability and equilibrium very intuitively, while being applicable to any aircraft regardless of its aerodynamic configuration. The disadvantage, and this is why it has not been discussed above, is that its use requires a thorough understanding of the distinction between the wing center of gravity and the aircraft center of gravity. Moreover, it encompasses within a single force and a single moment the functions of the wing, the horizontal tail and the fuselage, functions which it is wise to study individually both from the point of view of understanding the aerodynamic phenomena involved and from the point of view of their modeling.
- From the equilibrium of longitudinal moments, we can deduce that the elevator control influences the aircraft's pitch angle of attack via its overall center of mass (Cm), starting from a zero value in level flight (equilibrium: $\Sigma Cm = 0$). If the model is slowed down by pulling back on the elevator, simply releasing the control stick allows the model to regain a certain airspeed (a phenomenon more easily identified in gliders), which is therefore its equilibrium airspeed (also called the "natural airspeed"), corresponding to the equilibrium angle of attack. This is also true, of course, in the opposite direction; this is the well-known dive test, which we will detail later.
- As explained in the first point of this note, this principle applies to the particular case of a flying wing: the control stick and the elevator trim act on the moment of the airfoil which, at equilibrium, exactly compensates for the moment of the lift force around the CG.
- Similarly, the link between center of gravity and trim becomes easy to understand: changing the center of gravity alters the lever arms of the lifting elements (wing, horizontal tail, fuselage) relative to the CG, thus requiring an adjustment of the lift of one of these elements to balance the moments. Here again, the pitch control surface plays this role: moving the center of gravity forward requires a pitch correction, while moving it backward requires a pitch correction. Contrary to appearances, adding more weight to the front of a model does not require a pitch correction because this additional mass needs to be compensated for, but because the shift in the CG has altered the lever arms of the various lifting elements. The difference is subtle since the result is the same, but the underlying logic is radically different.
- The heavy feel at the elevator due to an excessively forward center of gravity is quite naturally explained: such a CG gives high stability, which strongly opposes any change of attack around the equilibrium position, including pilot commands.
- In the case of a canard (see photo below), the horizontal tail is a misnomer, since, being located in front of the wing, it actually destabilizes. The same applies to the fuselage, hence the very forward position of the center of

gravity on this type of aircraft, often in front of the leading edge of the wing's mean chord.

- If the center of gravity (CG) is vertically far from the wing, the point of application of the wing's lift shifts horizontally relative to the CG during a change in angle of attack, which mechanically contributes to stability. This effect, even in the case of a parasol wing except in extreme cases, is generally negligible.

The center of gravity (CG) position of these two models (photos by Patrice Pons and Christophe Rocourt) is radically different, while the wings and airfoil are relatively similar. This raises questions about the principle of CG positioning.

2.14 Lifting efficiency

Let us now turn to the concept of lift efficiency of a wing, which quantifies the ratio between the lift coefficient of the wing and that of the airfoil.

A wing is therefore considered less efficient the more it requires, for a given surface area, a significant angle of attack to provide a given lift. This efficiency depends primarily on the aspect ratio but also, in the case of the horizontal tail, on the wing's wake deflection, and cannot by its very nature be greater than that of the airfoil alone (also known as an "infinite aspect ratio wing").

2.14.1 Effect of aspect ratio

The airflow from the lower surface (intrados) to the upper surface (extrados) at the wingtip effectively reduces lift at the wingtip (wing or horizontal tail, it's exactly the same thing). In the case of a low-aspect-ratio wing, the entire lift along the wing is affected (Fig. 21), with a very clear break at the fuselage (which is therefore considered separately from the wings and acts as a partition between them). We will see this in detail later (§ 4.2.3 and § 5.6).

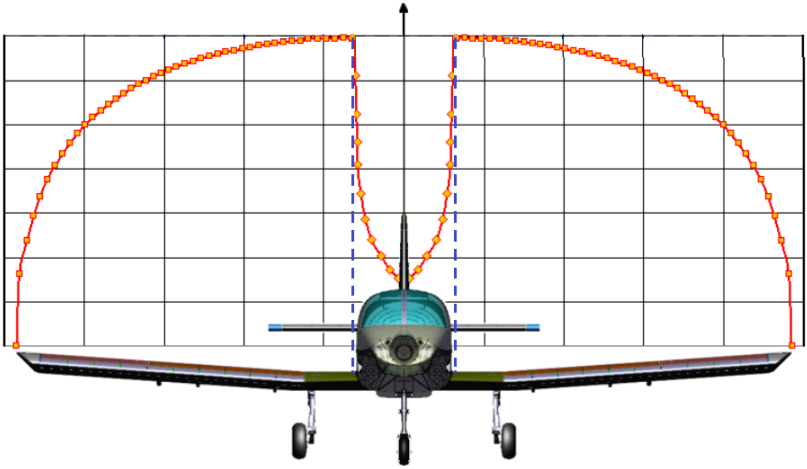

Fig. 21, lift distribution along a wing (illustration by Ivan A. Kostic).

Consequently, for a given angle of attack, the average lift coefficient of the wing (denoted Cl) will always be lower than that of the airfoil alone (denoted Clp for convenience), and this is all the more true when the aspect ratio is low.
This is described by the Prandtl correlation, valid for a lift distribution close to elliptical and for a not too small aspect ratio:

$$Cz = \frac{\lambda}{2+\lambda}.Cz_p$$

For the rest of this text, we will denote A (plus the suffixes a = wing and s = horizontal tail) as the lift efficiency of a wing:

$$A_a = \frac{\lambda_a}{2+\lambda_a} \text{ And } A_s = \frac{\lambda_s}{2+\lambda_s}$$

The proportionality between the lift coefficient (Cl) of a wing *x* and its angle of attack is therefore no longer simply 0.11, but rather:

$$\frac{dCz}{d\alpha} = 0{,}11.A_x$$

With: dα a small variation in angle of attack and dCl the corresponding variation in Cl.

The wing's lift-generating efficiency is therefore less effective the lower its aspect ratio. Conversely, the wing's efficiency approaches that of the airfoil as the aspect ratio increases. In some publications, Clp is even denoted Cl ∝(Cl at infinite wing aspect ratio).

By introducing the relationship between Cl and angle of attack (see §2.3), it is also possible to calculate the angle of attack required to obtain a given wing Cl:

$$\alpha = 9{,}1.\frac{Cz_a}{A_a} + \alpha 0$$

This equation can then be developed into a form frequently encountered in aerodynamic literature (although it is neither very intuitive nor very practical to use):

$$\alpha = 9{,}1.Cz_a + 18{,}2.\frac{Cz_a}{\lambda_a} + \alpha 0$$

The three terms of this sum are respectively identified as follows:

- angle of attack of wing section (or infinite aspect ratio wing angle of attack)
- induced angle of attack (to be added to compensate for the effect of the aspect ratio)
- zero lift angle of attack of the airfoil

2.14.2 Sweep effect

The greater the sweep, the more it tends to deflect the airflow towards the wingtip. The actual airfoil seen by the flow is then inclined relative to the direction of flight, which reduces the effective angle of attack (projected from the local angle of attack onto the forward plane) and therefore affects lift efficiency accordingly.

This effect is described by the Helmbold-Polhamus correlation (also called the "DATCOM formula"), an extension of Prandtl's:

$$A = \frac{\lambda . \eta}{\sqrt{\lambda^2 / \cos^2(\Lambda_{c/2}) + 4.\eta^2} + 2.\eta}$$

With :

Average angular deflection of the half-chords (°): $\Lambda_{c/2}$

Correction of the lift-airfoil/angle of attack relationship (/ 0.11): $\eta \approx 0.95$

In the general case (device with zero to moderate sag), this effect is of the second order and we will therefore neglect it in the rest of this work.

2.14.3 Wing wake effect

This is simply the descending layer of air generated by the wing (Fig. 22), whose angle (denoted as the deflection angle: αdfl or ε) changes proportionally to the wing's angle of attack. This angle is not the same everywhere: it is greatest at the wing's trailing edge and decreases the further it is measured from the wing, both horizontally and vertically. When the aircraft's angle of attack changes, the wing's deflection changes accordingly, thus reducing the actual angle of attack of the horizontal tail operating within this deflected layer of air (canard-type aircraft are therefore not affected): the lift of the horizontal tail working in the wing's wake therefore changes less rapidly than that of the wing itself.
In other words, the closer a horizontal tail is (axially and vertically) to the wing, the less effective it is, which is cumulative with the effectiveness related to aspect ratio.

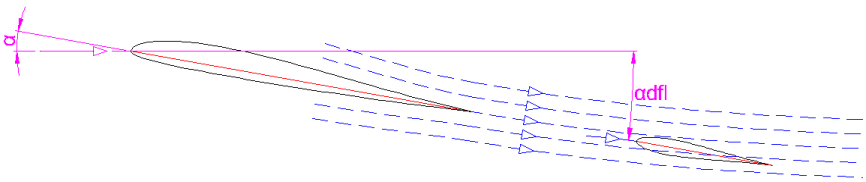

Fig. 22

The local deflection angle is calculated as follows:

$$\alpha_{dfl} = \varepsilon'.(\alpha - \alpha 0) = \varepsilon'.9{,}1.\frac{Cz_a}{A_a}$$

ε' being the local deflection coefficient, calculated using the Munk or Toussaint formulas (improved in the context of this dossier) which we will see later (cf. 4.6.1).

As, when the angle of attack of the model changes, the change in the lift of the horizontal tail can be written as:

$$dCz_s = 0{,}11.A_s.(d\alpha - d\alpha_{dfl})$$

From this, we deduce the proportionality between the lift coefficient (Cl) of the horizontal tail and the angle of attack of the model :

$$\frac{dCz_s}{d\alpha} = 0{,}11.A_s.(1-\varepsilon')$$

NOTE
It is important to distinguish between the wing's wake, in the overall sense as described here, and the direct wake, that is, the thin layer of turbulent air downstream of the wing's trailing edge, whose influence is negligible at normal flight speeds. This confusion can often lead people to believe that a T-horizontal tail is an optimal aerodynamic solution because it is free from any influence from the wing, which is doubly false: firstly, the overall deflection of the air by the wing extends well beyond its direct wake, both vertically and downstream of the wing; secondly, there is always an angle of attack at which the horizontal tail will pass through this thin turbulent layer (see §4.4.6).

2.14.4 Effect of structural flexibility

Although no mechanical structure is infinitely rigid, this effect is generally totally negligible in the context of a normally carried out construction.

However, there are two potential issues to be aware of: the flexural flexibility of the tail boom (made with an insufficient cross-section and/or a material that is too flexible, typically foam or a material similar to fishing rod material), and the torsional rigidity of the wings (very thin airfoil and/or overly lightweight construction). These two factors will affect the lift efficiency of the horizontal tail [relative to that of the wing], with potentially detrimental effects on balance and flight stability (see note in §4.6.1).

2.15 A quick word about the performance

An aircraft's performance is primarily measured in terms of sink rate (engine off) and glide ratio, both of which vary with speed (Vx). Both are directly derived from drag.

- **Sink rate (Vz)** : vertical speed at which the aircraft descends with the engine off. The minimum is found at a low airspeed, with the sink rate then increasing significantly with airspeed. The sink rate is directly related to the aircraft's drag and wing loading.
  One noteworthy point: the sink rate is a scale-independent concept. The order of magnitude of a minimum sink rate is approximately 0.5 m/s for a good thermalling glider, micro or full size, to 1.5 m/s or even much more for an average airplane; these guidelines are valid regardless of the aircraft's size.

- **Glide ratio (f)** : This quantifies the distance covered in a glide (in neutral air with the engine off) per unit of altitude. For example, a glider with a glide ratio of 20 will therefore cover 20 meters for every 1 meter of descent. The glide ratio is the best indicator of the aerodynamic efficiency of an aircraft, powered or unpowered, and can be assessed at any speed and angle of attack (level flight, tight turn, etc.). In level flight, the glide ratio is highest at a speed slightly above the minimum sink rate and decreases as the speed increases. Mathematically, the glide ratio is the lift-to-drag ratio (Fz/Fx), which is equivalent to Cl/Cd or Vx/Vz.
  The lift-to-drag ratio and maximum lift-to-drag speed evolve inversely with the wing loading: the higher the latter, the greater the sink rate of the aircraft, but the faster it flies, which ultimately benefits the lift-to-drag ratio because the gain in speed is proportionally greater than the increase in sink rate thanks to the better Reynolds number of the airfoil.
  Also due to the Reynolds number, the lift-to-drag ratio is particularly scale-dependent; achieving a good lift-to-drag ratio becomes increasingly difficult as the model gets smaller. The orders of magnitude for maximum lift-to-drag ratios are approximately 10 to 25 for gliders from 1 to 5 meters in diameter, and 5 to 10 for airplanes ranging from half-A class to small and large.

- **Aerodynamic power dissipated by the aircraft (Pw)** : this corresponds exactly to the change in potential energy during gliding in neutral air. In level flight, its calculation is therefore the product of the gravitational force (weight, in newtons) and the rate of descent ($Pw = mgVz$, where m = mass of the aircraft, g = acceleration due to gravity = 9.81 m/s^2). Like the lift-to-drag ratio, which is also related to the rate of descent, it varies with speed. For a given airspeed, the higher the corresponding rate of descent, the more engine power (or lift or slope effect for a glider) is required to compensate for it and thus maintain the aircraft at a constant altitude. Knowing the propulsive efficiency of an engine (propeller efficiency * engine efficiency) at the given

airspeed, the aerodynamic power allows us to directly determine the engine power required to achieve a given airspeed.

2.16 Summary of fundamental principles

- The laws of solid mechanics and aerodynamics are the same for all aircraft: a flying wing or a canard flies and is controlled in the same way as a normal airplane, regardless of scale.
- An aircraft flies because it has a source of energy (mechanical, potential, aerological) to move forward; this movement generates lift (through angle of attack and speed) and drag. Lift balances weight, while drag opposes movement and dissipates energy.
- An aircraft is a whole, not just a airfoil or a wing.
- The fuselage and horizontal tail are not neutral elements; they can also be load-bearing or load-bearing depending on the phase of flight.
- The wing airfoil, as well as the fuselage or horizontal tail airfoil, helps to limit drag and delay stalling, but does not affect lift, which is a purely mechanical consequence of the aircraft's mass and the current flight conditions.
- Wing aspect ratio is a very important element of aircraft performance.
- The airfoils mainly determine the flight qualities, the angle of attack and stall speed as well as the balance of longitudinal moments which, in order to maintain level flight (sum of moments = 0), is achieved via the stab setting and refined by the elevator trim.
- The aerodynamic center of gravity of an aerodynamic component is a fixed point, independent of flight conditions or airfoil shape, where the moment does not depend on the angle of attack. It is located at 25% of the chord for an airfoil, 25% of the mean chord for a wing, and at a value that depends primarily on the horizontal tail volume for a complete aircraft.
- Flight stability and therefore center of gravity do not depend on the airfoil(s) but solely on the overall geometry of the aircraft: the aircraft is a simple weather vane evolving in its relative wind.

3. Tools and reference documents

This initial introduction to the mechanics of flight was intended to familiarize you with the essentials of a designer's approach, which must first and foremost involve understanding the concepts they are working with. Unfortunately, my perfectionist side has noticed that modern humans have a regrettable tendency to focus on manipulating the tool and the final result rather than on the process itself. Yet, tools are useless without technical perspective and a bit of critical thinking, and can lead to absurdities.

Once this necessary perspective has been gained, using a tool is, of course, invaluable for saving time and getting to the heart of the matter. No one wants to go back to the abacus or slide rule, except perhaps for the intellectual pleasure of it. Certain tools may also prove useful (but not essential) to support this project.

3.1 A little reading

Reference books (paper):

- Mechanics of Flight, by Warren F. Phillips
- Fluid Dynamic Lift & Drag, by Sighard F. Hoener
- Theory of Wing Sections, by Ira H. Abbott
- Theory of Flight, by Richard Von Mises
- Introduction to Flight, by John Anderson
- Experimental Aerodynamics, by Pierre Rebuffet
- Aircraft Aerodynamics, by Jean Chaffois

Paper books for model makers:

- Model Aircraft Aerodynamics, by Martin Simons
- Airflow and Model Flight, by Martin Simons
- RCM Special Aerodynamics, by Serge Barth (1989)
- Aerodynamics, by Jean Champenois (1992)

On the Internet:

- Author's website: http://www.rcaerolab.eu
- Inter Action: http://inter.action.free.fr
- See how it flies: http://www.av8n.com
- Popular science works by Jean-Pierre Petit:
  http://www.savoir-sans-frontieres.com/JPP/telechargeables/Francais/ASPIRISOUFFLE.pdf
  http://www.savoir-sans-frontieres.com/JPP/telechargeables/Francais/mecavol/mecavol.pdf
- The Encyclopedia for the Budding Aerodynamicist, by Raphaël Gougnot:
  http://aerodynamique.chez.com
- Aerodynamics for Students:
  https://aerospace101.com/introduction/index.html
- Princeton University, reading slides for Aircraft Flight Dynamics:

http://www.princeton.edu/~stengel/MAE331Lectures.html

Some technical publications:

- Thin airfoil theory:
  http://fr.wikipedia.org/wiki/Théorie_des_profils_minces
- Longitudinal stability and center of gravity of an aircraft:
- https://fr.wikipedia.org/wiki/Stabilité_longitudinale_(aviation)
- NACA/NASA Archives:
  http://ntrs.nasa.gov/search.jsp
- NACA Archives:
  http://naca.central.cranfield.ac.uk
  https://howfliesthealbatross.com/Lift and Drag Review and Renew - Correlations of 50 Years of NACA and NASA Test Data on the Effects of Wing Planform and Thickness.pdf
- Introduction to aerodynamics of flight, NASA:
  http://ntrs.nasa.gov/archive/nasa/casi.ntrs.nasa.gov/19760003955.pdf
- Technical files by Olivier Caldara:
  http://bio-air-technologies.com/dossiers_techniques/Dossier_general.html
- Centering, stability and balance :
  http://pierre.rondel.free.fr/images2/tp_centrage/index.htm
  http://pierre.rondel.free.fr/images2/centrage_article/Centrage_2.htm
  http://adg.stanford.edu/aa241/stability/staticstability.html
  http://pierre.rondel.free.fr/Centrage_equilibrage_stabilite.pdf
  http://formation.ffvv.org/files/2009/06/chargement-et-centrage-du-planeur.pdf
  http://pouduciel.free.fr/trucs&astuces/stabilite-balligand.html
  http://www.aeroclub-versailles.com/doctech/Notices-Techniques /007 /41 /46 /48
- Study of the longitudinal V-shape:
  http://pierre.rondel.free.fr/images2/Volet2ndPart/ETUDE DU V 2.pdf
- Flap optimization:
  http://pierre.rondel.free.fr/images2/volets/volets.htm
  http://pierre.rondel.free.fr/images2/Volet2ndPart/volet2_bis.htm
  http://pierre.rondel.free.fr/images2/snapFlapPart3/SnapPart3.htm
- Tailplane stories:
  http://pierre.rondel.free.fr/images3/empennages
  http://pierre.rondel.free.fr/images4/HistoireDeStab
- Matthieu Scherrer's website:
  http://scherrer.pagesperso-orange.fr/matthieu/modeli.html
- Flight F3F (JL. Foucher):
  http://www.f3f-france.com/images/stories/Fichiers/PDF/f3fmecaniquedevol.pdf
- Electric motorization:
  http://web.mit.edu/drela/Public/web/qprop/motor1_theory.pdf
  http://web.mit.edu/drela/Public/web/qprop/motor2_theory.pdf
  http://web.mit.edu/drela/Public/web/qprop/motorprop.pdf

3.2 Some tools

Here is a small selection of mostly free software:

- Digital wind tunnels: these tools allow you to simulate airflow around an airfoil to deduce its characteristics. We can distinguish between software based on the XFoil calculation code and its graphical interface (Profili, XFLR5, PredimRC, and Gemini Aero Designer), those based on the Eppler code (JavaFoil, DesignFoil), and more specialized software like FoilWorks. The current standard is XFoil, which is generally more predictive (with some limitations) at low Reynolds numbers.
- Aerodynamic design tools: two approaches are possible, either semi-analytical (PredimRC), purely numerical (XFLR5), or a combination of both (Gemini Aero Designer). These tools are based on XFoil for airfoil analysis. The second approach allows for greater refinement in wing design, but the first offers a more comprehensive and complete approach, is simpler to use, and directly delivers optimized results (center of gravity, trim, optimal aspect ratio, etc.) without an iterative process. Gemini Aero Designer combines the best of both approaches. It's worth noting the existence of AVL software by Mark Drela, the creator of XFoil, but it is particularly difficult for beginners to use.
- Various utilities: some tools can be useful for specific needs, even if they don't replace the previously mentioned tools. Two excellent tools stand out: Mean Chord for calculating the position of the aerodynamic center (but not the center of gravity) of a wing or horizontal tail, and AirfoilConverter for deducing simple airfoil characteristics.

Download the tools from the internet:

- Airfoil: http://www.profili2.com/
- FoilWorks: http://users.skynet.be/fa496838/
- XFoil: http://web.mit.edu/drela/Public/web/XFoil/
- JavaFoil: http://www.mh-aerotools.de/airfoils/javafoil.htm
- XFLR5: http://www.xflr5.com
- AVL: http://web.mit.edu/drela/Public/web/avl/
- PredimRC: https://www.rcaerolab.eu/predimrc
- Gemini Aero Designer : https://www.geminiaerotools.com
- Average chord: http://tracfoil.free.fr/cm/index.html
- ProfilKonverter: http://members.aon.at/p-51/download/profkonv.zip
- PropCalc: http://www.drivecalc.de/PropCalc/
- JavaProp: http://www.mh-aerotools.de/airfoils/jp_applet.htm
- Airfoil database:
  http://tracfoil.free.fr/airfoils/ http://www.ae.uiuc.edu/m-selig/ads.html
- Calculation of the mechanical resistance of the longerons, skins and wing spars:
  http://voiletech.free.fr/Modelismeplaneur/calcul_longeron.htm

Magnificent and poetic 9Decker by Rainer Lange (photo Laurent Berlivet).

4. Analysis Methodology

4.1 Identify the need

Now we're getting to the heart of the matter. First and foremost, we need to define, at a minimum, the expected result through a specifications document. Don't worry, it won't be very complex, but it's essential for what follows.

Once the subject has been chosen (model, free creation, model intended for a specific competition category, etc.), the specifications must be used to characterize it via the following elements:

- Model scale: we will only need to determine the wingspan and fuselage length.
- Drafting a first sketch: the simplest approach is to create it on an A4 sheet of paper, ideally gridded or millimeter-marked. There's no need to spend too much time on it for now; two simplified views (top and side) will suffice. The important thing is to choose an appropriate scale (1/ ^{5th} , 1/ ^{10th} , etc.) and maintain it across all views to easily keep track of everything (fig. 24).
- We will make an initial estimate of the model's mass (denoted m), based on personal experience or by analogy with models of similar size. Later, we will discuss wing loading, but for now, mass will suffice.
- Definition of the flight domain, based for the moment on qualitative elements: are we looking for a slow and quiet model? Or a faster model that needs to be a little acrobatic? Or a sleek glider to fly in all weather conditions? etc.

The last aspect is essential, as it determines all aerodynamic choices (wing loading, aspect ratio, airfoils, trim, engine, etc.). It is embodied by the aircraft's "design point," which is a combination (wing lift coefficient, flight speed) for which the aircraft will be perfectly adapted, or even optimal.

While flight speed is a fairly intuitive concept, although not so simple to determine a priori, the design lift coefficient (Cl) is more difficult to grasp. Two approaches are possible: either the Cl corresponding to the level flight speed for which the aircraft will be specialized (in which case the design point is reduced to the Cl alone), or the average Cl of the flight envelope (in this case, design speed and design lift coefficient are separate).

Some typical values, which will also be used for adjustments:

- High-speed flight or aerobatics: Cla = 0.1
- Typical case, including pylon racing: Cla = 0.3
- Calm flight, thermals: Cla = 0.5

To delve a little deeper into the question, Matthieu Scherrer carried out a measurement campaign of the flight domain of a glider in 2007, the main summary graph of which is shown here (fig. 23).

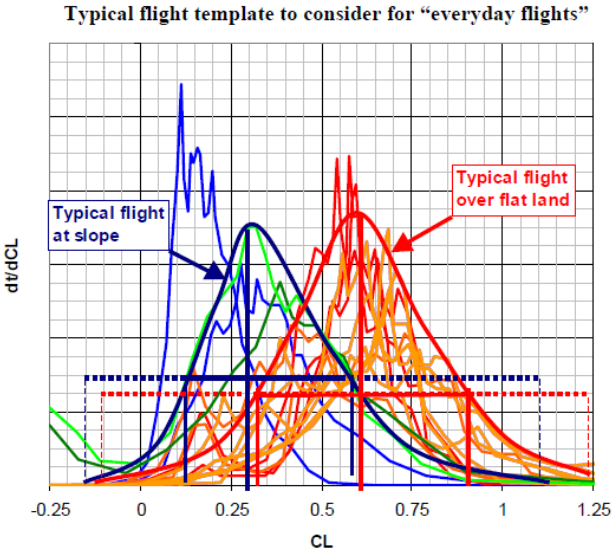

Fig. 23, Cl utilization rate of a glider

Regardless of the glider, slope soaring typically occurs at significantly lower lift coefficients (0.3) than flatland soaring (0.6). This study provides a useful starting point for optimizing a glider based on the type of flight performed, although it does not reflect all the flight conditions encountered in competition: F3F runs, F3B or F3J winch launches, F3K launches, etc. For these latter disciplines, the lift coefficient differences between two flight phases can be substantial, and determining the average lift coefficient that will yield the best overall results is crucial in the design of a competition glider.

We now have a starting point that will give us some initial dimensions (wing chords, lever arms) and the essential design point to begin the design process. These dimensions are currently estimates, even rough approximations; the designer's entire task is to adjust them to meet the various criteria that will ensure good flight characteristics.

In the case of an existing model, the main measurements recorded on a sketch will be more than enough to make a critical analysis, or simply to check the settings indicated by the manufacturer.

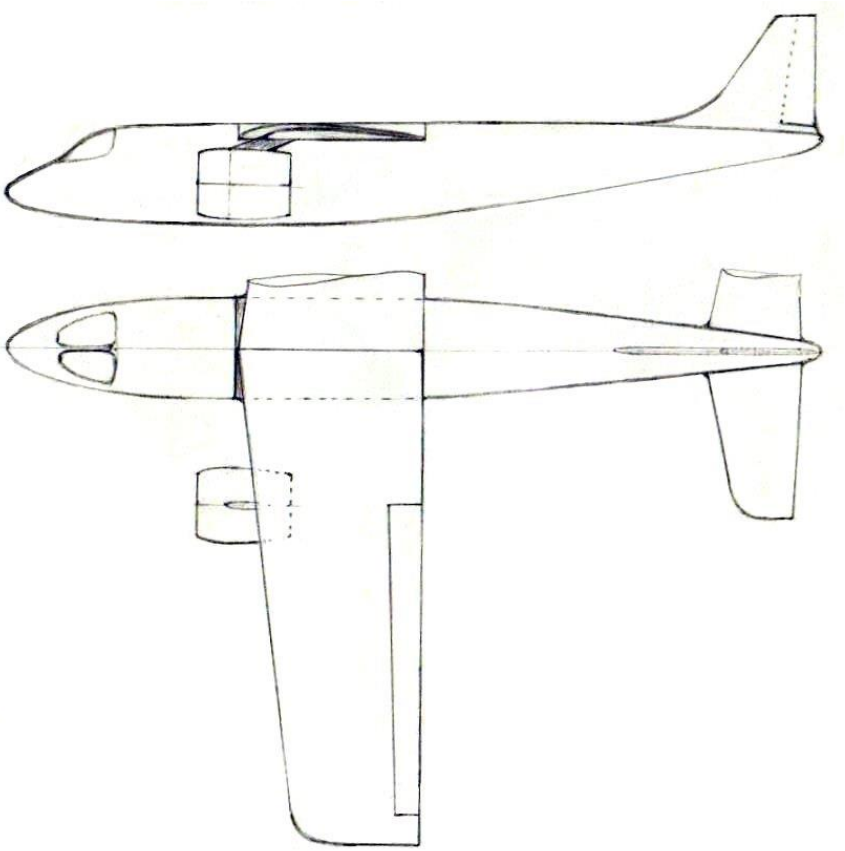

Fig. 24, author's sketch of a small twin-turbine electric liner drawn at 1/10th scale

4.2 Sizing the wing

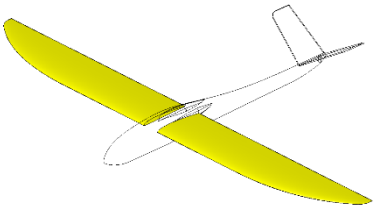

This milestone is valid regardless of the aircraft type, provided, however, that the wing is the aircraft's primary lift generator. The study of jet or tandem aircraft, whose fuselage or tail surface area is of the same order of magnitude as that of the wing, will therefore require some specific adjustments, particularly regarding wing loading.

First, we will calculate the basic characteristics of the wings, working on a single wing, assuming the aircraft is symmetrical about the vertical plane: the surface area, the aspect ratio, and the taper (ratio of the chord at the wingtip to the chord at the wing root). These will allow us to describe the wing's behavior, to verify its suitability as needed, and possibly modify the geometry accordingly.

Two possible scenarios:

- The wing is trapezoidal: in this case, the following calculations will be applied directly.
- The wing has a more complex shape: you can either use a tool (see §3.2) such as Mean Chord, or directly PredimRC (which will also perform all the other calculations mentioned here and much more), or simplify the wing into a single trapezoid (fig. 25). With a little care, this approximation gives very good results, so we will use it for its educational value in the context of this project. To do this, we will replace the leading edge and trailing edge each with a straight line that passes visually as best as possible (with the same surface area on both sides).

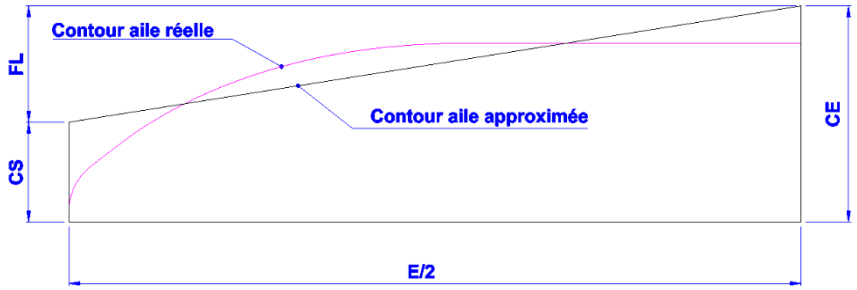

Fig. 25

4.2.1 Basic calculations on the wing

We will use the following designations and units, which are also valid for the horizontal tail (suffix "s" instead of "a"):

- Root/tip/medium chords: CE/CS/CMA (mm)
- Leading edge deflection: FL (mm)
- Wingspan: E (mm in general, dm for aspect ratio calculation)
- Aspect ratio: λ (lambda, unitless)
- Taper: Eff (unitless)
- Area: S (dm²)
- Mass: m (g)
- Wing loading: CHa (g/dm²)

Here are the details of the first calculations, also valid for other wings such as the horizontal tail, to be carried out on the basis of this first wing sketch (pay attention to the consistency of the units).

Wing area: $S_a = (CS_a + CE_a).E_a / 2$

Wing loading: $CH_a = m / S_a$

Aspect ratio: $\lambda_a = {E_a}^2 / S_a$

Taper: $Eff_a = CS_a / CE_a$

Mean aerodynamic chord: $CMA_a = \frac{2}{3}.\frac{{CE_a}^2 + CE_a.CS_a + {CS_a}^2}{CE_a + CS_a}$

Sweep BA MAC / BA emp.: $FL_{CMA\,a} = \frac{FL_a}{3}.\frac{CE_a + 2.CS_a}{CE_a + CS_a}$

The concept of mean aerodynamic chord requires some explanation, as it is sometimes confused with the mean chord, which is incorrect. The mean chord is the chord of a rectangular wing with the same surface area as the wing being studied, and is representative of the forces acting upon it.

Mathematically, this chord is the average of the chords weighted by their elementary areas (those more mathematically inclined will recognize the definition of an integral over the span in C.dS/S):

$$CMA = \frac{2}{S}.\int_0^{E/2} C^2(y).dy$$

With: S = wing area, C(y) = chord and C(y).dy = elementary area.

The same applies to the calculation of the wing area and the position of the mean chord relative to the leading edge of the wing root, the previous equations being deduced from the application of these integrals to the case of a trapezoidal wing.

The mean chord and its position can also be determined graphically, again within the framework of a simple trapezoidal wing. Simply transfer the root chord to either side of the wingtip, and vice versa at the root, then draw the diagonals, with the mean chord finding itself at the point of intersection (fig. 26).

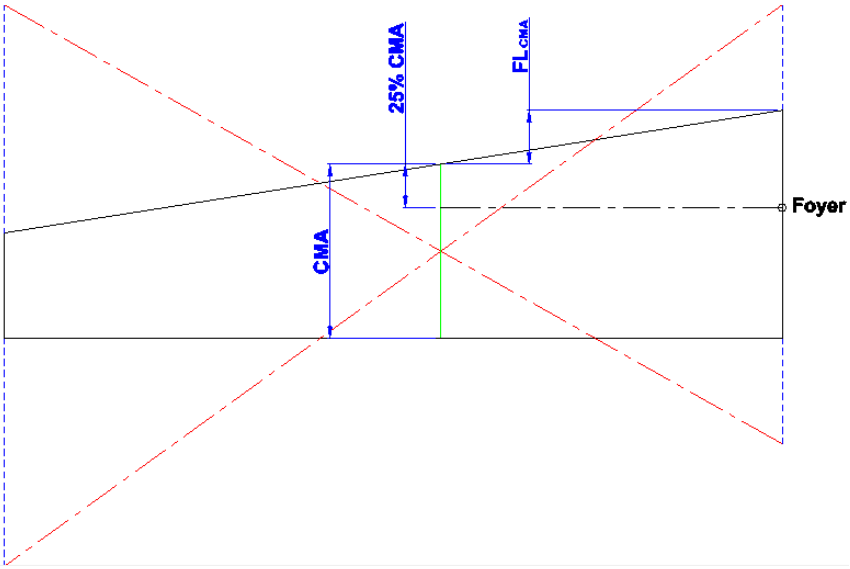

Fig. 26, neutral point and mean chord of a wing

The preceding formal calculations can be extended to a complex wing, by decomposing it into trapezoidal panels and calculating the area-weighted average of the lengths and sweeps (relative to the leading edge of the root chord) of the mean chords of these panels (p):

$$CMA = \frac{\sum CMA_p . S_p}{\sum S_p} \text{ And } FL_{CMA} = \frac{\sum FL_{CMAp} . S_p}{\sum S_p}$$

It can also be done graphically, but it is a tedious task which is of little interest - except for doing everything on paper without computer assistance - compared to dedicated software like PredimRC.

The mean chord allows us to find the wing apogee (Fa), located at 25% of this chord and which we project for convenience onto the wing root.

Distance from wing root to leading edge:

$$XF_a = FL_{CMA\,a} + 0{,}25.CMA_a$$

NOTE

- In the case of a complex wing (elliptical or multi-panel), the mean chord is generally not a physical chord of the wing.
- Do not confuse aerodynamic wingspan with actual wingspan. The latter takes the fuselage into account, while the former—the only one that concerns us here—considers only the wing (also applicable to the horizontal tail, of course) located outside the fuselage. The wing root is therefore the interface plane with the fuselage.

4.2.2 Wing loading

Wing loading is the primary indicator of a future aircraft's flight envelope, as a higher wing loading means the faster the model will perform, generally with a better glide ratio but a higher minimum sink rate. Conversely, a lower wing loading ensures smoother flight and contributes to good thermalling capabilities for gliders.

The assessment of wing loading is relative to the size of the aircraft, which conditions both the impression of speed for the pilot on the ground and the Reynolds effect (reminder: the higher it is, the better the airfoil works): a micro-model will start to be very loaded around 25 g/dm², while a VGM aerobatic aircraft will be comfortable with 100 g/dm².

To circumvent this difficulty, "Wing Cube Loading" adds a factor of 3/2 to the surface area, thus defining a rule of flight realism similarity valid at any scale, from micro-model to full-size (a scale model with the same WCL as the full-size model will have realistic flight). This factor simply reflects the fact that the surface area of an aircraft increases with the square of the scale while its mass increases with the cube. Guillaume Rouby improved this factor (renamed "Yomgui Wing Loading"), with a slightly larger coefficient (5/3) to incorporate the Reynolds number effect.

$$YWL = k.\frac{m}{S_a^{\,5/3}}$$

With :

k = 1 for an airplane and 2 for a glider or a flying wing.
m is the mass in g and S_{is} the wing area in dm².

The YWL scale ranges from about 4 for an aircraft that can move particularly slowly, such as a soaring glider or a very quiet debut aircraft, to about 25 for a

heavily loaded jet or dynamic soaring glider, passing through about 10 for a warbird or hotliner and 10 to 15 for a racer or pylon racing glider.

The target weight of the model and/or the wing area will be adjusted accordingly, depending on the requirements and the projected weight distribution. It is, of course, possible to decrease or increase these values depending on the intended use of the model and the pilot's skill level. Particularly with gliders, the weight can be increased by up to approximately 50% by adding ballast to optimize performance in rough weather. However, be mindful of the FAI limit, which normally requires that most competition models remain below 75 g/dm².

The following simple check allows us to complement this approach in a more scientific way by calculating the minimum flight speed (before stalling):

In stages, we have: $$Fz = m.g = \frac{1}{2}.\rho.S_a.Cz_a.V^2$$

Hence: $$V_{\min} = \sqrt{\frac{2.m.g}{\rho.S_a.Cz_{a\max}}}$$

With: $\rho = 1.225 kg/m^3$ (standard air density, at sea level at 15°C), V the forward speed (in m/s, to be multiplied by 3.6 to get the speed in km/h), S the wing area (in m²), m the mass of the aircraft (in kg) and g the acceleration due to gravity (approximately 9.81m/s²).
By default, a generic value (valid only for a reduced model) can be used for Cla_{max}: 0.8.

Of course, the calculation can be reversed to deduce the wing loading (= m/Sa) corresponding to a given stall speed:

$$CH_a = \frac{1}{2}.\rho.Cz_{a\max}.V_{\min}^2$$

4.2.3 Aspect ratio

Since the chosen topic allows for some flexibility, it is very interesting to optimize the wing geometry, starting with the aspect ratio (while maintaining the wing area defined above). This parameter reflects the relative size of the wingspan compared to the chords, for a given wing area.

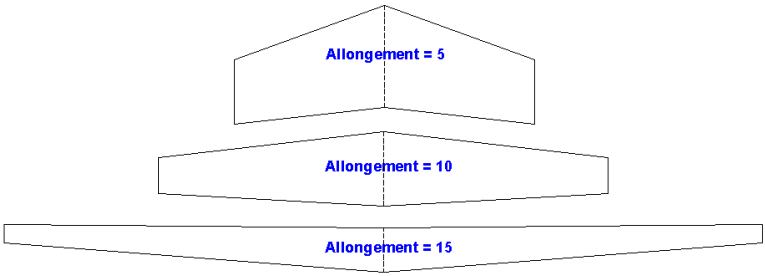

Fig. 27, wings of the same surface area but radically different aspect ratios

The aspect ratio has a very important physical meaning, due to two opposing aspects: on the one hand, the greater the aspect ratio, the smaller the wingtip is proportionally compared to the wingspan, and therefore the lower the induced drag (generated by the wingtip's wingtip vortex, Fig. 13). On the other hand, the lower the aspect ratio, the larger the chords, and therefore the less drag the airfoil will produce thanks to a higher Reynolds number (larger chord = higher Reynolds number = better airfoil performance). The choice of aspect ratio is thus closely linked to the choice of airfoil, but also to the size of the model, which influences the airfoil's aerodynamic performance (large model, large chords, etc.).

Choosing the aspect ratio therefore leads to a compromise between the airfoil drag and the induced drag. These two values change during flight depending on the lift coefficient and the speed, but in very different ways. Here is an illustration (Fig. 28), for a 30 dm² wing with an SB96 airfoil flying at a lift coefficient (Cl) of 0.5 and a speed of 10 m/s, whose aspect ratio is varied to study the evolution of the drag:

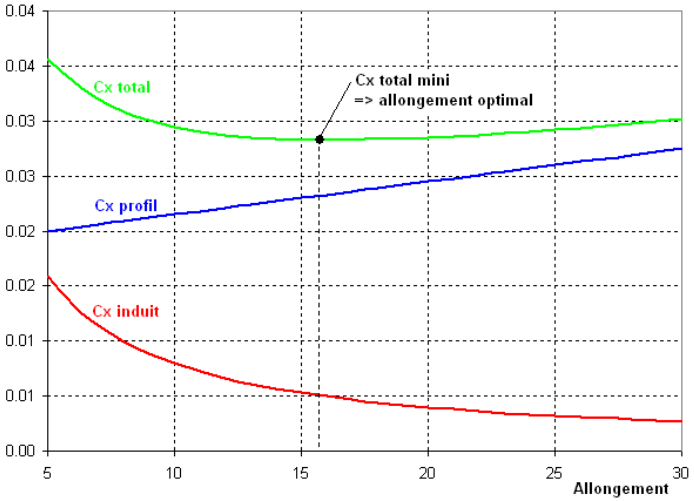

Fig. 28

In this example, the overall wing drag is minimal at an aspect ratio of 16. This aspect ratio is therefore optimal for the specific flight conditions considered (airspeed and lift coefficient) and the airfoil studied, with some leeway given that the total drag coefficient curve is relatively flat. If the calculation is repeated for different flight conditions or with a different airfoil, the corresponding optimal aspect ratio will not be the same.

Determining the aspect ratio of a wing therefore amounts to determining the flight conditions under which the wing will perform best overall. For a given airfoil, this optimal adaptation of the aspect ratio to a single, specific flight condition becomes evident when studying the lift-to-drag ratio of the wing alone. As previously discussed, the lift-to-drag ratio is calculated as the lift-to-drag ratio. In the case of a single wing, we therefore have: lift-to-drag ratio of wing alone = lift of wing / (airfoil drag + induced drag). This analysis is conducted using two complementary approaches: lift-to-drag ratio in level, stabilized flight and lift-to-drag ratio at high lift.

Firstly, the glide ratio in level flight, depending on the flight speed.

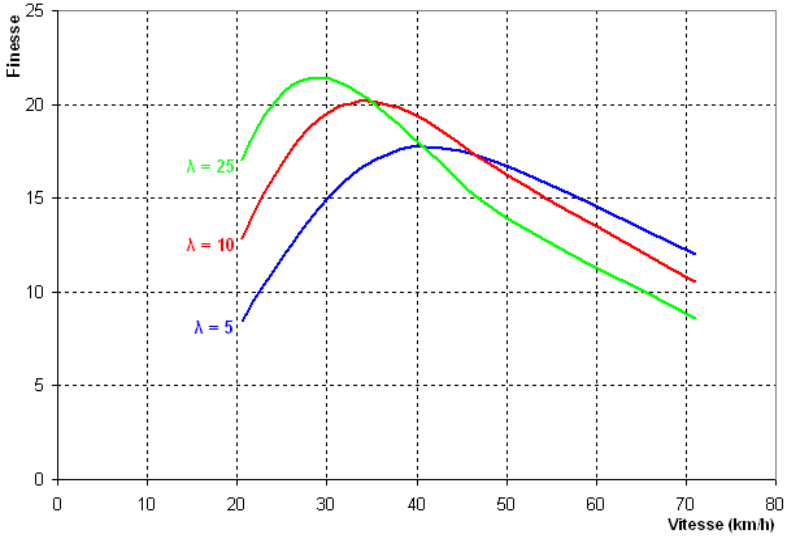

Fig. 29

An aspect ratio of 25 provides the best absolute glide ratio, while an aspect ratio of 10 is better from 35 km/h. As for an aspect ratio of 5, it becomes most efficient from 47 km/h. It can also be deduced that, depending on the flight speed considered, the best wing is not necessarily the one that provides the best absolute glide ratio; the key is that it be optimal for the chosen design point (see §4.1).

Second way of studying the question: at high constant angle of attack (tight turn or loop, here Cl = 0.8), always as a function of speed (fig. 30).

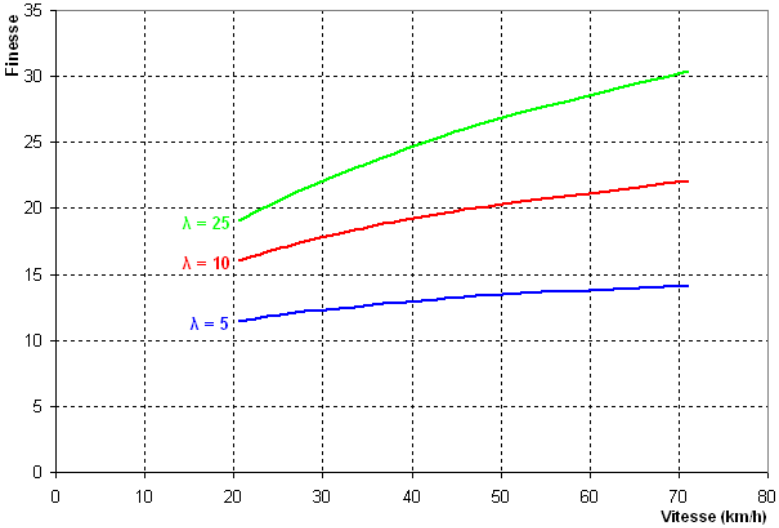

Fig. 30

Regardless of speed, a significant aspect ratio favors this maneuver thanks to good agility, while a small aspect ratio gives a serious braking effect.

In addition to all these aerodynamic considerations, there is a mechanical problem: a high aspect ratio generally requires sophisticated manufacturing techniques (composite for example) to guarantee correct strength and rigidity, whereas the compactness of a low aspect ratio wing naturally gives good mechanical characteristics even with light materials (sheeted polystyrene or balsa structure).

Consequently, a low aspect ratio will tend to be preferred when the aircraft's flight envelope doesn't require gliding or tight turning efficiency, such as in a training aircraft. The wing will be robust, the choice of airfoil will be less critical due to high Reynolds numbers, and landing will be easy for an average pilot thanks to a moderate glide ratio at high angles of attack, preventing the aircraft from overshooting the runway. Conversely, a glider will have a higher aspect ratio to minimize drag (and therefore energy loss) during low-speed phases (climbing, spiraling: seeking a low sink rate) and transition phases (seeking a high glide ratio).

In the case of competition aircraft such as pylon racers (F5D racers, F3F gliders, etc.), choosing the aspect ratio is a critical decision, as these aircraft must be as fast as possible in a straight line (low-lift phase) and as tight as possible in turns

(high-lift phase) while losing minimal speed. Therefore, unless the aspect ratio can be varied in real time (...), a compromise must be found between these two very different phases to achieve the least disadvantageous performance in each.

The reader will therefore understand that the choice of aspect ratio is by no means trivial, and is even significantly more important than the choice of airfoil. These two choices are interdependent, requiring experience and tools to be carried out successfully. In particular, PredimRC (see §3.2) includes an optimization module dedicated to aspect ratio, but this work can also be done with XFLR5, in a more laborious (iterative) but even more thorough manner.

Fortunately, since it's fairly easy to find an airfoil (see below) suitable for each scale (i.e., one that performs correctly at the relevant Reynolds numbers), the choice of airfoil can be relegated to a secondary concern at this stage. This will allow us to give a rough idea of the wing aspect ratio to use as a function of the wingspan (in meters), which, while not necessarily optimal, gives acceptable results:

- Gliders and racers: $\lambda_a = 7 + 3.E_a$
- Flying Wings: $\lambda_a = 2 + 3{,}5.E_a$
- Airplanes: $\lambda_a = 3 + 2.E_a$

In the case of Delta wings, aspect ratio, which is very low given the specialization of these aircraft for high-speed level flight, is not a very interesting criterion.

We can subtract 10 to 30% from these values for models that do not have a particular performance requirement or for aerobatic models whose lower aspect ratio than that of a conventional model increases acrobatic capabilities.

Next, we will see how to avoid ruining the efforts made on aspect ratio by a poor choice of airfoil.

NOTE
Depending on specific requirements, for example a wing area imposed by a competition category, it is also possible to start from the aspect ratio to deduce the corresponding wingspan.

A significant aspect ratio is, far more than the airfoil, the secret to the efficiency of sailing machines (NASA photo).

4.2.4 Taper

Tapering characterizes the ratio between the wingtip chord and the root chord. This somewhat simplistic concept is not at all suitable for characterizing wings with elliptical or nearly elliptical leading and/or trailing edges, nor for high aspect ratio wings, but it is perfectly adequate for working with a trapezoidal wing of reasonable aspect ratio. Tapering is an indirect way of optimizing the lift distribution of a wing, which we generally want to make as close as possible to an elliptical wing (like the famous Spitfire). The latter is characterized by maximum lift at the root, then decreasing progressively towards the wingtip. And, logically, low lift at the wingtip also means low induced drag. The gain is nevertheless limited, the induced drag of a simple rectangular wing being, depending on the aspect ratio, 10 to 20% greater than that of an equivalent elliptical wing (of the same surface area and aspect ratio).

This additional induced drag related to the wing geometry is characterized by the Oswald coefficient (denoted "e", see §4.8.2), which could be described as the planar geometry efficiency and which has a maximum value of 1 (wing with elliptical lift distribution). Its calculation principle consists of quantifying the angle of attack increment required for a wing to provide the same lift as an equivalent elliptical wing, an increment that locally induces an increase in lift coefficient (Cl), and therefore in induced drag. Like the lift and lift distributions (from which it is derived), it is calculated using numerical analysis methods, such as LLT (Lifting Line Theory, in 1.5D) and VLM (Vortex Lattice Method, in 2D), which are very well explained on the "Aerodynamics for Students" website. It is also possible to approximate it satisfactorily, as we will see in §5.6.

To put it simply, a taper ratio of approximately 0.5 to 0.6 gives good results on a single-trapeze wing (e = 0.92 to 0.96, representing 9% to 4% additional induced drag compared to an elliptical wing). Of course, even better results are possible with a multi-trapeze wing (Oswald coefficient = 0.99), thanks, for example, to PredimRC, which allows for very efficient and rapid optimization.

In the case of a taper of 0.6, the root and tip chords can be calculated directly:

$$CE_a = \frac{S_a}{0{,}8.E_a} \text{ And } CS_a = \frac{S_a}{1{,}33.E_a}$$

To illustrate the evolution of lift along the wingspan, here (Fig. 31 a and b), with the actual distribution shown in red and the ideal (i.e., elliptical) distribution shown in blue, is an example of a 60" racing glider, equipped either with a wing designed according to the simple criteria outlined here, or with an optimized wing. The difference in wing geometry efficiency is only 4% (95% versus 99%) and should give manufacturers pause, as the optimized wing presents significant manufacturing challenges, particularly regarding maintaining the airfoil airfoil and the risk of introducing undesirable twist towards the wingtip, thus negating all the

gains achieved through the geometry. Sometimes, the pursuit of perfection can be the enemy of good enough…

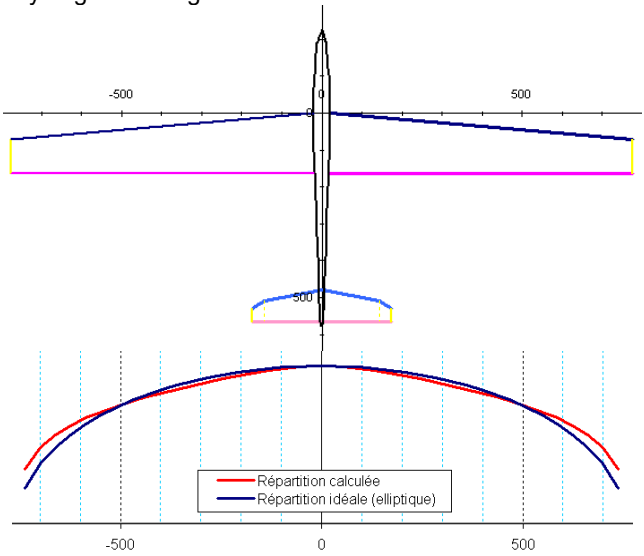

Fig. 31a, 60" racing glider with single trapezoidal wing

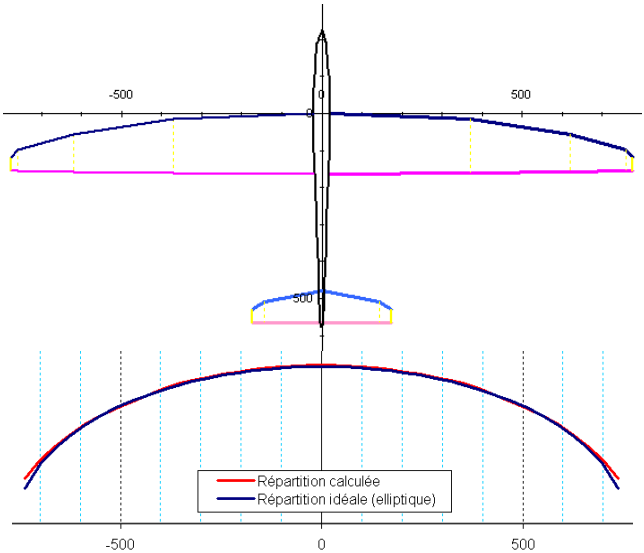

Fig. 31b, 60" racing glider with multi-trapeze wing

4.2.5 Twist

If simply reducing wingtip lift is enough to make it more like an elliptical wing, then why not introduce wing twist? Indeed, twisting a wing in the right direction reduces the local angle of attack of the airfoil (we speak of negative twist when the trailing edge rises), and therefore its lift. This is a solution that was often used a few years ago, sometimes for performance reasons, but also because it delays the stall of the wingtip in a tight spiral at low speed, a phenomenon very pronounced in lightly loaded aircraft with a high aspect ratio. But wing twist is by no means a miracle solution, because the lift distribution changes depending on the wing's angle of attack, and therefore on the speed. At high speed, and therefore low angle of attack, we can even end up with a wingtip that drifts outward, inducing significant forces in the wings and poor efficiency. Therefore, as far as possible, we will avoid any twisting, at least with a wing having a constant airfoil.

Conversely, the use of twist can prove useful in the case of an evolution of airfoil along the wing to compensate for any differences in Alpha0 between airfoils, in order to obtain the same distribution of Cl along the wingspan (see 5.6) as in the case of a constant airfoil.

Used in conjunction with sweep (see below), negative twist can also help balance the pitching moments of a flying wing with airfoil(s) having a Cm0 of zero or even slightly negative. The calculation is detailed at the end of this document.

An interesting way to manage wing twist is to "program" it according to the flight coefficient (Cl). This requires a positive sweep angle and a judiciously chosen torsional rigidity of the wing: consequently, significant lift forces in tight turns or loops induce negative wing twist, which tends to smooth out the aircraft's behavior during this phase of flight. Conversely, a negative sweep angle results in positive twist, which increases lift and makes pitch behavior more aggressive, as is the case with the Grumman X29. Caution is advised in this case, as the wing is subjected to particularly high stresses and requires rigorous structural design.

4.2.6 Wingtip

The shape of the wingtip is a frequent concern for designers in their quest for drag reduction, often inspired by the famous winglets that are flourishing in full-size aviation, primarily on airliners and some gliders. Regardless of the technique used (Dornier, winglet, elliptical, etc.), it's important to understand that optimizing the wingtip is a difficult and complex art, which can do far more harm than good, even when one believes they are acting with full knowledge of the facts. If I had to cite just two examples: makeshift solutions using tubing, whose actual gain is often inversely proportional to the conviction driving their creator, and "imitation Dornier" wingtips created by cutting off a wingtip, thus completely ruining the airfoil. This issue therefore goes well beyond the scope of this article, and the key

takeaway is that a simple straight wingtip will be far better than a pseudo-winglet, which at best will only look pretty or unusual and at worst will ruin all the drag reduction efforts made elsewhere.

That said, it is at least possible to explain how a wingtip device works: reducing induced drag (exactly as if the aspect ratio were increased), using three approaches. Either by optimizing the airflow around the wingtip to reduce the wingtip vortex, and therefore the induced drag. Or by significantly reducing the lift at the wingtip, so as to locally reduce the pressure difference and thus the airflow that creates the wingtip vortex—this is the principle behind Dornier wingtips. Or by installing a winglet, that is, a small vertical wing, which will generate counter-pressure (through a judiciously chosen airfoil and twist) opposing the wingtip flow and also providing lift with a driving component (forward, hence the specific angle of attack of a winglet airfoil).

In all cases, the major difficulty is that winglet circulation varies significantly with speed and angle of attack, making it very complex to define a winglet shape or device capable of functioning well at all flight regimes. Simply put, since a winglet improves induced drag, it is clearly useless at low lift. Furthermore, as it itself generates some drag, this becomes a disadvantage because it is no longer offset by the reduction in induced drag. For these reasons, winglets are generally not found on aircraft designed for use across a wide speed range, but rather on aircraft with a preferred flight envelope at high lift coefficients (airliners, long-range gliders).

The example (fig. 32) was carried out by the author as part of Crobe[2], and required the use of an industrial CFD-type calculation code to obtain a wingtip really optimized for a wide speed range, which also resulted in a shape of fairly simple appearance.

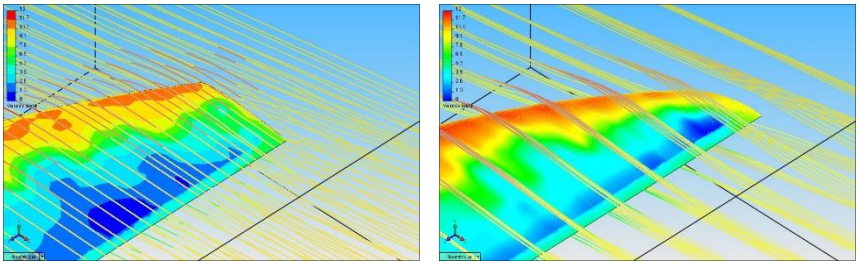

Fig. 32, CFD optimization of the Crobe wingtip (final shape on the right)

4.2.7 Sweep

Wing sweep is characterized by its average forward (negative) or aft (positive) inclination relative to the normal to forward motion. It is measured by drawing a straight line passing through the points located at 25% of the root and tip chords (fig. 33).

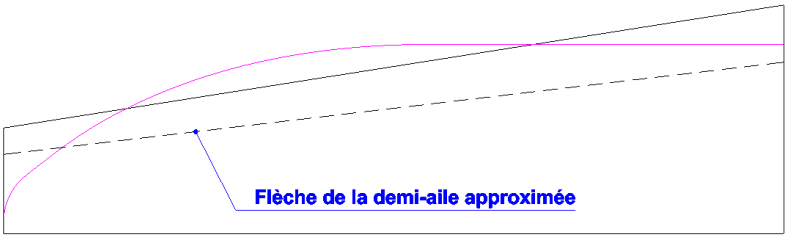

Fig. 33

In full-scale aviation, wing sweep is widely used for compressibility reasons in transonic flight, the most characteristic example being jet fighters. Since model aircraft applications are far removed from these concerns, we will focus instead on other, more traditional effects of wing sweep.

Sweep, within reasonable limits (below the maximum aerodynamic coefficient - CMA), has relatively little impact on wing lift distribution, and therefore on performance, and primarily serves to stabilize yaw. Again, there's nothing mysterious about it; it's a matter of drag. If a sideslip angle is applied in yaw, one wing half moves forward while the other moves backward. However, if the wing has a positive sweep, the advancing wing half presents a slightly larger surface area to the air than the retreating half, and will therefore create a little more drag, which tends to bring the wing back into line with the flight path. This principle is very useful on flying wings, which are inherently quite poorly stabilized in yaw (the fin is difficult to position far behind the wing, unless a fuselage is added, which is rather unfortunate). In this case, a significant sweep can be considered, on the order of 20 to 25°, which also allows the use of a negative Cm0 airfoil, provided that the balance of moments is ensured by twisting the wingtip (see §5.9: Panknin's formula). Conversely, using a reverse sweep increases maneuverability (typical example: Grumman X29, see paragraph above).

For the most common aircraft, it should be noted that the use of sweep is not critical, and a zero sweep at the control surface hinge (see below) can be used as a design criterion, generally around 66 to 75% of the chord. This approach can significantly facilitate the construction of multi-trapeze wings by aligning the panels relative to the aileron and flap hinges.

Another possibility, useful for minimizing torsional stress on wings subjected to high mechanical loads (winch-launched gliders, pylon racing gliders): adjust the sweep to align the centers of pressure of the airfoil on each wing chord and position this line perpendicular to the flight axis. The center of pressure is the point on which the lift force alone is applied, without any airfoil moment (see the very beginning of this document).

Its position on the local chord is given by the following relation:

$$xCP = 0{,}25 - \frac{Cm0}{Cz}$$

The Cm0 of the airfoil will be defined below, while the Cl to be used (by default, Cl = 0.8) is the one for which we wish to minimize the effects of torsion.

It is also possible to combine the two approaches, prioritizing mechanical resistance on the first third or half wingspan and then adjusting the sweep to align the control surface joints, or simply for aesthetic reasons.

4.2.8 Dihedral

All that remains is to discuss dihedral, which is the angle formed by the wings when viewed from the front relative to the horizontal. Dihedral has two roles: to provide stability in roll (the same principle as sweep for yaw) and to transform a yaw command (rudder) into induced roll (bank angle, as with ailerons).

Here's how it works, starting from an equilibrium configuration (fig. 34a):

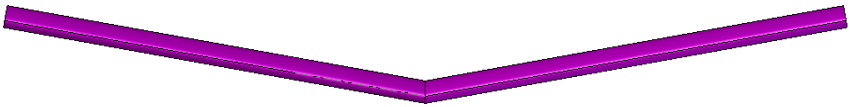

Fig. 34a

Let's apply a roll angle (fig. 34b):

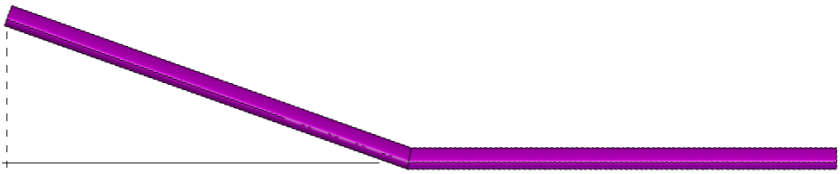

Fig. 34b

The lower wing has a larger lifting surface (horizontal projection) than the higher wing. At the same angle of attack, the former therefore generates slightly more lift than the latter, creating a restoring moment that tends to reduce the roll angle to zero.

Let's now apply a yaw skid (fig. 35):

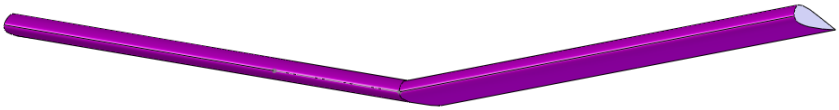

Fig. 35

Due to the dihedral angle, the apparent angle of attack (viewed along the direction of flight) is increased for the forward wing (leading edge of the apparent airfoil higher than its trailing edge) and, conversely, reduced for the aft wing (Fig. 36). The former generates more lift while the latter generates less, resulting in a roll moment in the same direction of turn as the sideslip.

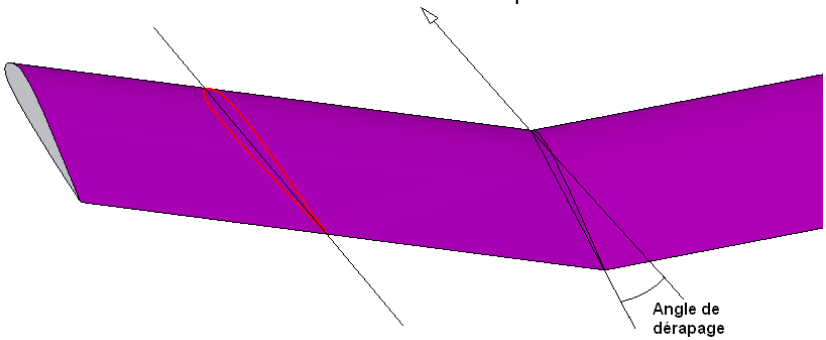

Fig. 36

This latter effect is particularly interesting for a two-axis model (rudder + elevator), lacking direct roll control (ailerons).

For other models, with ailerons, a little dihedral is useful for providing some comfort in yaw control. Dihedral is also beneficial in spirals: the inside wing in a turn has a larger effective (projected) area than the outside wing, but a lower speed, the former partially compensating for the latter and limiting the risk of stalling.

Standard values will be used, depending on the model's intended use:

- Aerobatics: 0° to 1° per wing
- High-performance 3-axis machines: 1 to 2° per wing
- Common use 3-axis, airplane and glider: 2 to 4° per wing
- Common use 3-axis, soaring glider: 3 to 6° per wing
- Common use 2 axes: 8 to 10° per wing

Ideally, the dihedral angle should be divided into three sections: a small central dihedral, then a larger dihedral at each end panel. This distribution provides even better handling and efficiency. In the case of a two-axis glider, for example, 4° to 6° could be set at the first central dihedral and 10° to 12° at the outer dihedral (always per wing half).

Note that these are only orders of magnitude; the interactions between the dihedral angle and other aerodynamic contributors, particularly the tail assembly, can lead to some unexpected results. Whenever possible, it will be advisable to allow for testing several dihedral angles (for example, using a dihedral key made of piano wire, which can be bent at different angles) to achieve the best outcome. A very common example: sluggish induced roll behavior is frequently interpreted

as a sign of an undersized rudder, whereas in most cases it is the dihedral angle that is insufficient.

The presence of sweep can also contribute to induced roll, with a similar, though significantly less effective, effect to that of dihedral. This induced roll effect of sweep is dependent on the angle of attack, with no effect at zero angle of attack. Therefore, completely replacing dihedral with sweep is not suitable for a two-axis model. This sweep/dihedral equivalence is described in NACA Report No. 177 (Munk), which concludes that, for a typical flight angle of attack, the sweep value must be approximately three to six times the dihedral value to achieve an equivalent result. In other words, at this angle of attack, a sweep of approximately 30° to 60° will produce the same result as a 10° dihedral. Conversely, it is also possible to compensate for the roll effect induced by a strong sweep by a negative dihedral; this is a technique quite commonly used in jet aircraft (e.g., Saab 105, Alpha Jet, Mirage F1, etc.).

In the same vein, the effect of an inverse sweep can also be compensated by an additional dihedral to that identified above; this is typically the case on gliders like the ASK13 or the L-13 Blanik.

4.3 Choose the wing airfoil

Given everything we've just read, it's almost disappointing to be talking about airfoils now. After all, the heart of flight as most modelers imagine it is practically a myth… but that would be forgetting that, just like the wings, fuselage, or horizontal tail, the airfoil is an important part of the whole of an airplane. Neglecting it is just as detrimental as relying solely on it.

4.3.1 Definitions

The airfoil is a closed curve representing the cross-section of a wing in a vertical plane. From a distance, the typical airfoil resembles a more or less elongated teardrop, with the convex part pointing in the direction of flight (leading edge) and the pointed part towards the rear (trailing edge). But the simple board, more or less smoothed with a sandpaper, used by some indoor pilots is also an airfoil… a rustic one, certainly, but an airfoil nonetheless.
This curve is usually discretized into a set of points, 30 to 200 for the most part, points through which the said curve (usually a spline) best passes.

That's the basic principle, because having the points of a airfoil doesn't tell us much at the moment. The important thing lies in the deduced characteristics, in two forms:

- Geometric: thickness, camber, leading edge radius, position of maximum thickness and maximum camber. The list is not exhaustive, but will be more than sufficient to describe a airfoil within the scope of this document.
- Aerodynamics: these are obtained in wind tunnels, real or digital (XFoil, etc.), and are described by curves called polars. The concepts involved are numerous; we will limit ourselves to the simplest: lift, drag, moment, all in relation to the essential Reynolds number.

For practical reasons, we will not use the aforementioned physical values, but dimensionless values to facilitate interpretation and comparisons:

- For geometry: we will talk about thickness, curvature, etc., relative [to the chord]. For example, 10% relative thickness means that the physical thickness of a airfoil with a 150 mm chord is 15 mm.
- For aerodynamics: as seen previously, the lift coefficient (denoted Cl or Cz in French), drag coefficient (Cd or Cx), and moment coefficient (Cm) will be used extensively. We will also discuss airfoil polars (graphs plotting the relationship between one coefficient and another), the same formalism being used for all aerodynamic elements, from the wing to the complete model.

The aerodynamic approach is obviously much richer in information than the geometric approach. To draw another analogy with the automotive world: knowing that an engine has a 2-liter displacement (geometric equivalent) is good, but knowing that it develops a certain power and torque at a certain engine speed (aerodynamic equivalent) is much more relevant. However, calculating polar diagrams requires computer tools that are not necessarily accessible to everyone, so I will propose an approximate method for deducing the main aerodynamic characteristics of an airfoil from a geometric analysis.

4.3.2 Geometric analysis

Here (fig. 37) is a airfoil with its main geometric characteristics highlighted.

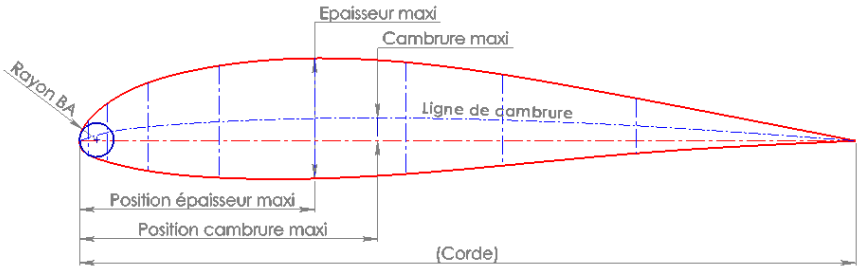

Fig. 37

These five geometric characteristics (position and maximum thickness, position and maximum camber, leading edge radius), generally expressed as a percentage of the chord, will allow us to classify and characterize the airfoils. We should note a somewhat unusual concept, camber, which is defined as the line equidistant from the lower and upper surfaces. This line is drawn by passing through the midpoints of several vertical segments drawn from the lower to the upper surface.

The first rule for using an airfoil concerns its maximum thickness, commonly called relative thickness (Ep, in %). As we saw earlier, the thicker an airfoil is, the more difficult it is for air to follow its contour, especially as the Reynolds number decreases. This Reynolds number adaptation issue can be simplified, as a first approximation, to a relationship with the airfoil chord (in mm):

$$Ep_{conseillée} \leq \sqrt{Corde}$$

Here are some rules of influence that allow for a basic comparison between airfoils:

- As maximum thickness increases, maximum load-bearing capacity increases, minimum resistance increases.
- Maximum thickness position, advance: Minimum thickness decreases
- As camber increases: maximum lift increases, minimum drag is located at higher lift, and moment increases.
- Maximum camber position moves back: better adaptation to high R-values
- As the BA radius decreases, minimum drag decreases, resulting in a more abrupt stall.

These influence rules teach us an important point: ideally, for a given wing, it's not a single airfoil, but rather a progression of airfoils from the root to the tip, so that each airfoil is perfectly adapted to the local operating conditions. This isn't strictly necessary, of course, but it's good to know when you start seeking performance, particularly in gliders. This is also beneficial for flight comfort: for example, for a large wing with a high aspect ratio, it's advantageous to use a thinner airfoil at the tip than at the root to ensure smooth operation at low speeds. However, this shouldn't be overdone, as a airfoil that's too thin will have reduced maximum lift, which can be counterproductive. Here again, it's all about compromise.

A simple rule for adapting the relative thickness of the airfoil to the local chord gives good results as a first approximation:

$$Ep_{corde2} = Ep_{corde1} \cdot \sqrt{\frac{Corde\,2}{Corde\,1}}$$

It is possible to conduct a quantitative analysis of each airfoil to better support the choice. This will allow the determination of the zero-lift angle of attack (Alpha0) and the corresponding moment coefficient (Cm0), these values being essential for model adjustments and horizontal tail sizing.

Here is an empirical formulation developed within the framework of this work:

$$\alpha 0 \approx -61. \frac{CambMax}{100 - PosCambMax}$$

$$\mathrm{C}m0 \approx -61. \frac{CambMax\,.\,PosCambMax}{100000}$$

Compared to those produced by a digital wind tunnel (XFoil or JavaFoil) or by thin airfoil theory (ProfilKonverter), the results obtained are particularly respectable. However, this is contingent on meticulous graphical analysis, which ultimately likely takes more time than using the aforementioned software.

4.3.3 Simple polar

The aim here is not to explain all the intricacies of using a digital wind tunnel, but to give you a foundation for understanding the data it provides. This data, in the form of curves called polars, describes the aerodynamic behavior of the airfoil. We will also define the key elements for relating these airfoil polars to the aircraft's performance.

Let us begin with the simplest of the polars (fig. 38), which shows the evolution of the lift coefficient (Cl) as a function of the angle of attack (α).

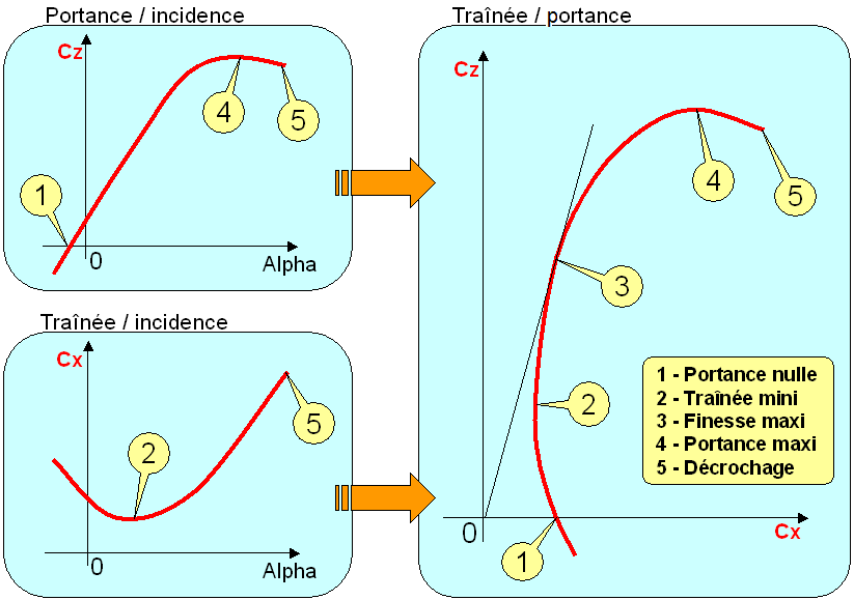

Fig. 38

Lift increases proportionally to the angle of attack up to maximum lift, then drops; this is stall. At Cl = 0, the angle of attack with zero lift α0 appears.
As already mentioned, the slope of the line is the same regardless of the airfoil; only α0 changes, according to the following relationship:

$$Cz_p = 0.11.(\alpha - \alpha 0)$$

Next, the polar curve of the drag coefficient (Cd) with respect to the angle of attack (α): drag improves up to a certain angle of attack, then gradually increases until stall. Each Cd curve is unique to each airfoil and can differ significantly from one airfoil to another.

Since the angle of attack is only really interesting for determining α0, we then dispense with it to transform these first two polars into one, the drag/lift polar (Cd/Cl, called the Eiffel polar… and yes, the same one who built the eponymous tower) which is much more telling.

Beware of the risk of confusion: by similarity with the reference frame of the flight (the x axis is horizontal and the z axis is vertical), the abscissas and ordinates of this polar are reversed, the input data for its reading being Cl (and not Cd).

The value of this polar diagram can be understood with another automotive analogy: for example, rather than studying fuel consumption as a function of engine speed on one hand and power output on the other, it is much more informative to establish a direct curve of fuel consumption as a function of power. This makes it easy to objectively compare two engines of the same power but running at different nominal speeds and therefore requiring different gear ratios between the engine and the wheels. Alpha0 then corresponds to the gear ratio, while drag is to fuel consumption what lift is to power. Like the ideal engine, which is very powerful and consumes little fuel, the ideal airfoil can handle high lift and low drag; this is precisely what we see on the lift/drag polar diagram.

The drag coefficient (Cd/Cl) polar diagram also offers the advantage of showing the lift-to-drag ratio, which reflects the airfoil's efficiency: it's the maximum lift-to-drag ratio, which in reality corresponds to the distance traveled by the aircraft (with the engine off) for a loss of altitude of 1 unit of height. Note that the airfoil's lift-to-drag ratio is always much better than the aircraft's lift-to-drag ratio, because while the lift is almost the same, an aircraft's drag is much greater: it's the sum of the airfoil's drag plus the induced drag, the fuselage drag, the horizontal tail drag, and also the drag of all the extraneous elements (protruding control surfaces, wing root fairings, etc.).

Reminder: Due to the reduction in lift at the wingtip (effect of aspect ratio: **λ**), the average lift of the wing (Cla) is not quite equal to the lift (Clp) of the airfoil:

$$Cz_a = \frac{Cz_p}{1 + 2/\lambda_a}$$

Lastly, the moment coefficient polar (Cm, fig. 39), which can be drawn with respect to the angle of attack, or better with respect to the lift coefficient.

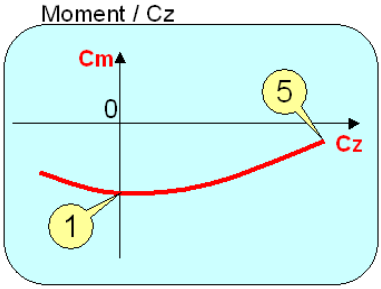

Fig. 39

This polar curve contains the value of Cm0, which is the moment coefficient at zero lift. This polar curve is generally flat or nearly so when the airfoil is functioning correctly, which usually allows it to be summarized by the single value of Cm0. However, analyzing this polar curve is useful to ensure the airfoil is functioning correctly, especially at low Reynolds numbers. For example, at Reynolds numbers < 100 000, the latest generation airfoils show significantly less variation in Cm than older airfoils such as Eppler or others, which makes them much healthier at low speeds.

Here is an order of magnitude of the values manipulated, which vary depending on the airfoils and flight conditions:

- Lift coefficient Cl: from -0.2 to -0.5 up to +0.8 to +1.6
- Drag coefficient Cx: from 0.005 to 0.05
- Moment coefficient Cm0: from -0.15 to +0.05 (flying wing)

Once the principle of polars is understood, we'll make things a bit more complex by introducing the Reynolds number (Re) at which the polar is plotted. Indeed, we emphasized at the beginning of this book that an airfoil performs better the higher the Re, which is reflected in the polars. During a flight, the aircraft encounters a wide range of Re values (remember: 68 * airspeed * mean chord), from the lowest speeds (landing/takeoff) to the highest (full-throttle level flight or airspeed adjustment).

This speed can be calculated for different level flight situations according to the equation already seen previously for the calculation of minimum speed.

This gives us: $\mathrm{Re} = 68.CMA_a \sqrt{\frac{2.m.g}{\rho.S_a.Cz_a}}$

To define, as a first approximation, a realistic flight envelope at our scales, we will use the following different values of wing lift coefficient (Cl):

- Minimum speed: Cla = 0.8
- Average speed: Cla = 0.3
- Maximum speed: Cla = 0.05

4.3.4 Multiple Reynolds polar

When studying an airfoil (or a given chord on a wing), one does not plot a single Cx/Cl or Cm/Cl polar, but as many polars as there are Re values needed to correctly describe the entire flight range [in terms of speed] of the aircraft under study. And rather than using Re values specific to each study, the most efficient approach is to systematically use a set of judiciously chosen standard Re values. As a general rule, the following five Re values (50 000, 100 000, 250 000, 750 000 and 1 500 000, which we will denote for the rest 50k, 100k, etc.) are more than enough to describe the majority of common devices, from the "micro" to the "small fat".

To illustrate this, here is a set of Cd/Cl polar diagrams (fig. 40) of the FAD14 airfoil, intended for gliders from 2.5 m to 4 m with camber flaps.

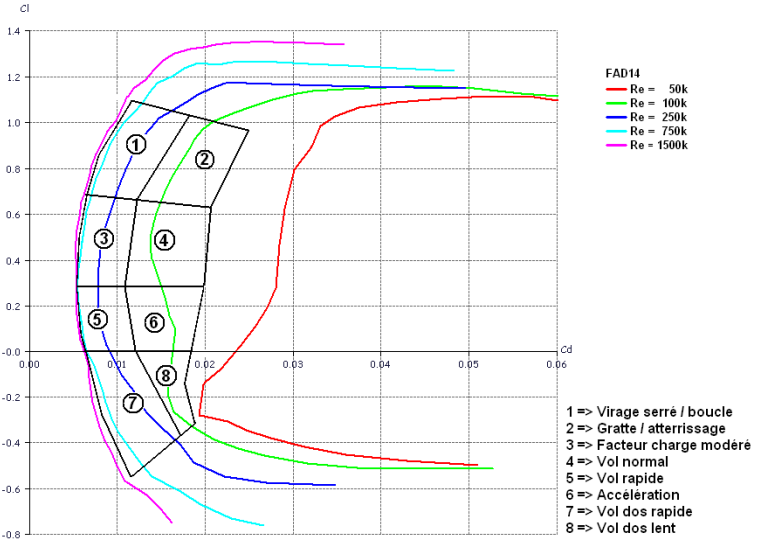

Fig. 40

In this study, a simplified breakdown shows the correspondence between the polars and the different phases of flight (many thanks to Marco Ricci for this excellent idea), here for the flight envelope of a hotliner. Note the areas outside the breakdown, in which it is not advantageous to optimize the airfoil because, even if there is still some lift margin, the drag begins to become significantly excessive.

This breakdown allows for a very easy comparison of different airfoils: after overlaying their polars, simply compare them (the best being the one with the least drag) for the flight phases (Cd, Re) that you wish to prioritize. For example, phase 1 (fast turn) is irrelevant for a transition aircraft, whereas it will be vital for a racer or a racing glider. Conversely, phases 7 and 8 will be important for an

aerobatic aircraft, while a hand-launched glider will gain absolutely no advantage from them.

The transitional phases can also be highlighted: simply remember that a change in lift coefficient (Cl) corresponds to an action on the elevator. In other words, examining a polar curve at a given lift coefficient (Re) shows the instantaneous behavior of the airfoil under the action of the elevator (loop, dive).

4.3.5 Type 2 polar

While airfoil polars with variable lift coefficient (Cl) and constant lift coefficient (Re) are ideal for analyzing constant-speed maneuvers, typical of powered flight, they are inadequate for accurately representing level flight. Since level flight is performed at constant lift and variable lift coefficient (Re), its description requires a specific polar, called a "type 2" polar (Fig. 41), which proves to be an excellent tool for comparing airfoils, particularly for gliders and aircraft with a wide speed range in general.

The principle is simple: starting from the simplified lift equation written for constant lift ($1/2.\rho.V^2.Cl = mg$), we can observe that the airspeed (and therefore the Reynolds number) during level flight varies inversely with the square root of Cl. Consequently, it suffices to plot the polar curve of Cd for $Re.Cl^{1/2}$ = constant to describe the behavior of the airfoil in level flight.

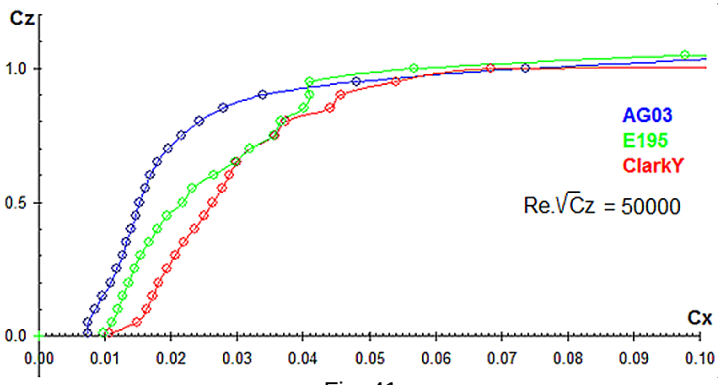

Fig. 41

The constant "Cste" is by definition derived from an arbitrary flight condition, for example Cl = 1 for simplicity, for which the corresponding flight speed is calculated from the lift equation, and then finally Re (= 68V.Chord). The chord used can be, depending on the need, the average of the wing chords, or a local chord that one wishes to study in more detail (as long as it is not too close to the wingtip, whose Cl is generally significantly lower than the average Cl of the wing).

Next, a relevant range of lift coefficients (Cl or Re) is chosen to describe the level flight envelope, and this range is discretized into a number of points. At each point, the corresponding Re (or Cl) is calculated using the previous equation, and then the airfoil drag coefficient (Cd) is determined for each pair (Cl, Re) from existing polars or by generating them as needed (Xfoil, Eppler). The type 2 polar can then be plotted on all the points (Cl, Cd) thus calculated.

While the exercise is interesting for understanding the principle, it is nevertheless quite laborious, hence the interest in automatic computer processing as offered by software such as Xfoil, XFLR5, PredimRC or Gemini Aero Designer, for example.

Note that this method, in addition to the classic type 2 polars described here, offers a more elaborate approach, taking into account the horizontal tail's contribution to overall lift, for calculating the operating points (Cla, Vx) of the level flight envelope. In this case, the polar is therefore not drawn at Re.Cl^0.5 = constant, but at Rz = constant. Furthermore, this method converts Cla into local Clp for each chord studied, based on the wing's Cl distribution curve (see 5.9), which allows for a detailed analysis of each chord. This proves particularly useful for optimizing the airfoil and twist of the chords near the wingtip.

4.3.6 Critical Reynolds

Simultaneous reading of polars at various Re also makes it possible to highlight a Reynolds number below which the airfoil does not function correctly, a number which is called critical Re and which differs significantly from one airfoil to another.

For example, on this set of polars (fig. 42) plotted for the Eppler 201 airfoil, we can clearly distinguish at Re = 100k (green curve) and especially 50k that (red curve):

- The Cl curve (/ angle of attack) has a slope that is no longer quite constant and equal to the coefficient of 0.11 predicted by the theory of thin airfoils (see also §5.5).
- The airfoil moment coefficient (Cm) varies excessively, whereas at higher Re values, especially above 200k, Cm can be considered relatively constant (except at angles of attack close to stall).
- The airfoil exhibits significant drag and varies abruptly when lift increases.

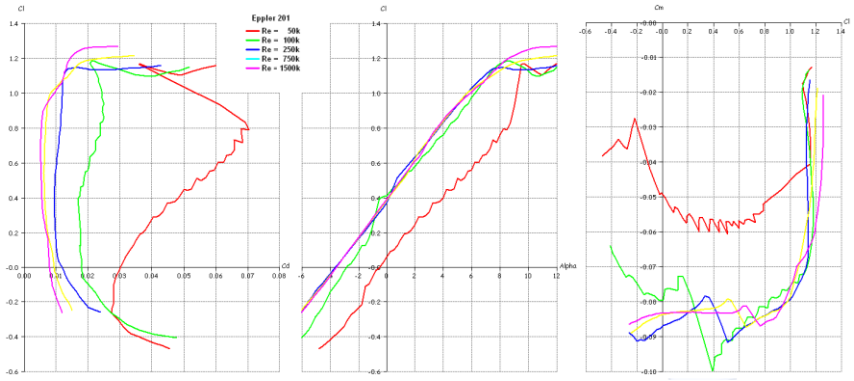

Fig. 42

Here, the critical Reynolds coefficient (Re) is at least 100k, which corresponds to approximately 50 km/h for a 100 mm chord. Therefore, this airfoil should not be used on a small machine or on the wingtip of a larger machine.

A more refined way of approaching the critical Re is to construct, as a function of the Cl, the curves (fig. 43) at zero lift (Cl=0) of drag (Cd0), zero lift angle of attack (α0) and moment coefficient (Cm0):

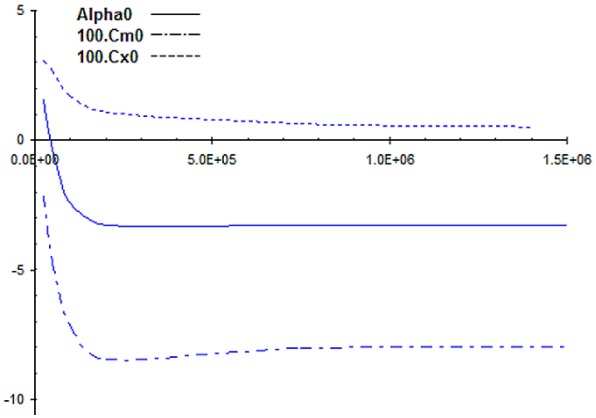

Fig. 43

This time, the interpretation is unambiguous: the critical Re of this airfoil is approximately 200k (2.0E+05 in scientific notation). Below this value, the airfoil's characteristics are no longer constant, and the device's behavior will be problematic.

NOTE

- To emphasize this crucial point: the effects of critical refraction detected on the airfoil polars result in very real parasitic reactions, typically problems with neutrality and pitch non-linearity. These reactions can, at best, make flight uncomfortable (a feeling of forward and aft center of gravity at times, the need for constant elevator re-trimming, and elevator more responsive at certain deflections than others), and at worst, lead to particularly hazardous, even dangerous, behavior. This latter point typically manifests as a sudden and difficult-to-anticipate stall, which can degenerate into a spin.
- These phenomena are often attributed to an excessively aft center of gravity, which is partially true since non-linearities in Cl and variations in Cm caused by the poor functioning of the airfoil affect the variations in the model's moments, and therefore the position of its aerodynamic center, which is normally invariant (see § 2.2). At the airfoil level, the aerodynamic center position becomes xF = 25% - dCm/dCl. Here, in the case of the Eppler 201, at Re = 50k and Cl = 0.8, dCm/dCl is approximately +0.05, representing a 5% advance of the aerodynamic center (or, consequently, a corresponding reduction in the static margin for this operating point!).
- But fundamentally, it's due to a poor choice of airfoil. This inherent difficulty with low Reynolds numbers is the main reason for the failure of many micro-models, leading to the emergence in model-making culture of a rule of thumb advising against going below a 100mm chord. So, with wingtip chords of around 30mm, a Crobe seems daunting, and yet its flight characteristics and performance are simply astounding.

4.3.7 Synthesis

We will focus here on the analysis of airfoils, knowing that there is still much to explore, and we will see more on this at the end of this document. For example, a digital wind tunnel allows us to study the airfoil deformed by a deflected control surface, aileron, or camber flap. The latter is crucial for high-performance gliders, which must minimize drag in all phases of flight. By lowering the camber flaps, we generally reduce drag at high lift (and not increase lift, as is often mistakenly believed), which minimizes the glider's braking in tight turns. We can also study the position of a turbulator, a sawtooth-shaped device attached to a strategic location on a wing (5% to 10% of the chord length in front of the maximum thickness is a fairly common value), which helps an airfoil to perform better, particularly below its critical drag coefficient. Or, even better, you can also create your own airfoils, and above all ensure that they are at least as good as existing airfoils…
But the important thing is, I hope, acquired: if you now know how to decode a polar diagram, then you will be able to use the functions of a digital wind tunnel without difficulty, since you will know how to interpret the results it delivers.

Of course, one might be tempted to believe in a hypothetical airfoil that " *works well everywhere* ," with very little drag across a wide range of lift conditions, both

positive and negative, and regardless of the Reynolds number considered. But, as we glimpsed earlier, the miracle airfoil doesn't exist; it's all a matter of compromise: an airfoil that performs very well in thermals (high maximum lift coefficient and minimum drag coefficient set at a fairly high lift coefficient) will very likely be poor at low lift coefficients (inverted flight, high-speed maneuvers), while an airfoil suited to low Reynolds numbers will be mediocre on a large model.

Therefore, it is not the "m*ost fashionable airfoil*" that should be chosen for your model, but a airfoil well suited to the flight domain of said model.

The Fractale, a small 60" all-aspect-ratio glider designed by the author, demonstrates that it is possible to combine high performance with simple and proven construction methods. All this with impeccable flight characteristics, which is ultimately the most demanding aspect, especially with a small model.

4.4 Sizing the tail assembly

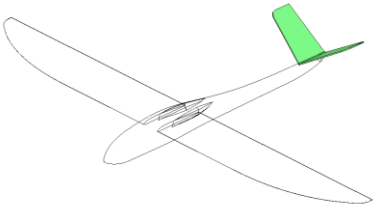

The tail assembly is a set of small wing-like structures, called the fin for the vertical plane and the horizontal tail (or horizontal tail) for the horizontal plane. In the case of a V-tail, there is no fin or horizontal tail; each of the two tail halves performs both roles.

The tail assembly fulfills several functions:

- Yaw axis (vertical plane): its function is obviously to stabilize and control this axis. Generally, a single vertical plane is used, but some specific devices (models, tugboats) may use two.
- Pitch axis (horizontal plane): it's a similar concept, but less straightforward. From a pitch perspective, the horizontal tail is never neutral: it's subject to the wing's wake (air deflected downwards), which varies depending on the speed and the horizontal tail's position relative to the wing, as well as the wing's moment (actually the airfoil's moment), which also varies with speed. Therefore, the horizontal tail's design must take all these parameters into account for optimal performance.

Generally, a tail assembly is located at the rear of the aircraft, but it may be partially or completely absent (classic flying wing with a fin, or Horten wing without a fin), or decoupled in the case of a canard, with the horizontal tail at the front and the vertical horizontal tail at the rear. However, the vertical horizontal tail cannot be placed at the front, as this positions the yaw center (weather vane effect) in front of the center of gravity, resulting in unstable yaw behavior.

4.4.1 The different types of tail assembly

Before sizing the tail assembly, you must first choose its design. There are fervent supporters of the V-tail, those who swear by the cruciform tail, while fans of the T-tail find it more elegant. In short, there's a lot of passion involved, which we'll move beyond to stick to the facts. Once again, let's dispel a myth: the miracle tail assembly doesn't exist! The most obvious proof is seen in glider and racing competitions, where the pursuit of optimal performance is constant, and where no tail assembly design has demonstrated a significant difference compared to another.

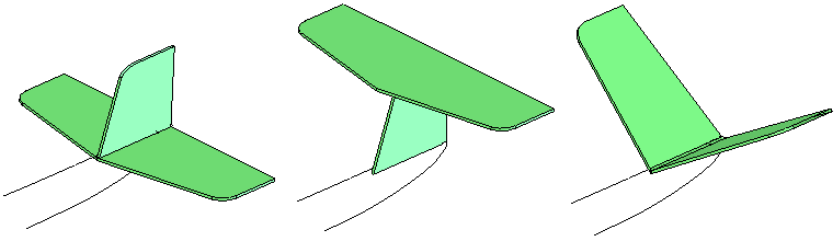

Fig. 44, different tail configurations

Here are the advantages and disadvantages of each:

- Cross-shaped tail: this is the most classic design, both easy to build and without major drawbacks. The height of the horizontal tail relative to the fuselage can vary: being close to the fuselage simplifies construction but slightly increases drag in the junction area between the horizontal tail and the fuselage plus the fin (referred to as the interaction or connection point), while high-performance aircraft often have their horizontal tail positioned at the first third of the fin.
- T-tail: it functions in exactly the same way as the cruciform tail but is theoretically slightly better thanks to lower drag at the fin (no connection to the upper surface) and greater efficiency due to less wake deflection. On the downside, it has a suspended mass at the top of the fin, which often causes mechanical problems at the base of the fin during rough landings.
- V-tail: often criticized for its relative sluggishness in yaw and sometimes poor decoupling between the yaw and pitch axes, it is primarily misunderstood and more demanding in terms of adjustment than the other two horizontal tail designs. However, when properly sized and adjusted, it proves just as effective, with the advantages of good ground clearance and greater simplicity in construction and installation. On the other hand, it is often attributed with the virtues of lightness, which is incorrect when its effectiveness is equal.

4.4.2 Equivalence V / classic

In the specific case of the V-tail, there is no horizontal or vertical plane; the projections of the tail onto these planes play this role. At first glance, one might think that the equivalence between a normal tail and its V-tail equivalent is simply a matter of projection, but in reality, things are a little more complicated (fig. 44):

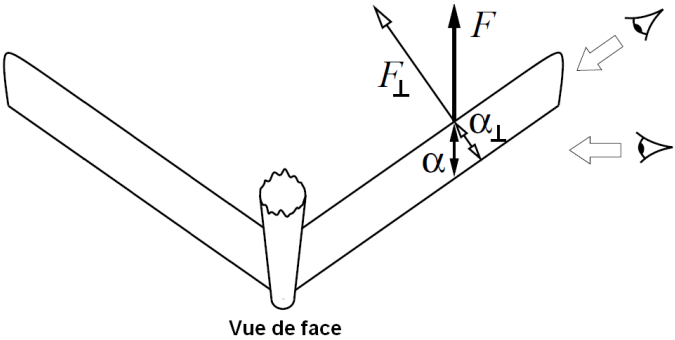

Fig. 45, projection of lift onto a V-tail (sketch by Mark Drela)

Let β (beta) be the opening of the V-tail. First, since the lift force of each half-tail is perpendicular to its plane, the resulting vertical force (acting on the pitch axis) is therefore projected as sin(β/2): this is the classic projection. However, when the angle of attack of this tail changes around the pitch axis, the actual change in angle of attack—and therefore in lift—of each half-tail (when viewed along its wingspan and not from the side) is also projected, with a factor of sin(β/2).

From a pitch perspective, the actual geometric equivalence between normal and V is therefore $\sin^2(\beta/2)$. This is exactly the same for the equivalence on the vertical plane (yaw) in $\cos^2(\beta/2)$, except that it will be a consequence of the choice of the dimensions of the horizontal plane and the aperture.

Remarkably, this equivalence in $\sin^2/\cos^2$ results in a V-tail with the same wetted surface area as an equivalent conventional tail. Consequently, the drag and mass of these two equivalent tails are virtually the same.

Since the horizontal plane is dictated by significant constraints (see below), the tailplane angle becomes a variable for adjusting the yaw axis. Two approaches are possible, depending on whether one seeks good yaw efficiency or a reduction in mass and drag. In the first case, a 90° angle is used, while in the second case, the classic 110° angle is perfectly suited.

To maintain a correct equivalent aspect ratio, the equivalence will be distributed across both the wingspan and the chords. Therefore, we will have the following relationship between the dimensions (chords, panel lengths) of the two tail configurations (C = conventional tail, V = V-tail):

$$\dim_C = \dim_V . \sin(\beta / 2)$$

For those allergic to mathematics, here are the values corresponding to the most common stab openings:

- 110°: equivalence coefficient = sin(55) = 0.82
- 90°: equivalence coefficient = sin(45) = 0.71

It should be noted that the V-tail introduces two opposing effects when the yaw control is applied: on the one hand, a yaw sideslip, identical to that of a conventional fin, and on the other hand, a roll moment opposite to the turn (like two mini ailerons). A conventional fin also generates this moment, but approximately half as much (one control surface versus two). This generally necessitates slightly increasing the wing dihedral to maintain good induced roll efficiency with a V-tail.

For what follows, we will only work on a classic tail assembly; it will then be sufficient to use the rules above to transform it into an equivalent V-tail assembly.

The F3K is a very active area of research, particularly concerning the shape of the tail assembly, typically cruciform with a lower fin and varying aspect ratios. X-shaped tail assemblies are also encountered, as well as this inverted V variant designed in 2009 by the author and validated by comparative tests under identical conditions thanks to a quick-release tail tube mounting system. Other experimenters have also had the same idea, such as in Poland where this horizontal tail has been used successfully since early 2011.

4.4.3 Tail volume and Cl

To dimension the horizontal plane or horizontal tail, we will use the -geometric- concept of horizontal tail volume, based on the following diagram (fig. 46), in which the wing and horizontal tail roots have been placed on the same axis (important for what follows):

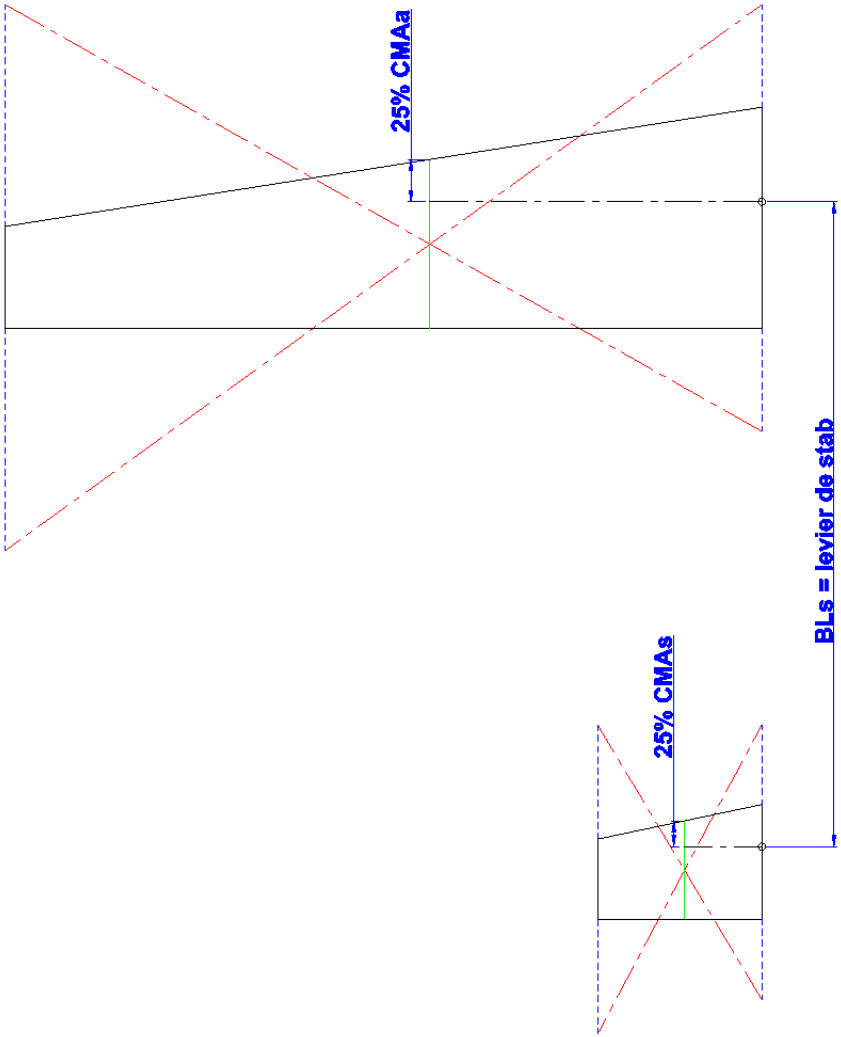

Fig. 46

The formula for the stabilizing volume is as follows:

$$V_s = \frac{BL_s.S_s}{CMA_a.S_a}$$

With: BLs = distance between the wing and horizontal tail apogees, Ss = horizontal tail area, MAC = mean wing aerodynamic chord, Sa = wing area. The apogee and horizontal tail area are calculated in the same way as for the wing (fig. 25).

The principle of the stabilizing volume is quite intuitive to understand:

- A small horizontal tail far from the wing is equivalent to a large horizontal tail close to the wing.
- A small wing with a large mean chord will have a pitching moment (given by the airfoil) as large as a large wing with a small mean chord.

The sizing of the horizontal tail volume essentially involves finding a compromise between drag and proper operation. Proper operation is characterized by the horizontal tail's ability to balance the wing's moment across the entire flight envelope, whether in level flight or under load. If the horizontal tail volume is too small, it will struggle to "hold" the wing and may even stall during certain phases of flight, while if it is too large, it will generate unnecessary drag. Furthermore, an excessively large horizontal tail volume also poses a center of gravity problem by moving the model's aerodynamic center aft (see §4.6), which ultimately contributes to excessive stress on the horizontal tail. Therefore, fine-tuning the horizontal tail volume is complex, as it involves factors such as the wing airfoil, the center of gravity, and the model's flight envelope. For this last point, an example: an aerobatic pilot will often work the wing at significant negative Cl (back loop) whereas a beginner aircraft will rarely fly at negative wing Cl.

Since this optimization is a matter of horizontal tail lift, this is an opportunity to learn how to calculate it. Here is the formula, derived from the equilibrium of moments around the center of gravity, neglecting the effect of the fuselage (fig. 47) and a possible Cm0 of the horizontal tail airfoil (generally symmetrical, therefore Cm0 = 0).

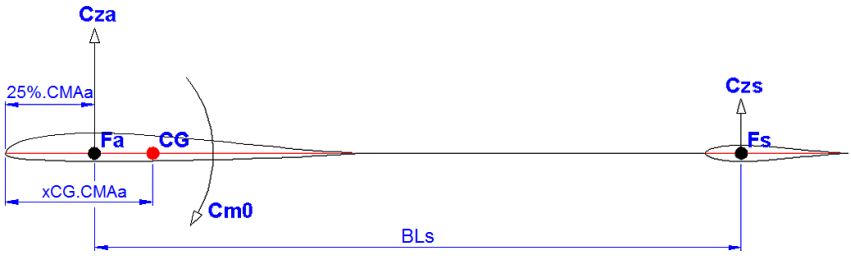

Fig. 47

Horizontal tail lift coefficient:

$$Cz_s = \frac{S_a.CMA_a(Cz_a.(xCG - 0{,}25) + Cm0)}{S_s.(BL_s - CMA_a.(xCG - 0{,}25))}$$

If the distance between the center of gravity and the wing center is sufficiently small compared to the horizontal tail's lever arm, then:

$$Cz_s \approx \frac{Cz_a.(xCG - 0{,}25) + Cm0}{Vstab}$$

With: xCG = relative position of the CG on the mean chord (ex: 0.3 if position = 30%), Cm0 = Cm0 of the airfoil and Cla = wing Cl.

In practice, it is generally observed that reducing horizontal tail drag primarily involves reducing its wetted surface area. Consequently, optimizing the horizontal tail volume can be summarized as reducing the horizontal tail lift coefficient (Cl) across the entire flight envelope to ensure proper operation. This reduction can be achieved either iteratively in XFLR5 or PredimRC, by testing different horizontal tail volumes to identify the one that yields the lowest possible Cl curve, or formally. For the latter, the lift coefficient (Vs) is calculated so that the horizontal tail's Cl is zero at the wing's average flight Cl. This distributes the horizontal tail load evenly on either side of this average Cl, thus minimizing the horizontal tail's extreme Cl values.

If Cls = 0, then we have:

$$Cz_a.(xCG - 0{,}25) + Cm0 = 0$$

Using the simplified formula for xCG (see chapter on centering §4.6.1), with a zero static margin (xCG = xF, which represents the most unfavorable case), we then find:

$$V_{s\,opti} \approx \frac{1}{Ceff_s}(K_f - \frac{Cm0}{Cz_{a\ moy}})$$

With: Ceffs = relative efficiency coefficient of the horizontal tail, Kf = correction coefficient of the fuselage.

The average lift coefficient (Cl) for flight can be defined by considering the aircraft's flight envelope a priori, with 0.3 being a value fairly representative of most applications, while 0.15 is relatively well-suited to aerobatic aircraft. A more refined approach is proposed by Thierry Platon in his publication on horizontal tail

volume optimization, which consists of using the average of the two stall lift coefficients (positive and negative, taken from the polar diagrams) of the airfoil to define the aircraft's actual flight envelope.

$$Cz_{a\ moy} = A_a . \frac{Cz_{p\ \max} + Cz_{p\ \min}}{2}$$

By default, the following generic table can be used, obtained with very classic values (Ceffs = 0.6, Cf = 0.1) and constituting a relatively correct working basis:

Cm0 Airfoil	Vs @ Cla moy. = 0.15	Vs @ Cla moy. = 0.30
-0.02	0.4	0.3
-0.04	0.6	0.4
-0.06	0.8	0.5
-0.08	-	0.6
-0.10	-	0.7
-0.12	-	0.8

In the case of an aircraft with a fairly wide fuselage (Cf = 0.15), such as a training aircraft, 0.1 should be added to the generic values to account for the fuselage's effect on the center of gravity. In all cases, it is not advisable to go below a horizontal tail volume of 0.3, as this is the bare minimum for adequate longitudinal damping.

NOTE

- Since this approach no longer works with zero Cm0 airfoils, typically used on aerobatic machines that move identically on their backs and stomachs, general-purpose Vs values of 0.5 for a glider and 0.6 for an airplane will suit the majority of uses.
- The horizontal tail lift formula indicates that, in level flight, horizontal tail lift is generally positive (directed upwards) at low speed (high Cla), zero for a given speed (or Cla) and negative at higher speed (low Cla).
- A very forward center of gravity (CG) (canard or conventional aircraft with a center of gravity much too far forward) can result in a high horizontal tail lift coefficient (Cl). In extreme cases, when this Cl is the same value as the maximum Cl supported by the horizontal tail airfoil, the latter is no longer able to balance the aircraft: this is the definition of the forward limit of the center of gravity. It should be noted that this forward limit depends on the wing loading: the heavier the aircraft, the smaller the usable center of gravity range (from the aerodynamic center to the forward limit).
- This formula also highlights a rather unusual observation: the pitch-up maneuver during a high-lift phase of flight (low speed, tight turn, loop) results in a lifting horizontal tail if the center of gravity is behind the wing's aerodynamic center (the general case), whereas intuitively one would think it

would become a lifting horizontal tail under the action of the elevator. The same is true for a pitch-down maneuver during a high-speed phase. This apparent paradox disappears when considering the elevator's action as a control of the horizontal tail's lift based on its equilibrium lift in level flight, itself conditioned by the wake deflection, which is proportional to the lift. The elevator action will therefore modulate this lift without necessarily canceling or reversing it. This is not intuitive at first glance, but perfectly logical.

- At the same time, we can deduce that a pendulum horizontal tail (also called a monobloc horizontal tail) always generates slightly less drag at high wing lift than its conventional rudder-type equivalent. Indeed, the latter's airfoil operates in an unfavorable manner and therefore generates more drag, being deflected in the direction of lift (its polar is "shifted to the 'wrong side'", see §5.3).
- The concept of horizontal tail volume applies equally to a conventional model and a canard. Only the sign of BLs changes, and therefore that of Vs as well; they are considered negative when the horizontal tail is positioned in front of the wing. However, in this particular case, it is observed that regardless of the designer's efforts, the leading edge—by its very nature—is particularly loaded during flight phases at high lift coefficients (Cla). It is therefore relevant, starting from the complete Cls formula, to work instead on the wing airfoil's Cm0 to relieve the horizontal tail and prevent it from stalling.

4.4.4 Horizontal tail lever arm

Now the challenge is to find the right compromise between horizontal tail surface area and lift. It all depends on the model: on a semi-scale model, the lift is a fairly fixed parameter, so the surface area will be adjusted accordingly. Whereas on a less constrained model, the horizontal tail surface area will be set at approximately 8 to 15% of the wing area for a glider or racer, and 15 to 25% for an airplane, from which the corresponding lift can then be calculated using the horizontal tail volume formula.

$$BL_s = \frac{S_a}{S_s}.CMA_a.V_s$$

With: Sa/Ss = 0.08 to 0.25 as defined above.

In the case of aircraft primarily designed for gliding (F3J or F3K gliders), increasing the horizontal tail lever arm is highly advantageous for improving pitch damping (a concept discussed in more detail at the end of this document). Consequently, a relatively small horizontal tail surface area, on the order of 8 to 10% of the wing area, should be chosen.

4.4.5 Tail level arm

Once the surface area is defined, a standard value of 5 to 7 for the horizontal tail aspect ratio (λs) is used, or even approximately 50% of the wing aspect ratio for aesthetic reasons if the wing has a low aspect ratio. This aspect ratio can be increased in the case of a canard, where the horizontal tail is as heavily loaded as the wing, in order to reduce its induced drag. In all cases, this value is not critical. Similar to the wing, a taper of around 0.6 can also be used to improve geometry efficiency, along with a minimal sweep if possible. Regarding this last point, a principle of zero sweep can be adopted at approximately 66 to 75% (see 4.2.7) of the chord length from the leading edge, which will simplify the positioning of the elevator hinge.

4.4.6 Vertical positioning

To conclude the discussion on the horizontal tail, a word about its vertical positioning, ranging from the T-shaped horizontal tail (positioned at the top of the fin) to the cruciform horizontal tail (directly mounted in the fuselage). Since the horizontal tail is located behind the wing, one might imagine that the higher the horizontal tail is positioned, the less it will be affected by the wing's "disturbance." This is partly true: as the wing deflects air downwards, proportionally to its angle of attack (or lift coefficient - Cl), the horizontal tail will encounter a layer of air that is more inclined the closer it is to the wing and/or the lower its position. This wake deflection changes the horizontal tail's actual angle of attack (by a few tenths of a degree). However, the term "disturbance" is largely unfounded because a wing's wake is actually relatively laminar (uniform flow), especially from the perspective of the horizontal tail, which is significantly smaller than the wing and therefore not affected by the wing's wingtip vortices.

The only point of concern concerns flight at high angles of attack, i.e., at a high angle of attack and therefore close to stalling, as the wing's direct wake becomes thicker and more turbulent. In this flight condition, a T- or V-shaped horizontal tail is very likely to operate within this direct wake, which will therefore affect its proper functioning and reduce its effectiveness. In contrast, a cruciform horizontal tail will be free of this turbulence and will therefore operate in a cleaner layer of air, hence the systematic use of this type of horizontal tail on aerobatic aircraft where the best possible pitch control is sought in extreme flight conditions.

The canard configuration presents a completely different situation, as its wing operates non-uniformly: the area downstream of the horizontal tail is subject to wingtip vortices and its wake, thus locally affecting its performance. Contrary to popular belief, the canard configuration is therefore aerodynamically less efficient than a conventional configuration.

4.4.7 Vertical tail

Let's now turn to the vertical tail, which acts as the rudder and is significantly less critical than the horizontal tail. We'll use a starting point of a surface area equal to 60% of that of the horizontal tail, again with a zero sweep at 66-75% of the chord. Just as with a wing, the taper can be around 0.6 to limit drag when the rudder generates lift (rudder deflected or yaw). The root chord will be approximately between 100% and 120% of that of the horizontal tail. As you'll have gathered, this dimensioning is inherently included in the case of the V-tail through the dimensioning of the horizontal tail and the angle of attack.

For an aerobatic machine, approximately one third of the surface area of the fin will be positioned below the horizontal plane passing through the wing, in order to reduce the induced adverse roll.

For sailing machines, again for reasons of damping, this time in yaw, a fin lever arm greater than that of the horizontal tail can be used. This configuration is particularly advantageous in F3K, where the fin is under extreme stress during launch, requiring high yaw efficiency to minimize energy loss during this phase.

In the case of a flying wing, lacking a horizontal tail as a reference point for calculations, the sizing of the fin(s) requires addressing the concept of lateral center of gravity and therefore lateral stability. This is detailed in section 4.6.2.

4.4.8 Tail airfoil

The commonly accepted rule is that a "well-designed" model should always use a horizontal tail and fin airfoil to minimize drag. While this rule holds true for most aircraft, it's not at all essential, or even true, for small models (say, less than 1.5 meters wingspan), for two reasons: the Reynolds numbers encountered by the horizontal tail are low, as is its lift (Cls = approximately 10% to 15% of the Cla when the model is well-designed). In this context, a thin, plank-shaped airfoil (approximately 5 to 6% relative thickness) works just as well as a true airfoil, or even better on micro-models like the Crobe, due to the very low Reynolds numbers encountered, with the sharp leading edge acting as a turbulator (see §5.5). Therefore, there's no valid reason to complicate things with a horizontal tail airfoil on small models.

For larger models, a symmetrical NACA airfoil is typically chosen, with a relative thickness of approximately two-thirds that of the wing. In the case of a highly loaded horizontal tail (Cls > 0.3 over a significant portion of the flight envelope), an asymmetrical airfoil may be used to minimize drag around this Cl value. This is generally the case with canards, whose aerodynamic design places a heavy load on the horizontal tail, typically resulting in a horizontal tail Cl equivalent to the wing Cl.

This SZD-55 micro-glider by the author uses a plank horizontal tail airfoil, which is as efficient as, if not more efficient than, a classic airfoil on a reduced scale.

4.5 The fuselage

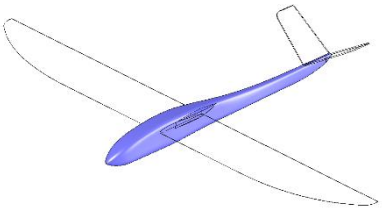

The fuselage acts as a link between the various components—the engine, wings, and horizontal tail—and as a container for the radio, batteries, and fuel tank. Its aerodynamic impact is often misunderstood or even ignored, with many modelers believing the fuselage to be "neutral." Nothing could be further from the truth, because, as we saw at the beginning, the fuselage follows the wing's angle of attack. Consequently, a maneuver with a significant angle of attack (say, 6 to 8° for a tight turn or a loop) will place the fuselage "across" the airflow, generating considerably more drag than in a straight line. This is, in fact, one of the undeniable advantages of models with full-angle or snap-flap design, since the fuselage maintains almost the same flight axis regardless of the wings' angle of attack.

At the same time, the fuselage contributes to the balance of moments and influences the model's center of gravity, and therefore its balance. Furthermore, it provides the majority of the lift in knife-edge flight, in equilibrium with the rudder. In short, it's anything but neutral…

4.5.1 Airfoil

The first thing to remember is to always think of a fuselage in terms of its airfoil. Yes, we're always told about the maximum cross-section (the section viewed from the front), whereas a fuselage is actually a continuous shape from front to back. It's like an airfoil: a thick but efficient airfoil is better than a thin but poorly designed one: obvious, but…

The advantage of streamlined the fuselage is twofold:

- Its wetted surface area will be reduced, therefore the associated friction drag will also be reduced.
- Its sensitivity to angle of attack will be reduced, with a smaller increase in drag at high angles of attack.

The profiling can be done by bringing out the big guns (for those who have them…) with a 3D CFD calculation code, or much more simply: empirically, by using our common sense to try and imagine the path of the fillets along the fuselage. We will therefore ensure that the contours flow smoothly and harmoniously from front to back, avoiding steep slopes, steps, and obstacles, which are major drag generators. We will also remember a simple rule: whether viewed from above or from the side, the maximum thickness of the fuselage will be positioned at approximately 25% of its length.

At the same time, the desired level-flight attitude of the fuselage will be determined, with a slightly high tail to provide a pleasing visual appearance in flight and allow for a slight pitch-up angle without excessive drag. On the drawing, this level attitude is then represented by a horizontal line on the side view; this will serve as the fuselage reference line.

4.5.2 Master couple

Once this exercise is completed, we can, of course, work on the fuselage cross-section to reduce the wetted surface area and facilitate airflow around the fuselage at an angle of attack. Particular attention will be paid to reducing the fuselage width and rounding the corners, as these two aspects are the main contributors to fuselage drag when it is at an angle of attack. In the specific case of F3K gliders, where a large portion of the launch energy is dissipated by the significant drag of the fuselage during sideslip, it is possible to do the opposite (fuselage wider than it is tall), at the expense of flight performance (unless devices such as full-angle-of-attack or camber-changing flaps are used to limit the fuselage's angle of attack in the different phases of flight). Again, it's all about finding the right compromise to achieve the best overall result over the average flight.

In the case of the aircraft used as an example in this report, the Crobe[2], this pursuit of streamlined flight and reduced width, essential for achieving good performance, is clearly evident. As we saw in the introduction, the fuselage can account for up to a third of the drag of even the most streamlined competition glider, so one can easily imagine the result when dealing with a less aerodynamic model. Some beginner aircraft, for example, have enormous fuselages, often referred to as "soapboxes," which is a real heresy: more drag necessarily means a more powerful engine, therefore more weight, and therefore a higher landing speed… It's a vicious cycle that the beginner suffers from, when what they need most is a lightweight aircraft (less inertia in case of impact) capable of very low-speed flight. The worst part is that this type of fuselage is not even justified by the equipment on board, which swims freely in this large empty volume, with the added risk of being poorly secured (a receiver battery that "moves around" is commonplace and can cause some centering problems).

4.5.3 Lever arm

The sizing of the horizontal tail allowed us to define its lever arm, and therefore the rear length of the fuselage. All that remains is to define the forward length. This distance is measured from the wing's center of gravity to the leading edge, a distance that we will set, as far as possible, between 30 and 40% (Fig. 48) of the distance from the wing's center of gravity to the horizontal tail's center of gravity.

Fig. 48

This point is not entirely insignificant, as it has consequences for longitudinal stability, and therefore for the calculation of the center of gravity (see §4.6.1 and §5.7), as well as for performance. In particular, an excessively long forward lever arm will—through its destabilizing effect—contribute to excessive stress on the horizontal tail, which will then drag more. This also affects the lateral center of gravity, which is important for both yaw stability and knife-edge flight maneuvers.

4.5.4 Vertical positioning

The vertical positioning of the fuselage relative to the wing is referred to by the established terms "low," "mid-wing," or "high" wings. The first criteria that naturally come to mind when designing a custom aircraft are the ease of landing gear installation (on the fuselage or wing), aesthetics, radio control accessibility, wing attachment method (rubber bands, screws, through-wings), etc. From a handling perspective, this positioning is relatively unimportant, except during knife-edge flight where a mid-wing reduces the inter-axis effects during this phase of flight. It is often stated that a "high-wing" aircraft is more stable than its "low-wing" counterpart because its center of gravity will be located slightly lower relative to the wing, but in reality, this effect is negligible most of the time and is therefore not a design criterion for the majority of applications. Only weight-shift control microlights or paragliders can really feel it because of the significant vertical distance between the center of mass and the wing.

Conversely, the wing's placement relative to the fuselage has a significant impact on performance. A very interesting study, directly applicable to our scale models, is available in the University of Maryland's knowledge base: http://drum.lib.umd.edu/handle/1903/8141
Experimentally, it demonstrates that the configuration least affecting wing performance is a high-mounted wing with its lower surface tangent to the upper surface of the fuselage. The other tested configurations (mid-mounted wing, wing on an F3K-type pod at varying heights) proved less efficient, both in terms of maximum lift and drag, with the latter sometimes showing significant differences. In the same vein, NACA Report No. 678 also contains a lot of information on this subject.

The Wasabi is an aerobatic glider, designed by Thierry Platon, Jérôme Bobin and François Lorrain, which benefits from an in-depth study of the fuselage for the phases of knife-edge flight (photo Jérôme Bobin).

4.6 The settings

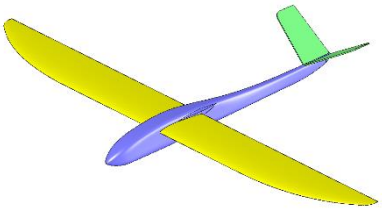

The adjustments are studied in a very specific order: first the center of gravity (CG), then the wing and horizontal tail settings. While the CG depends only on the aircraft's geometry, the wing and horizontal tail settings depend not only on the geometry, but also on the airfoil airfoils and the chosen CG. This sequence also forms the basis of the fine-tuning methodology detailed in Chapter 4.8.

4.6.1 Centering and neutral point

We saw in §2.13 the principle of the center of gravity, which determines the center of gravity (CG). Now we need to see how to calculate it. To do this, we will refer back to the top view of the model (fig. 46), which shows the wing and horizontal tail centers of gravity, to deduce their common center of gravity. Then we will incorporate the effects of the fuselage to find the overall center of gravity of the model. The center of gravity will be positioned just in front of this.

Several coefficients must be determined beforehand:

Static margin (ms): This is the distance between the global center of gravity and the center of gravity (CG), relative to the mean aerodynamic chord of the wing, which determines the level of stability. Its typical value ranges from 0% for a neutral aircraft (aerobatics) to approximately 10% for a very stable aircraft, with 3 to 5% generally used for common applications. The usable static margin can be greater, within the limit of the forward center of gravity defined in §4.4.3 (under "Note"), but this is pointless and even detrimental in model aircraft (see §2.13). In this case, we will use a value of 5% to cover the small approximations made here. At worst, this will result in a slightly forward CG, which will be inconsequential and perfectly adequate for a safe first flight.

Fuselage center of gravity correction: this allows for the consideration of its destabilizing moment related to the angle of attack. Although this correction is closely dependent on the dimensions and position of the fuselage and can vary significantly depending on these parameters, a standard value of 10% (of the mean aerodynamic chord) for a thin fuselage and 15% for a wide fuselage gives a relatively good result in most cases.

Relative efficiency coefficient of the horizontal tail (Ceffs): established relative to the wing, it incorporates into the horizontal tail's lift variation the difference in aspect ratio with the wing and the wake effect. A value of 0.6 can be used as a

first approximation for general cases, while for greater precision, the following formula should be used:

$$Ceff_s = \frac{dCz_s}{dCz_a} = \frac{0{,}11.(1-\varepsilon').A_s}{0{,}11.A_a} = (1-\varepsilon').\frac{A_s}{A_a}$$

With :

Wing and horizontal tail efficiency coefficients (see §2.14.1):

$$A_a = \frac{\lambda_a}{2+\lambda_a} \quad \text{And } A_s = \frac{\lambda_s}{2+\lambda_s}$$

Deflection coefficient (Munk, see §2.14.3): $\varepsilon' = \frac{4}{2+\lambda_a}$

Although this deflection coefficient formula works quite well in most cases, it is possible to do better thanks to the Toussaint formula improved by the author, which takes into account the position of the horizontal tail in the wing wake.

Deflection coefficient (Toussaint +):

$$\varepsilon' = \frac{1}{2+\lambda_a}.(4{,}5 - \frac{BL_s + 5.H_s}{\lambda_a\,.CMA_a})$$

With: BLs and Hs = axial and vertical distances between the wing and horizontal tail foci (fig. 46), CMAa = mean aerodynamic chord of the wing.

Caution: these formulas provide an average deflection coefficient and are therefore only valid when the horizontal tail's span is significantly smaller than that of the wing, which is the common case. With a tandem horizontal tail (Mignet type), the results will therefore be subject to some error, tending to underestimate the effectiveness of the downswing (thus calculating the aerodynamic center further forward than the actual center of pressure).

With this relative efficiency coefficient of the horizontal tail, it becomes possible to find (Figs. 49 and 50) the wing/horizontal tail aerodynamic center using the centroid of their aerodynamic centers weighted by their respective areas. Graphically, from a central axis (on which the wing and horizontal tail roots have been "glued"), two segments are drawn from the wing and horizontal tail aerodynamic centers, their length proportional to the area of the opposite element (for example, 1 cm for 1 dm²), knowing that for the horizontal tail, this is its area multiplied by its relative efficiency coefficient. The intersection of the line connecting the two ends of these segments with the central axis then gives the

position of the wing + horizontal tail aerodynamic center. By advancing this center by 10 to 15% of the CMAa (Closed Mass Attenuation Area) to account for the fuselage, we obtain a fairly realistic aerodynamic center for the complete model. To which we add 5% of CMAa towards the advance for the static margin, which gives us the CG.

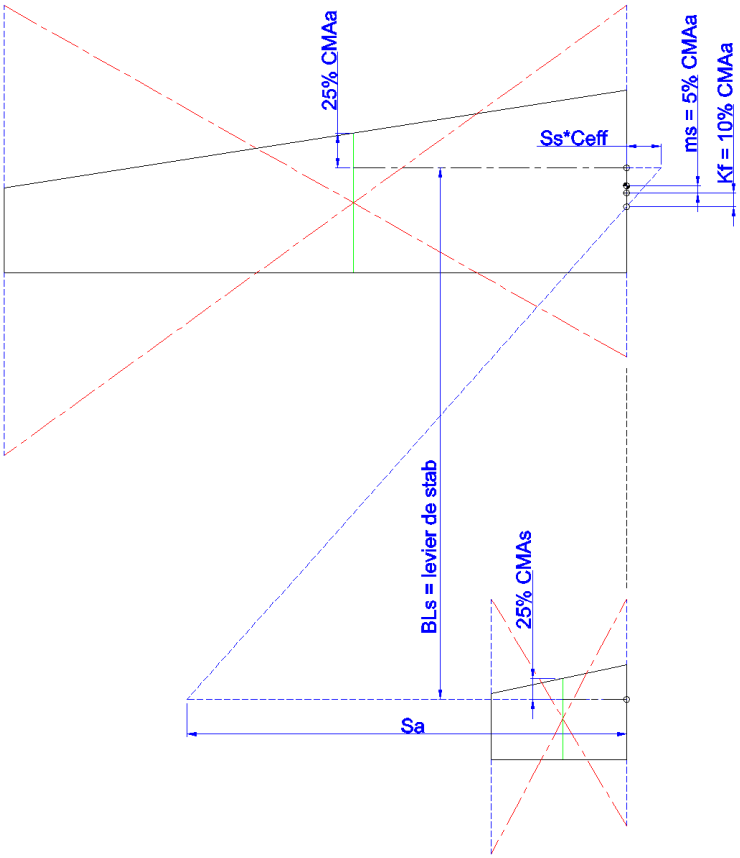

Fig. 49

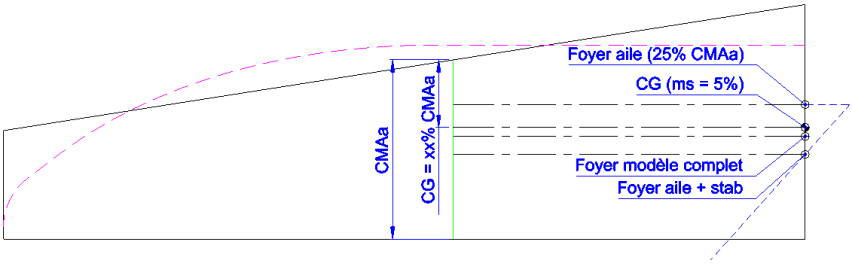

Fig. 50

This weighting can also be done formally, by calculating the position of the neutral point of the complete model (same as the graphical plot above) on the mean aerodynamic chord **:**

$$xF = 0{,}25 + \frac{BL_s.S_s.Ceff_s}{CMA_a.(S_a + S_s.Ceff_s)} - K_f$$

Therefore, if Ss*Ceffs is negligible compared to Sa:

$$xF \cong 0{,}25 + Ceff_s.V_s - K_f$$

With: 0.25 = wing center of gravity (= 25% CMAa), Kf = fuselage correction coefficient

For the latter, rather than the flat rate of 10 to 15% proposed above, we can use the following correlation which gives a rather satisfactory result in the context of the simplified modeling of xF:

$$K_f \approx 0.15.(0.3 + V_s)$$

Note that some full-size aviation manuals offer a very simplified formula, known as Lapresle's formula, whose connection to the general equation of xF - which is preferred - is obvious (Kf = 0.075 and Ceffs = 0.37):

$$xF \approx 0{,}225 + 0{,}37.V_s$$

Once the aircraft's center of gravity is found, the position of the center of gravity on the mean chord is deduced in proportion to the chord:

$$xCG = xF - ms$$

For easier handling, this result is then transferred to the root airfoil (the calculation of Fl_MAC is detailed in paragraph 4.2.1):

$$XCG = FL_{CMA\,a} + xCG.CMA_a$$

Four specific cases deserve further explanation:

- V-tail: Hs will be measured from the point at 40% (by default) of the height of the fin.
- Canard: With the horizontal tail positioned in front of the wing, the wake coefficient ε' is 0 (in reality, it is very slightly negative because the wing experiences the horizontal tail's wake, which slightly reduces its effectiveness). Also note the sign of the horizontal tail volume; it is negative because the lever arm between the wing apex and the horizontal tail apex is the inverse of a standard model. On these models, xF and xCG can be negative (located in front of the leading edge of the mean aerodynamic chord).

- Flying wing/delta: in the absence of a fuselage and horizontal tail, the center of gravity (CG) is simply placed 5% forward of the wing's aerodynamic center. If a small fuselage exists at the front of the wing, a standard correction factor of approximately 3% of the aerodynamic center of gravity (ACG) can be used.
- Biplane: the calculations presented here will be carried out using an equivalent wing with the following characteristics:
  - Wing area: sum of the areas of the two wings.
  - Aerodynamic center and mean chord: barycenters weighted by their respective areas (fig. 51), exactly as between a wing and a horizontal tail to find their center.
  - Aspect ratio: average of the aspect ratios weighted by the areas.

$$\lambda_{équiv} = \frac{\lambda_{a1}.S_{a1} + \lambda_{a2}.S_{a2}}{S_{a1} + S_{a2}}$$

  - Relative wing angle adjustment: the upper wing's underside (under positive pressure) and the lower wing's underside (under negative pressure) influence each other; a correction is necessary to ensure both wings operate homogeneously. A formal calculation is provided in NACA report #362, but it is too complex to detail here. By default, an angle of attack correction of +1.5° will be applied to the lower wing if the wings are at the same longitudinal level, +1° if the lower wing is set back approximately 25% of its chord relative to the upper wing, and +0.5° for a setback of 50% of the chord.

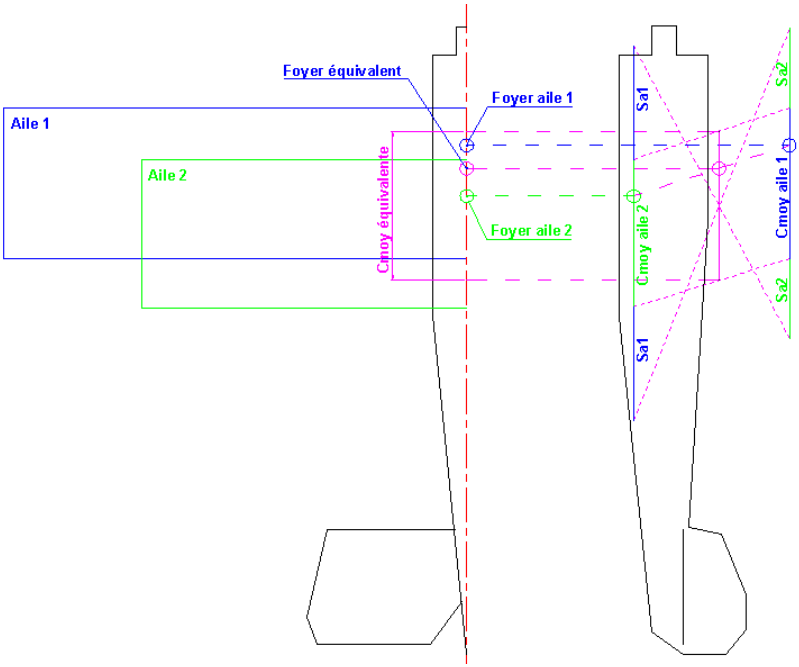

Fig. 51

NOTE

- The term Ceffs.Vs can be defined as the volume of aerodynamic stab, by similarity with Vs which is the volume of geometric stab.
- Since the calculation of Ceffs relies solely on the aircraft's geometry, it is implicitly assumed that this geometry must remain constant during flight (for the calculation to remain representative). However, this is not always true, as aircraft components do not possess infinite mechanical rigidity. In particular, a tail boom or horizontal tail that is too flexible, respectively in bending and torsion, will de facto reduce this coefficient, necessitating a more forward center of gravity than anticipated. Given this, it is far preferable to account for the boom's flexibility, thus avoiding various secondary problems (flutter, piloting inaccuracies, etc.).
- The static margin is also equal to -dCm $_{@CG}$ /dCl, that is, the opposite of the slope of the Cm $_{@CG\ curve}$ (global moment coefficient around the CG) as a function of Cl. This slope is negative for a stable aircraft, zero for a neutral aircraft, and positive for a stable aircraft, while the curve is a straight line when the airfoil is functioning normally. This representation is used in some software, with one straight line per moment (wing, horizontal tail, possibly fuselage, plus the complete model). It is important to remember that what matters is not so much the set of straight lines presented by this software, but solely the slope of the Cm/Cl line of the model and the point of intersection of this line with the y-axis (the equilibrium Cl of the model, see 4.1 and 4.6.3).
- We can observe that the center of gravity (CG) value for an aircraft with ultra-classic proportions (Vs = 0.45, Ceffs = 0.5, Cf = 0.10) is the equally classic one-third of the chord (mean chord, never forget that!). So far, so good, but it's crucial to remember that this CG value is simply a consequence of a particular model geometry. Modifying this geometry, especially the horizontal tail volume, changes the position of the center of gravity, and therefore the CG. This is further demonstrated by canard aircraft, whose CG is inevitably further forward than the wing center of gravity at 25% of the mean chord, since the horizontal tail is positioned in front of the wing.
- A more precise calculation of the center of gravity (CG) requires a more detailed consideration of the fuselage. This will be addressed at the end of this document, but the resulting equations make manual calculation tricky. Once again, I highly recommend using PredimRC for this. Thanks to the work of Thierry Platon, who has dedicated considerable effort to this subject, this software calculates the CG and trim for most models with astonishing accuracy. XFLR5 also allows this type of calculation, iteratively trying several CGs until finding the one that yields a horizontal overall moment curve (Cm/Cl). The horizontality of this curve indicates that the corresponding CG is neutral (i.e., positioned at the model's aerodynamic center) since the restoring moment (Cm) of the model's wind vane is independent of the lift (Cl), and therefore of the angle of attack. These results should be interpreted with caution because, to date, this tool's handling of fuselage lift is not yet satisfactory.

Here (fig. 52) are some examples of determining focal points/CGs using the PredimRC software. Unsurprisingly, the CG positions of the classic model, the

flying wing, and the canard are radically different, even though these aircraft share strictly the same wing geometry.

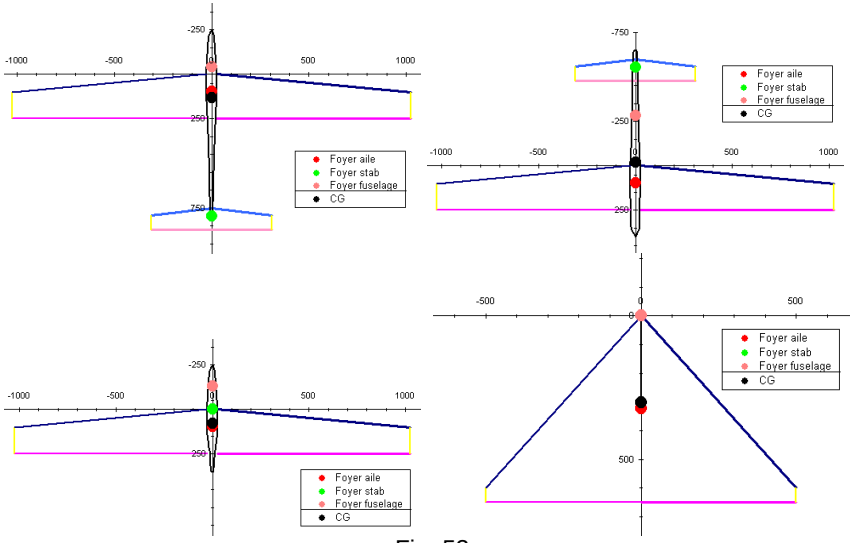

Fig. 52

4.6.2 Lateral neutral point

Now that we have placed the center of gravity (CG) (5% of the maximum aerodynamic center (MAC) in front of the longitudinal aerodynamic center), we need to verify that it is also in front of the lateral aerodynamic center to ensure proper yaw stability. To do this, we will work on the side view of the model and simplify the fuselage/wing assembly into a rectangle of equal length, from which we will deduce the area. In the case of a flying wing, this is simply the wing root airfoil that will be simplified. By default, the aerodynamic center of this surface will be considered to be at 20% of the fuselage length for a standard aircraft and 40% for a canard (these values take into account the average shape of a fuselage). The fin will also be simplified into a rectangle with its aerodynamic center at 25%, and then we will perform the same graphical weighting exercise as for the longitudinal aerodynamic center (but without an efficiency coefficient).

Note that for a V-tail you must project the total area with the squared cosine of half the stab opening (see above the rules of equivalence between normal and V tails), while you must sum the different fin areas of an aircraft with several distinct fins.
The result will be approximate, but nevertheless sufficient to give an idea of the yaw stability. It will be considered correct if the lateral neutral point is located behind the longitudinal neutral point (fig. 53), which implies a greater static margin in yaw than in pitch.

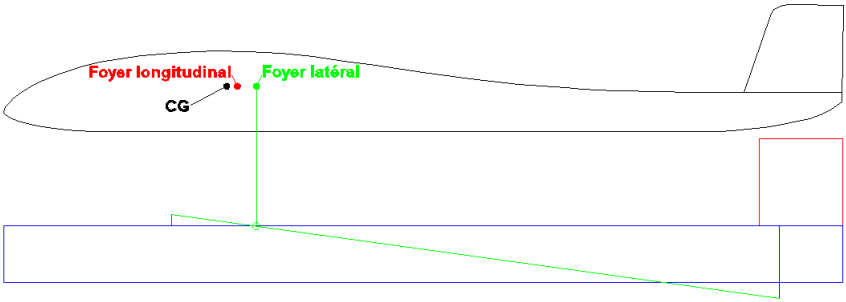

Fig. 53

The exercise is trivial in the case of a conventional aircraft, but can become considerably more interesting in the case of a flying wing or a canard, on which the rudder lever arm (relative to the center of gravity) is often reduced. Similarly, some aircraft (typically jets) have a very prominent forward fuselage, requiring a large tail surface area at the rear to maintain adequate yaw stability.

Alternatively, it is possible to use wingtip drag control devices, either passive (Horten wing principle) or active (wingtip airbrakes, as on the B2 flying wing), the variation of which (increase on the side that "advances" and, possibly, reduction on the side that "recedes") generates a yaw restoring moment and thus ensures stability on this axis.

The yaw stability of this Twister, which could be improved at low speed - despite an apparently comfortable fin area - due to the large forward surface of the fuselage, is here elegantly improved by the addition of two small sub-fins (design and photo Jean-Claude Talbert).

4.6.3 Wing/horizontal tail adjustments and balance coefficient (Cl)

It now remains to determine the geometric angles of the wings and horizontal tail (denoted α K), which are the "natural" angles of attack (corresponding to the equilibrium lift coefficient, towards which the model converges in the absence of

pilot input) of the wings with the flight line (fig. 54), that is to say with the trajectory of the aircraft.

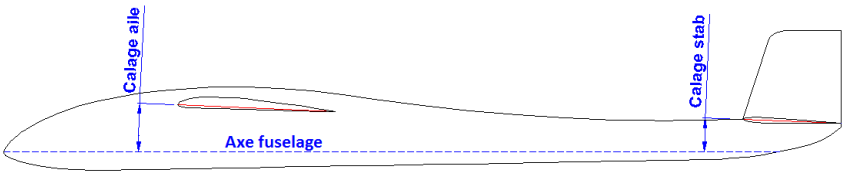

Fig. 54

In the case of models with a tail assembly, we often speak of the longitudinal V, which is simply the difference between the wing and horizontal tail angles:

$$V_{longi} = \alpha\kappa_a - \alpha\kappa_s$$

The longitudinal V is a concept we will use sparingly, as each calibration serves a very distinct purpose:

- The wing's shape gives the visual appearance of the fuselage, hence the fact that the latter (more precisely its median axis) generally serves as a reference for the adjustments.
- The stab ensures the balance of longitudinal moments, and therefore defines the equilibrium lift coefficient (Cl).

The usual values of these angles are generally between -1° and +2° but, being intimately linked to the geometry of the aircraft and its wing airfoil, no generic value can be defined a priori.

Calculating wing trim requires first defining the equilibrium lift coefficient (Cl) to be satisfied. The most logical strategy is to use the design lift coefficient defined in §4.1, in order to align the fuselage (via wing trim) with the average trajectory of the flight envelope and thus minimize its average drag. This rule can be deviated from, for example, to favor a high (aesthetic) attitude at certain flight regimes. In this case, the wing trim is decoupled from the equilibrium lift coefficient, and a pitching moment of the fuselage appears, which requires more complex calculations, detailed in §5.8.

The fuselage's median axis, roughly corresponding to its zero-lift angle of attack, can be determined by estimation, simply by eye, especially since it is not a very sensitive parameter. The important thing is not to be precise with this parameter but rather to avoid a significant error in judgment.

Since wing angle is its angle of attack for a given Cla setting, we arrive at a well-known equation:

$$\alpha\kappa_a = 9{,}1.\frac{Cz_a}{A_a} + \alpha 0_a - \alpha 0_{dec\_moy\ a}$$

The last term is the average wing twist, which can be calculated as follows in the case of a single-trapezoid wing with linear twist from root to tip (negative = upturned trailing edge):

$$\alpha 0_{dec\_moy\ a} = \frac{\alpha 0_{dec\_saum\ a}}{3}.\frac{CE_a + 2.CS_a}{CE_a + CS_a}$$

The formula is analogous to that of the mean sweep. The terminology used here equates twist to a shift in the zero-lift angle of attack of the airfoil, allowing, if necessary, the introduction into this term of the difference in Alpha0 between the root and tip airfoils, if they differ.

Calculating the horizontal tail trim is more complex and involves the required horizontal tail lift to balance the wing moments (lift moment + airfoil moment) around the center of gravity. From this, we deduce the corresponding aerodynamic angle of attack (αs), which is then corrected for the zero-lift angle of attack of the horizontal tail airfoil (α0s) and the wake deflection angle imposed by the wing (αdlf) to finally obtain the geometric trim to be used:

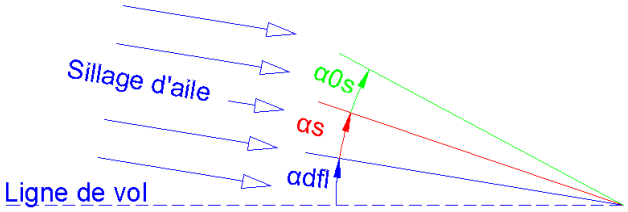

Fig. 55

Horizontal tail geometry adjustment: $\alpha\kappa_s = \alpha_{dfl} + \alpha_s + \alpha 0_s$

Or, expanding the formula: $\alpha\kappa_s = 9{,}1.(\varepsilon'.\frac{Cz_a}{A_a} + \frac{Cz_s}{A_s}) + \alpha 0_s$

With :

Local wake deflection angle: $\alpha_{dfl} = \varepsilon'.9{,}1.\frac{Cz_a}{A_a}$

Impact of the horizontal tail on the local airflow: $\alpha_s = 9{,}1.\frac{Cz_s}{A_s}$

Horizontal tail Cl (simplified formula):

$$Cz_s \approx \frac{Cz_a.(xCG - 0{,}25) + Cm0}{V_s}$$

In flight, the horizontal tail pitch can be corrected (or simply modified to adjust the equilibrium speed) using the elevator trim (see §4.10.1). This pitch – control surface deflection equivalence is generally not very intuitive, but it becomes clearer when compared to pitcheron wings or rotating horizontal tail.

NOTE

- Pay attention to the signs in the Cls equation: in the case of a canard, Vs is negative and XCG can also be negative (CG in front of the leading edge of the mean chord), which gives a horizontal tail Cl (and therefore horizontal tail trim) that is always strongly positive. However, with a conventional aircraft, Cls has a low absolute value and can be either negative or positive depending on the position of the CG and the value of Cm0 (which is generally negative).
- Similarly, if αdfl is always positive by nature, αs and α0s can be negative, zero or positive.
- The full formula for the horizontal tail lift coefficient (Cl) is preferable to the simplified formula as soon as the horizontal tail volume is sufficiently large. In this case, the distance between the center of gravity (CG) and the wing center is no longer negligible compared to the horizontal tail's leverage arm.
- Since most fuselages are relatively symmetrical, their Cm0 is considered negligible in the calculation of the moments determining the horizontal tail angle. Otherwise, this simplification may slightly affect the result, but rarely by more than a few tenths of a degree.
- The horizontal tail's position, and therefore the longitudinal V, depends on the CG setting. Moving the CG forward (= reducing the xCG value) leads to reducing αs, which is equivalent to trimming for nose-up attitude.
- When the static margin is zero (neutral center of gravity), the longitudinal dihedral becomes independent of the trim lift coefficient (Cl). This is logical since, with a neutral center of gravity, the longitudinal moment is independent of the angle of attack (definition of the center of effort). In this case, the very notion of trim lift coefficient loses its meaning, since there is no longer a natural airspeed. However, it retains its full importance with regard to performance, via the wing's incidence angle (relative to the fuselage axis).
- In the case of the flying wing, adjusting the longitudinal balance is simply a matter of adjusting the airfoil's Cm0 via the elevator trim (see ².12): *Cm0 = ms.Cla_reg*

For the exercise, we can also directly describe the local deflection angle:

Munk: $$\alpha_{dfl} = \frac{36{,}4.Cz_a}{\lambda_a}$$

Toussaint +: $$\alpha_{dfl} = \frac{9{,}1.Cz_a}{\lambda_a}.(4{,}5 - \frac{BL_s + 5.H_s}{\lambda_a \,.\, CMA_a})$$

For those curious, here is the original Toussaint formula:

$$\alpha_{dfl} = \frac{Cz_a}{\lambda_a}.(43 - 3{,}25.\frac{BL_s - 0{,}75.CMA_a}{CMA_a} - 0{,}45.\frac{H_s}{CMA_a})$$

A final deflection formula, provided by Matthieu Scherrer on his website and derived from a more general formulation presented in Warren F. Phillips' "Mechanics of Flight" (p. 372), is based on Prandtl's lifting line theory and the Biot-Savart law. Like Toussaint's formula, it relies on Munk's formula with a correction for the relative position of the horizontal tail, but it proves to be significantly more accurate. However, and this is why it is not detailed here, it is too complex to be used with a simple calculator and requires computer programming.

This is precisely the formula used in the PredimRC software, and it has also been used to improve Toussaint's formula based on a sample of values (λ, BLs/CMAa, Hs/CMAa) representative of common cases, with convincing results (Fig. 56). This graph shows the evolution of the various wake deflection coefficients as a function of the aspect ratio λ (from 4 to 20) and for several BLs/CMAa ratios (from 3 to 7) and Hs/CMAa ratios (from 0 to 1.5), hence the sawtooth curves. The correlation between Toussaint's improved formula and Matthieu's formula is particularly good.

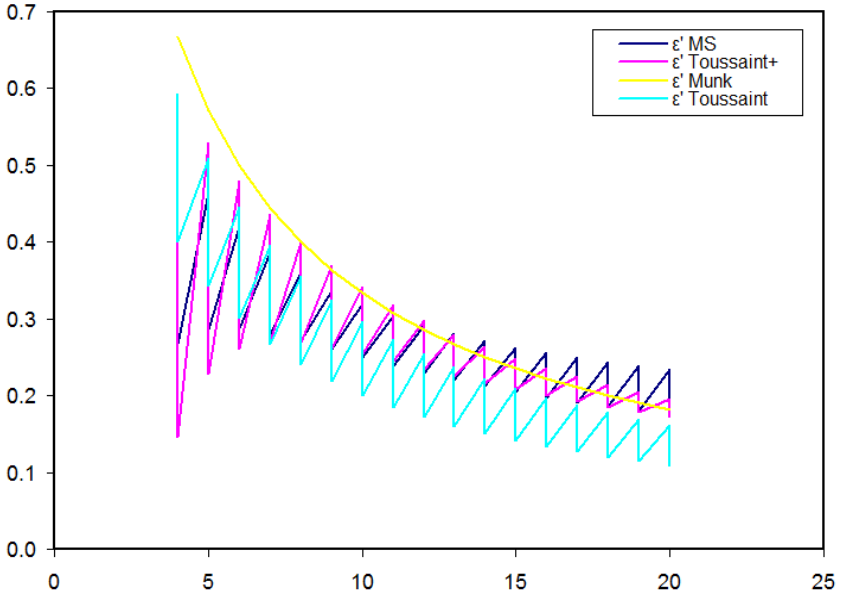

Fig 56, comparison of different wake deflection calculations as a function of the aspect ratio and relative position of the horizontal tail

4.7 The control surfaces

Control surfaces are generally sections of the wing that occupy a portion of the trailing edge and allow the aircraft to be steered. Their operation is quite simple: deflecting a control surface changes the shape of the airfoil (specifically its camber, and therefore ultimately its zero-lift angle of attack α0) and its angle of attack (since the trailing edge moves). The two combined effects increase, decrease, or reverse the wing's lift. Because the aircraft pivots around its center of gravity (always the same…), the control surfaces operate indirectly, especially for the yaw and pitch axes. For example, to climb: the elevator deflects upwards, generating downward lift from the horizontal tail, thus lowering the tail, which increases the wing's angle of attack… It sounds complicated, but it's actually quite simple in practice. In the case of ailerons, the operation is a little more direct: the aileron that rises reduces or even reverses the lift of the half-wing concerned, while the one that lowers increases the lift of the other half-wing, both contributing to a rotation around the roll axis.

This explanation of how the control surfaces work allows for an immediate understanding of the principle of flight control by varying the angle of attack, whether for the wings or the horizontal tail. The control chain is simply more direct, especially for the wings in terms of pitch. For example, to climb, you simply increase the wing's angle of attack or decrease the horizontal tail's angle of attack; it's as simple as that.

In all cases, to change a trajectory, the control surface must exert force to counteract the model's inertia and, above all, the restoring force generated by stability. Just like a wind vane: the more stable it is, the more effort is required to make it angle into the wind. Excessive stability is therefore detrimental, as it leads to having to over-steer the control surfaces for the same change of trajectory, which generates additional drag.

The sizing of the control surfaces is carried out along three axes: the first concerns the positioning of the joints, the second the deflections while the third is concerned with the torque required by the servo to ensure the control of each control surface.

4.7.1 Position of the joints

- Conventional control surfaces (ailerons, camber flaps, elevator, rudder): the hinge point should be positioned at approximately 20 to 30% of the chord to achieve the best efficiency/drag ratio. This optimal position varies slightly depending on the airfoil and is determined through successive iterations in XFoil, but it's a significant amount of work for a relatively small gain. Whenever possible, control surfaces should cover the entire span of the component in question, extending to the wingtip (better from a drag perspective than a control surface that stops a few centimeters before the wingtip, as is often observed). In the case of ailerons, if it's not possible to have them along the entire span, they should be positioned at the wingtip and cover approximately 55% of the span, either alone (but this isn't ideal in terms of drag), or extended towards the wing root by camber flaps that also function as ailerons.
- One-piece horizontal tail with pitcheron wings: to ensure the stability of this control surface (due to the weathervane effect), its hinge will be positioned in front of the apex of the relevant plane. A position will be chosen at 20% of the corresponding mean chord (which will then be projected onto the root chord), providing a good compromise between control surface stability and maneuvering effort.
- Pitcheron wings: the positioning of the hinge (wing spar) is critical, as the servo torque is essential for maneuvering the wings in all phases of flight. This hinge must be neither too far forward nor too far back, and its optimal position is calculated on the mean aerodynamic chord by aligning it with the center of pressure (Cp) for an average flight lift coefficient (Cl) of 0.25 (just below the generic design lift coefficient of 0.3):

$$x_{Clé} = 0{,}25 - \frac{Cm0}{0{,}25}$$

4.7.2 Travels and differential

Here is a first working basis that will be adjusted in flight according to the aircraft's behavior:

- Conventional control surfaces: +/-15° for the aileron function, +/-10° for the elevator function, +/-30° for the rudder function, +/-7.5° for camber-changing flaps used as ailerons
- One-piece horizontal tail (or classic horizontal tail with rudder > 50%): +/-6°
- Pitcheron wings: elevator function +/- 6°, aileron function +/- 3.5°
- Flying wing: elevator function +/-7.5°, aileron function +/-15°

Generally speaking, it will likely be necessary to introduce aileron differential, which consists of deflecting a control surface more in one direction than the other (Fig. 57). This is due to a drag issue, not of the control surface itself as often described, but of the airfoil: the change in lift of the airfoil, as well as its own

change in camber when the control surface is deflected, results in a change in its drag, potentially differently on the side where the aileron is raised and the side where it is lowered. If these two drags do not evolve in the same way, the result is a drag differential that tends to cause the aircraft to yaw, most frequently (but not always, depending on the phase of flight and the airfoil) in the opposite direction of the turn; this is adverse yaw.

To counteract this unwanted effect, we will then increase the upward deflection and decrease the downward deflection, from 10 to 50% depending on the airfoil and aspect ratio. These values will of course need to be fine-tuned in flight and are not critical; however, it should be noted that the difference will be greater the more cambered the airfoil.

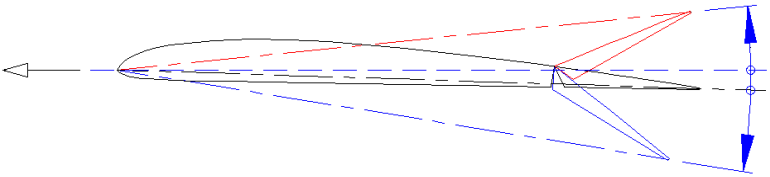

Fig. 57, aileron differential

Adverse yaw can be reduced at the source by means of Frise-type ailerons, using secondary airflow to balance drag (fig. 58).

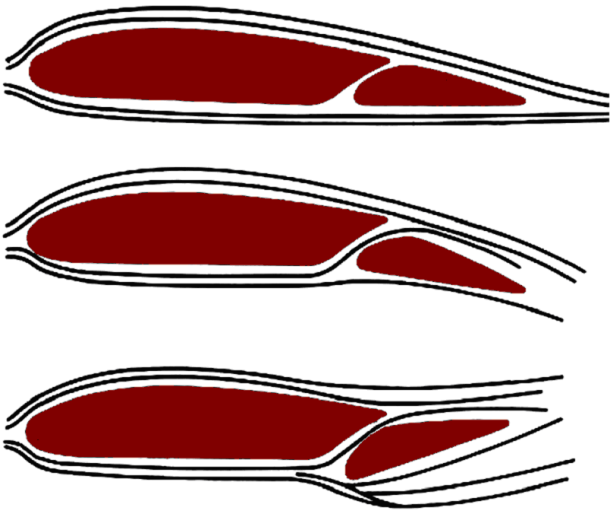

Fig. 58, Frise-type ailerons

NOTE

- In the case of a V-tail or a flying wing / delta wing, yaw differential may be introduced to counteract any potential pitch interaction when the yaw axis is used.
- Differentiating the control stick travel for functions that share the same servos (ailerons and elevator on a flying wing, for example) is done using the "Dual-Rate" menu (a historical term, gradually being replaced by "Sticks" or "Inputs") on our radios. This menu modulates the control stick travel, and therefore the functions, independently of each other. This differs from the Servo/End-of-Trip menu, which is often misused and affects the servo travel regardless of the origin of the command sent to it.

4.7.3 Servo sizing

Turning a control surface in the air generates a resisting force, called the hinge moment, which the servo must overcome to position the control surface at the desired angle. The sizing of a servo therefore boils down to calculating the moment to be provided for the maximum deflection.

This calculation involves the kinematics of the control system, but since the rudder travel is generally quite linear compared to that of the servo, we can use approximate formulas, which are perfectly adequate. The results are in kgf.cm, so they can be directly compared with the manufacturer's data.

Conventional rudders, with or without a compensation surface upstream of the hinge:

$$M_{servo} = \frac{C^2 . L}{200.r} . (1 - 3. \frac{C_c^2 . L_c}{C^2 . L}) . \delta . V^2$$

With :

δ = rudder travel (in degrees)
r = reduction ratio between the radius of the control horn and that of the servo horn, generally 1 to 4
V = average flight speed (in km/h)
C, L = chord and rudder length (in m)
C_c , L_c = chord and length of the compensator (in m)

In the common case of a rudder without a compensator, the term relating to the latter (in parentheses) is simply 1. Note the coefficient 3, which reflects the difference in lever arm between the foci (75% in front of the rudder hinge, 25% behind) of each surface.

Pendulum horizontal tail or pitcheron wings with symmetrical airfoil:

$$M_{servo} = \frac{CMA_s.S_s}{40000.r}.\delta.V^2$$

With :

δ = rudder travel (in degrees)
r = reduction ratio between the radius of the control horn and that of the servo horn, generally 3 to 4
V = average flight speed (in km/h)
CMAs = mean chord of the horizontal tail (in m)
Ss = surface of the stab (in dm²)

Pitcheron wings requires a bit more trigonometry, based on the sketch in Fig. 59 which defines the complete kinematics of the system. Assuming that the opening at full steering angle (Cl = 1) has the same amplitude as the toe-in at neutral (desirable for linearity of the steering travel), and after some simplifications, we obtain a relatively easy-to-use relationship:

$$M_{servo} = \frac{-Cm0.CMA_a.S_a}{200.r}.V^2$$

With :

r = reduction ratio R2 / R1, usually 4 to 5
V = average flight speed (in km/h)
CMAa = mean wing chord (in m)
Sa = wing surface area (in dm²)
D3 = R1 * 3 (recommended control lever length)

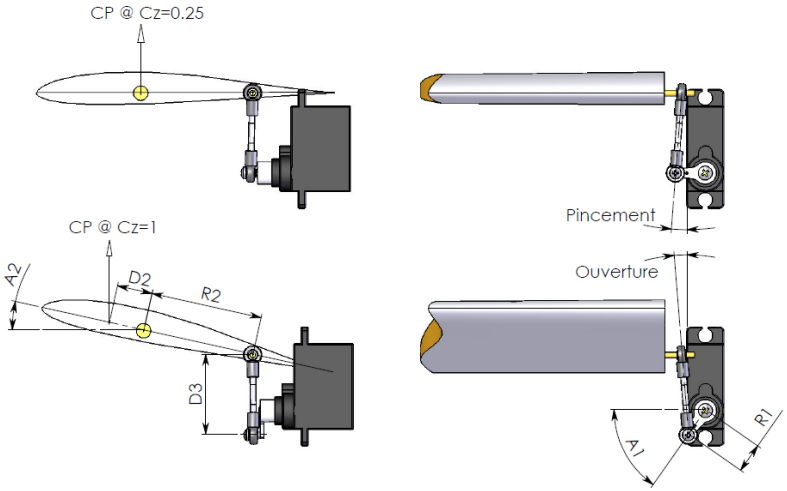

Fig 59

NOTE

- The leverage ratio between the servo and the control surface has a significant impact on the result. Carefully adjusting this ratio to achieve the correct control surface deflection, by moving the clevis mounting points on the servo horn or control horn, is therefore far preferable to electronically limiting the servo's travel. This also improves flight precision, thanks to the full utilization of the servo's positioning resolution, and reduces the servo's cost and weight, as these are directly related to the required torque.
- These raw results must be increased by a safety factor, generally 50%, to account for calculation approximations and the inevitable friction or stiff spots in the control system. One must also be wary of manufacturer figures, which more often reflect the servo's breaking point or reversibility point than its usable torque (generally 2 to 3 times lower than the former).
- The surcharge will need to be much greater in the case of control surfaces that are highly exposed during landing, such as flaps. This is especially true on slopes where landings are sometimes hard due to the small size or irregularity of the landing zone, putting significantly more stress on the wing servos during impact (due to the inertia of the control surfaces) than on the airflow during flight.

4.7.4 Air brakes

The last type of control surface discussed here is the airbrake, designed to generate drag. This is either to facilitate landing (possibly by reducing approach speed) or to control the yaw axis (B2-type flying wings, through asymmetrical use). Numerous variations exist, each with its own advantages and disadvantages:

- Vertical blade airbrakes: this system relies on one or more retractable blades integrated into the wing's thickness and extending beyond the upper surface (extrados) as needed via a lever system. This system is very effective but is also somewhat heavy and, above all, difficult to integrate into thin airfoils.
- Simple tilting airfoil: consisting of a single plate embedded within the thickness of the airfoil's formwork, generally on the upper surface (spoiler) but sometimes on the lower surface, and tilting around an axis. Its effectiveness can be increased by the presence of holes, but this complicates the construction because additional bosses must be incorporated to ensure the airfoil airfoil is correctly maintained.
- A tilting airbrake with a circulation system: this is a control surface located on the trailing edge that, when deployed, creates a gap between the upper and lower surfaces. Braking can be remarkably effective if the control surface operates downwards and with a hinge at one-third of its chord. See, for example, the author's Hypnosys2 glider, the plans of which were included in issue no. 690 of Modèle Magazine, published in March 2009 (fig. 60).
- Flaps: also called flaps and widely used in full-size aviation, these control surfaces are deflected approximately 45° to 60° downwards to generate

adequate braking. They are generally used with elevator compensation to cancel out any unwanted pitching moment and thus maintain the flight path.

- Aileron: The principle is the same as with the flap, but the control surface is raised by approximately 30° to 45°. This is the simplest solution because it repurposes existing control surfaces, but the braking effect is only moderately effective and poses control kinematic problems in maintaining aileron deflection when the airbrake function is used. With ailerons covering the entire wingspan, it may be advantageous to lower them rather than raise them if the airfoil is concave, as raising them will more easily increase drag.
- Butterfly: also called AF crocodile, this system combines the action of lowered flaps and raised ailerons. It is the most common system on all performance gliders, providing good braking while avoiding the need for a separate braking device. It can also be used on a flying wing, but its fine-tuning, to find the correct proportionality of flap deflection (between lowering flaps and raising ailerons) to avoid any pitching effect, requires a certain degree of precision.
- Split flap: This flap is a trailing-edge control surface that occupies only the lower surface of the wing (the upper surface remains fixed). Effective and relatively simple to manufacture, this type of flap was particularly used on fighter aircraft during World War II. A variant involves also hinged the upper surface in the opposite direction (upwards), as on the Messerschmitt ME109. This system is used, for example, on the vertical horizontal tail of the American space shuttle… or on that of the author's Fractale (a 60-inch glider with pitcheron wings).
- Fowler-type slotted flap: this is not strictly speaking a braking device, but rather a stall delaying device (more details in §5.4). Thanks to an offset hinge mechanism, this flap retracts as it lowers. This allows both an increase in wing area and the re-bonding of the boundary layer thanks to the slot it exposes (allowing airflow from the lower surface to the upper surface, as with Frise ailerons, see Fig. 58).

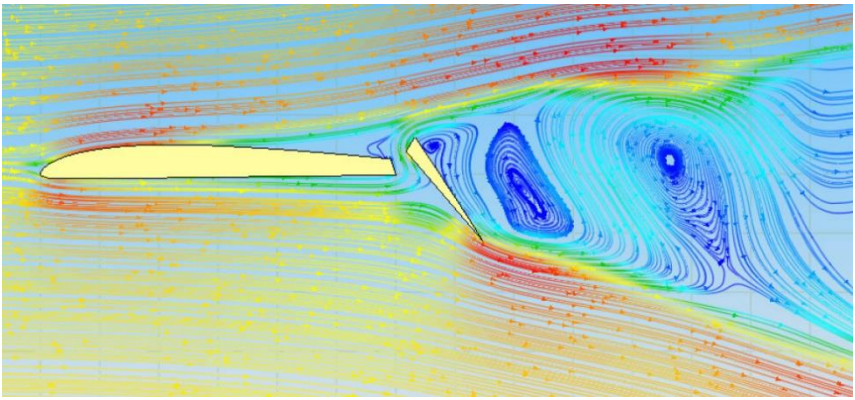

Fig. 60, simulation of the flow around the tilting AF of the Hypnosys2. The braking is due to the significant depression downstream of the wing, with clearly identifiable recirculation structures.

Hypnosys2 with AF deployed… it brakes hard!

4.8 Evaluate performance

Flight performance is studied mainly in level flight, i.e. at variable speed and constant lift, through a plot of two polars as a function of speed: the sink rate and the glide ratio (fig. 61).

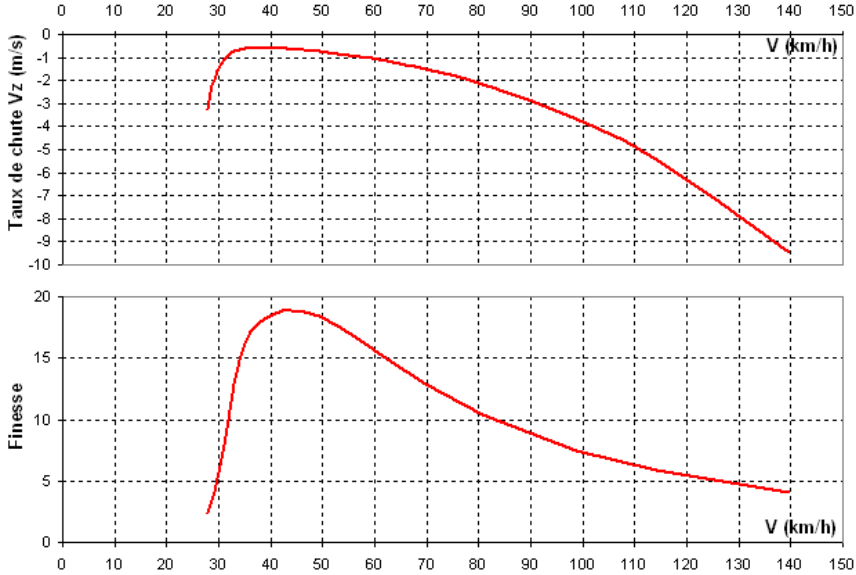

Fig. 61

These polar diagrams allow you to determine key performance elements: minimum sink rate, maximum glide ratio, and associated speeds. Not only does this provide a good understanding of your aircraft's flight envelope, but it also makes comparison with other aircraft possible on paper. This last point is essential, for example, for successfully designing a competition aircraft, which by its very nature is intended to compete with rival models.

For pylon-running type flights, taking place at relatively constant speed and variable lift, it is interesting to also plot several drag polars (one per flight speed studied) allowing to verify the efficiency of the machine both in straight line (low Cl) and in tight turn (high Cl), by means of the Cd/Cl polars of the complete aircraft.

Two reference frames will be manipulated (fig. 62): (x,z) for the aircraft reference frame and (h,v) for the ground (horizontal and vertical axes), the two being linked by the slope of the trajectory (γ) .

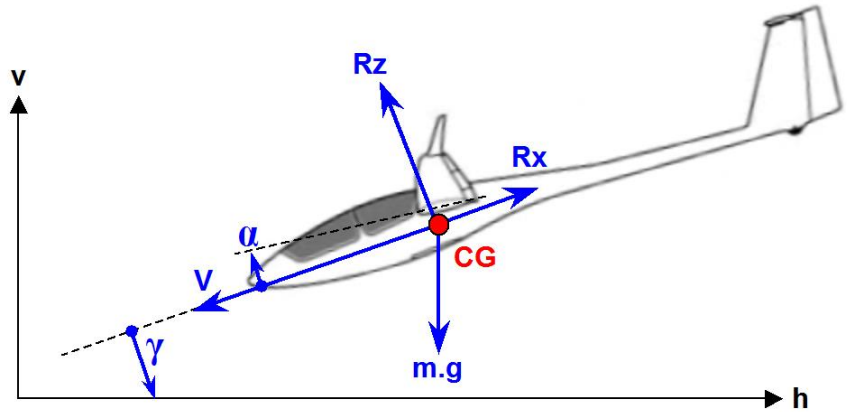

Fig. 62

In the aircraft frame of reference (x,z), the aerodynamic resultants are:

Drag: $Rx = \frac{1}{2}.\rho.S_a.Cx.V^2$

Lift: $Rz = \frac{1}{2}.\rho.(S_a.Cz_a + S_s.Cz_s).V^2$

The contribution of the fuselage to lift does not appear because it is anecdotal, while that of the horizontal tail can be neglected in the general case (excluding canard and tandem).

We then have: $Rz \approx \frac{1}{2}.\rho.S_a.Cz_a.V^2$

The equilibrium of forces on the z-axis (aircraft frame of reference) and the projection of the flight speed onto the horizontal axis (ground frame of reference) give:

$$Rz = m.g.\cos(\gamma) \qquad \text{And} \qquad V_h = V.\cos(\gamma)$$

The slope of descent in level flight is a small angle (a very poor glide ratio of 5 corresponds to an 11° slope, or only a 2% difference on the cosine), so we can write:

$$Rz \cong m.g \qquad \text{And} \qquad V_h \cong V$$

Hence the horizontal speed in level flight: $V_h \cong \sqrt{\frac{2.m.g}{\rho.S_a.Cz_a}}$

We also possess, by definition, finesse: $f = \frac{1}{\tan(\gamma)} = \frac{V_h}{V_v} = \frac{Cz}{Cx}$

SO : $V_v = \frac{Cx}{Cz}.V_h$

Hence the rate of descent in level flight without an engine: $V_v \cong \sqrt{\frac{2.m.g.Cx^2}{\rho.S_a.Cz_a^3}}$

Whether gliding or powered flight (where $\gamma = 0$ and the equilibrium of forces on the x-axis is: Rx = engine thrust), the difficulty in determining the aircraft's performance boils down to knowing only the drag coefficient Cd. Like speed, this coefficient is calculated based on the wing's lift coefficient (Cl), allowing us to then plot the evolution of Vz and f as a function of speed. The points on these polars can, for example, be plotted for lift coefficients ranging from 0.05 to 1.25 in increments of 0.05.

As a first approximation, the total Cd can be broken down into the following elementary Cd values:

- Wing and horizontal tail: airfoil drag coefficient + Induced drag coefficient.
- Vertical tail: Cd airfoil only.
- Fuselage: wetted area drag coefficient + Bypass drag coefficient.
- Landing gear, stays, etc.: Form Cd.
- Interaction between elements: approximately 10% of the sum of the Cd.

All that remains is to calculate these coefficients… Hold on tight!

NOTE

- "Vv" is generally written "Vz": the associated z axis is indeed the ground vertical and should not be confused with the aircraft z axis used for Rz or Cl.
- Substituting the term Cla into the equation for horizontal velocity, we obtain the following relationship:

  $$V_v \cong \frac{\rho.S_a}{2.m.g}.V_h^3.Cx$$

  For a given airspeed, the sink rate depends only on drag and not at all on lift. This is perfectly logical: in the pseudo-isolated system of an aircraft in balanced glide, energy dissipation occurs through changes in potential energy. Drag opposes forward motion, so the link between sink rate and drag is immediate. Lift, implied in the verb "to climb" in the classic phrase "lower the flaps to climb higher in the thermals," is a false friend: in the air frame of reference, the glider is always descending (more or less rapidly).

4.8.1 Airfoil drag (Cdp)

Using numerical wind tunnels like XFoil (or even Eppler) is unavoidable when you want to go into detail. Their analysis can be done directly by calculating the airfoil drag coefficient (Cd) for each Cl and Reynolds number pair studied. This approach is the most accurate but also the most time-consuming and the most sensitive to convergence errors in the numerical wind tunnel. It is significantly more efficient to use a set of pre-calculated polars (at predetermined Reynolds numbers, as proposed in 4.3.4) which are extrapolated to the Cl and Reynolds number pair under study through numerical processing. This can be done either directly by constructing an equation of the form Cd = f(Re, Cl), which proves very complex, or more simply in two steps. First, at the Cl number being studied, a linear interpolation is performed to find the two Cd values corresponding to the two predetermined Reynolds numbers located on either side of the Reynolds number being studied. Then, a simple model of the form Cd = a + b/Re is applied.

A simplified analytical approach can also provide a fairly good overview. The principle involves approximating a single Cd/Cl polar curve, calculated in a numerical wind tunnel, with a parabola. The coefficients of this parabola are determined for a reference Reynolds number, and then the result is adapted to the Reynolds numbers being studied. Like any simplified approach, this one has its limitations and only works reasonably well far from the stall point and for flight Reynolds numbers not too far removed from the reference Reynolds number.

$$Cx_p \approx Cx_{ref} .(\frac{\mathrm{Re}_{ref}}{\mathrm{Re}})^{1/2} \text{ And } Cx_{ref} = Cx_{\min} + k.(Cz_p - Cz_{opt})^2$$

With: Clp = Cl airfoil, Re_ref = Reynolds number at which the drag of the reference airfoil (Cdref) is calculated, Cdmin the minimum drag of the airfoil at Re_ref, Clopt the Cl at which the minimum drag is found and k a coefficient of evolution of the drag.

Re is the Reynolds number of the mean aerodynamic chord (= surface area / wingspan) - and not of the average chord, this time - of the wing being studied, which will be calculated for each speed V deduced from the current wing lift coefficient (Cl).

Since the calculation reference is the wing's lift coefficient (Cl), it will be necessary to convert the first lift coefficient (Clp) to the wing's aspect ratio (Cla) by incorporating the wing's aspect ratio. In the case of the horizontal tail, the same procedure will be followed, using the relationship that gives its lift coefficient as a function of the wing's lift coefficient and parameters such as the center of gravity (CG) position or the airfoil's lift coefficient (Cm0).

The following typical values can be used, given at a reference Reynolds number of 200. 000:

- Initial airfoil: Cdmin = 0.010, Clopt = 0.5, k = 0.011
- Transition airfoil: Cdmin = 0.009, Clopt = 0.3, k = 0.011

- Quick airfoil: Cdmin = 0.008, Clopt = 0.1, k = 0.011

For the horizontal tail, we can simplify things by setting Cdref = 0.01 (biconvex airfoil) to 0.02 (plank airfoil) with a reference Reynolds number of 100 000.

To refine the modeling, the 1/2 interpolation coefficient for Re can be replaced by an adjustable coefficient depending on the airfoil airfoil to better match the polars imported from the numerical wind tunnel. Typically, coefficients of 1/1.5 and 1/3 give good results for Re values below and above Re = 200, respectively. 000.

4.8.2 Induced drag (Cdi)

Although the phenomenon at its origin is physically complex and therefore difficult to model, it can nevertheless be described by a very simple equation:

$$Cxi = \frac{Cz^2}{\pi.\lambda.e}$$

With : λ = wing aspect ratio and e = Oswald coefficient (which is at most 1 for a wing with elliptical lift distribution).

In the case of the horizontal tail, a secondary induced drag is added to the drag directly generated by the horizontal tail's lift. This is a unique effect of the wing's wake, as the horizontal tail's lift is not perpendicular to the direction of flight but inclined backward by the wake deflection angle: the projection of this lift in the aircraft's frame of reference opposes forward motion. Conversely, negative horizontal tail lift has a forward component in the aircraft's frame of reference and consequently generates a driving force. Since the deflection angle is very small, these induced components can obviously be neglected, but it is always useful to be aware of their existence.

In the case of vertical tail, the angle of attack of which (angle of skid) is generally zero to very low, the induced Cd is not considered.

NOTE
Most aerodynamics textbooks and publications on the Oswald coefficient consider it through a highly simplified model of wing drag, based on zero-lift drag (Cd0, viscous drag) supplemented by lift-related drag (incorporating the effect of aspect ratio). In this context, the Oswald coefficient implicitly covers airfoil drag by correcting it for the lift effect (equivalent to the k factor in parabolic modeling in §4.8.1). The approach adopted in this book, which incorporates the actual airfoil drag through its Cd/Cl polars, uses the Oswald coefficient in its precise definition, that is, as the difference in induced drag compared to an equivalent elliptical wing. This is a more intellectually satisfying approach, as each contributor to drag is correctly identified, and, more importantly, it is more accurate.

4.8.3 Fuselage drag (Cdf)

The following equation (Prandtl/Von Karman in turbulent flow for Re < 10^6) is found in the literature , providing a satisfactory estimate of the wetted surface drag coefficient of the fuselage, also including an estimate of the form drag (stub) at zero angle of attack . :

$$Cx_{fSm} = \frac{0{,}074}{\mathrm{Re}_f^{1/5}}$$

With: Ref = Reynolds number of fuselages (= 68.Length.V)

For the bypass drag under angle of attack, I propose a personal empirical formulation which, to a first approximation, gives fairly satisfactory results:

$$Cx_{fc} \approx 0{,}006.\frac{l}{h}.k_f.\alpha_f{}^2$$

With: l and h = fuselage width and height, kf = shape coefficient ranging from 1 (very streamlined and well rounded fuselage) to 2 (box fuselage with sharp angles), αf = angle of attack of the fuselage in the relative wind.

Since the angle of attack of the fuselage is usually mechanically linked to that of the wing by the wing/fuselage angle (α K), we can therefore write:

$$\alpha_f = \frac{9{,}1}{A_a}.(Cz_a - \frac{0.11}{A_a.(\alpha\kappa_a - \alpha 0_a)})$$

Hence:

$$Cx_{fc} \approx 0{,}05.\frac{l}{h}.k_f.(\frac{Cz_a - 0.11/A_a.(\alpha\kappa_a - \alpha 0_a)}{A_a})^2$$

If the wing/fuselage alignment corresponds to the angle of attack of the adjustment Cl, it will be replaced at the following point:

$$0.11/A_a.(\alpha\kappa_a - \alpha 0_a) = Cz_{a\ regfuse}$$

In the case of an aircraft with pitcheron wings, the angle of attack of the fuselage is linked to that of the horizontal tail. Therefore:

$$\alpha_f \approx \frac{9{,}1}{A_s}.Cz_s \text{ Hence: } Cx_{fc} \approx \frac{l}{h}.k_f.(\frac{Cz_s}{A_s})^2$$

The two coefficients Cdf will be used below with the wetted surface area of the fuselage (Smf), which can be approximated from the surface area of a cylinder with the same major cross-section (width l, height h) and length (L) as the fuselage:

$$Sm_f \approx 0{,}65.(\pi.\frac{l+h}{2}.L).k_f \approx (l+h).L.k_f$$

4.8.4 Accessory drag (Cdu)

This is a shape trail, which we will break down into three levels:

- $Cx_u = 0.2$ for a highly streamlined element, such as a wheel fairing or a stay with a thin airfoil
- $Cx_u = 0.6$ for a rounded element, such as a wheel or stay
- $Cx_u = 1$ for any form

These approximations are valid for turbulent flow (below the critical Reynolds number of the object), which is generally the case at our scales.

Each time, we will use these coefficients with the apparent surface area seen from the front (height x width) of the element considered (Su).

4.8.5 Total drag

Now that we have all the basic building blocks, it is possible to construct a fairly realistic estimate of the total drag of the model using the sum of the basic drag coefficients (p = airfoil, a = wing, s = horizontal tail, f = fuselage, d = fin) relative to the wing area:

$$Cx_{total} \approx 1{,}1.(Cx_{pa} + Cxi_a + (Cx_{ps} + Cxi_s).\frac{S_s}{S_a} + Cx_d.\frac{S_d}{S_a} + (Cx_{fSm} + Cx_{fc}).\frac{Sm_f}{S_a} + \sum Cx_u.\frac{S_u}{S_a})$$

In short, it's not simple at all, but very instructive because it highlights the consequences of all the choices made during the model's design: mass, airfoil, aspect ratio, geometry, center of gravity, etc. Similarly, we can manipulate air density to study the effect of altitude and temperature on performance, which will allow us to conclude that it's better to try to break a speed record in hot, dry weather rather than at the seaside in cold weather.
As a first approximation, the density of air can be calculated as follows:

$$\rho \approx 1.293.\frac{273}{273+T}.\frac{20-H}{20+H}$$

With: T = temperature in °C and H = altitude in km relative to sea level.

It then becomes possible to construct this type of graph (fig. 63, extracted from PredimRC), allowing for detailed analysis of the contribution of each element to the drag and for making fine comparisons between models.

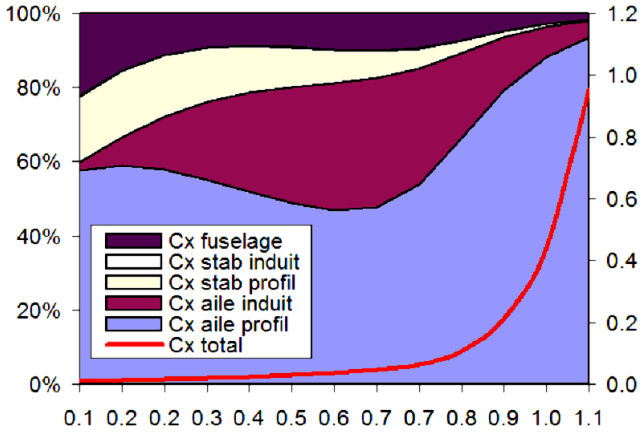

Fig. 63, distribution of Cd and total Cd, as a function of Cl

4.8.6 Polar in a turn

In addition to level flight polars, it is also useful to plot polars in a stabilized turn (or spiral). If φ is the wing bank angle with the horizontal, the projection of the forces onto the vertical axis of the ground frame gives:

$$Rz.\cos(\varphi) = \frac{1}{2}.\rho.S_a.Cz_a.V^2.\cos(\varphi) = m.g$$

Hence: $V_h = \sqrt{\frac{2.m.g}{\rho.S_a.Cz_a.\cos(\varphi)}}$ and $V_v = \sqrt{\frac{2.m.g.Cx^2}{\rho.S_a.(Cz_a.\cos(\varphi))^3}}$

4.9 Powered flight

4.9.1 Level flight

Let us equip a glider with a wingspan of 2m, aspect ratio 10, airfoil SB96, wing loadings of 20 g/dm² (empty) and 40 g/dm² (ballasted), equipped with an emergency motorization (7x5 propeller, 60W electric), and draw the graph of the evolution of the powers as a function of the level flight speed (fig. 64).

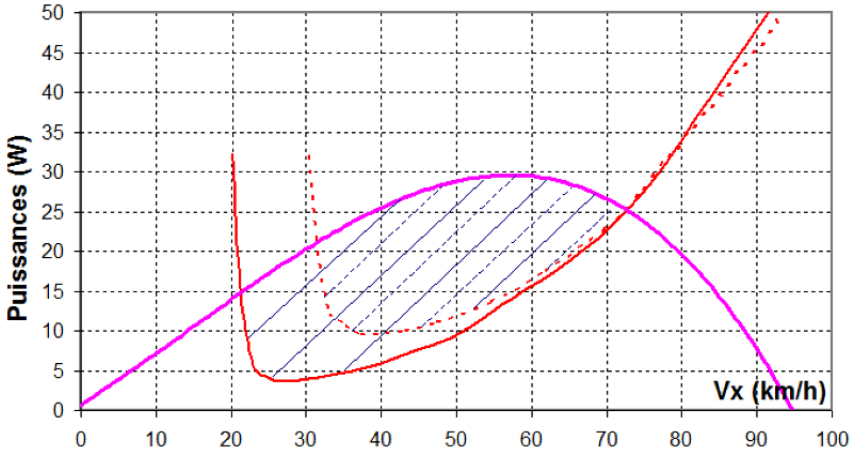

Fig. 64

The two red curves (one per mass studied) represent the aerodynamic power dissipated by the aircraft (Pw) in level flight as a function of speed, calculated from its rate of descent (which the model would have if it were not supplied with energy to remain at a constant altitude):

$$Pw = m.g.V_v = m.g.V_h.\frac{Cx}{Cz}$$

The magenta curve corresponds to the evolution of the power (Ph) transmitted by the propeller (full throttle) to the model, zero on the ground and when the flight speed catches up with the engine's no-load speed, maximum for the optimal propeller adaptation point:

$$Ph = T.V$$

With: T the propeller thrust (or the thrust of a turbine).

Four key areas can be distinguished:

- The first intersection (on the left) between the two types of curves (Pw, Ph) indicates the minimum engine speed, called the second regime (here approximately 22 to 32 km/h depending on the aircraft's weight). Below this speed, the engine power is no longer sufficient to overcome drag, and the aircraft descends despite full throttle. The only way to recover from this situation is to apply airspeed to regain power... logical, but requiring overcoming the natural reflex to continue pulling back on the elevator.
- The second intersection gives the level flight speed with the engine at full throttle (here approximately 73 km/h, almost independent of mass).
- Between these two intersections, the area between the two curves represents the power reserve in level flight at intermediate speeds (since the engine is not at full throttle at these speeds).
- The greatest vertical distance between the curves indicates the maximum propulsive efficiency speed.

By playing around a bit with the input data, we can draw the following conclusions:

- At high speed, aerodynamic power depends almost exclusively on flight speed, as drag differences related to the mass of the aircraft are small (low Cl => low induced drag).
- Performing the same exercise but changing only the airfoils reveals that the performance differences are fairly insignificant, except for very different airfoils. Again, the airfoil isn't everything…
- A large propeller isn't necessarily better than a small one. The best propeller is actually the one best suited (i.e., providing the greatest thrust, therefore power, and thus propulsive efficiency) to the operating point in question. Except for slow-flying models like 3D or indoor models, the advantage often goes to "semi-square" to "square" propellers, meaning those with a pitch between 70% and 100% of their diameter.

A similar study, valid as long as the climb gradient is not too steep (i.e., comparable to level flight), can be performed for the rate of climb, using this simplified formula:

$$V_h \approx \frac{Ph - Pw}{m.g}$$

The following graph is obtained (fig. 65).

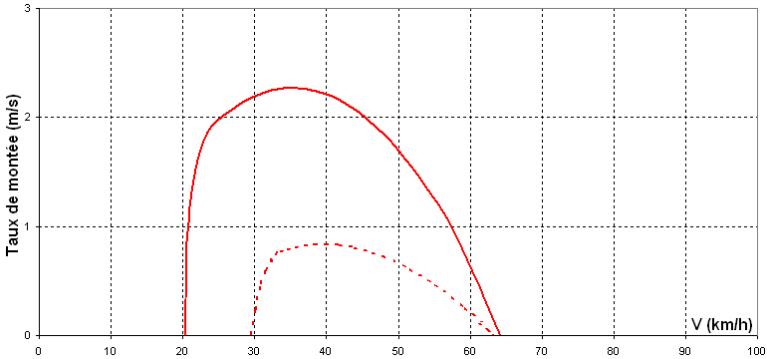

Fig. 65

Controlling the flight speed, and therefore the climb angle, is essential here [for a low-powered aircraft] for efficient climbing.

4.9.2 Climb performance

As soon as the climb gradient becomes significant, it becomes necessary - for the accuracy of the results - to perform the calculations in the aircraft frame of reference, considering that the engine thrust is aligned with the flight speed (fig. 66):

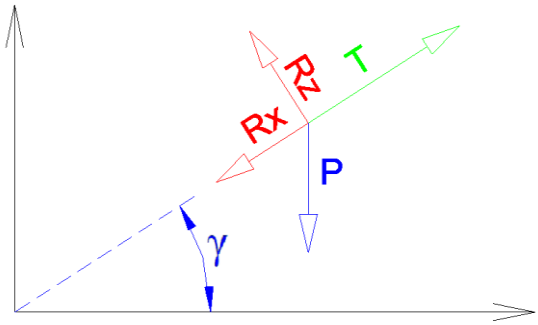

Fig. 66

The principle consists of finding, for each angle of climb from 0 to 90°, the solution - if it exists - in terms of velocity on trajectory (Vx) and Cl to the following equilibrium equations of forces (lift, drag, weight, traction):

$$T = Rx + P.\sin\gamma \qquad \text{And } Rz = P.\cos\gamma$$

Since the first equation can hardly be solved formally, it involves an iterative calculation with, for each Vx considered in a range and with an adapted step, the calculation of the total drag Rx (for the Cl calculated with the second equation) and the engine thrust T.
All that remains is to project the velocity onto the trajectory in the ground frame of reference:

$$V_h = V.\cos\gamma \text{ And } V_v = V.\sin\gamma$$

By repeating the exercise for different configurations (propellers, airfoils, etc.), the various results obtained can be superimposed to enrich the study. The following polars are obtained (Fig. 67), as a function of horizontal speed and climb angle:

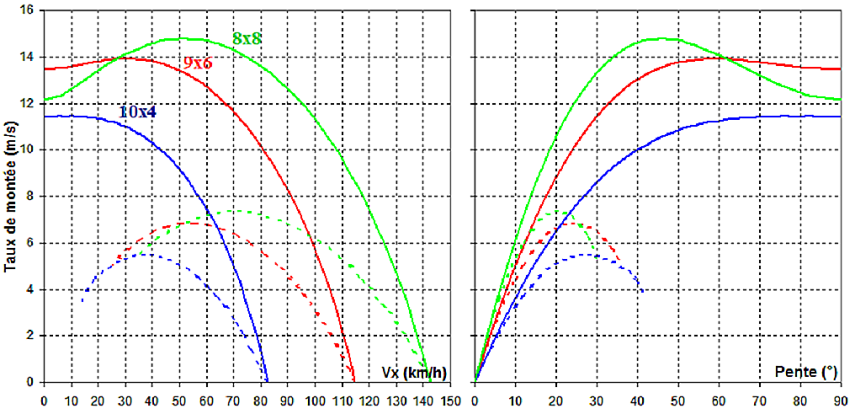

Fig. 67

In this case, the simulation was carried out with the same model as before, with the same electrical input power (400W this time) and by only playing on the propeller size (chosen to stay at the same engine speed, in order to introduce the minimum of parameters in the analysis) and the mass (still 20 and 40 g/dm², in dotted line).

The results are particularly informative:

- For a given configuration (aero + GMP), the maximum rate of climb is, to the first order, proportional to the mass (no surprise…).
- Contrary to popular belief, the best propeller [for the fastest climb] is not necessarily the one with the largest diameter, but rather the one with the largest relative pitch (pitch versus diameter). Indeed, while at the same engine speed, the static thrust (on the ground) of a large-diameter, low-pitch propeller is significantly greater than that of a smaller, square propeller (in this example, approximately 19 N versus 13 N), the thrust of the latter decreases much less rapidly with increasing airspeed and therefore becomes greater at high airspeeds.

- The greater the input power, the less critical the climb angle is to achieve the best climb rate.
- The value of V at Vv = 0 directly gives the maximum level speed, for the propeller and engine studied.

The analysis can be taken further, still at the same electrical power but considering the engine speed as an adaptation variable, in order to broaden the range of propellers studied and be much more selective (fig. 68):

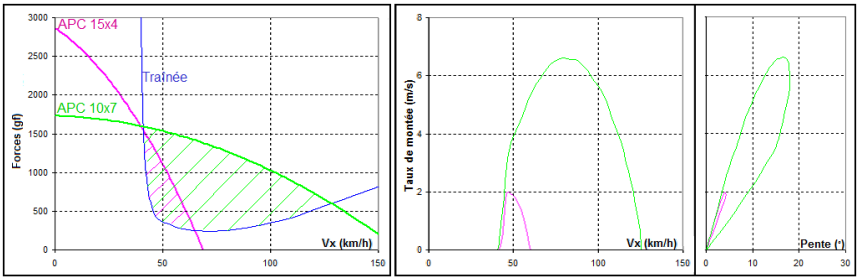

Fig. 68, study of a fast trainer with 600 W electric

This time, the forces (propeller thrust vs. model drag) are considered on this graph to analyze level flight. The result is easier to interpret than with power, but obviously identical. As already demonstrated above, a propeller with a low relative pitch, despite its high static thrust, proves unsuitable for this type of airframe, both in terms of thrust reserve (hatched area) and rate of climb or speed.

4.9.3 Propeller model

In order to carry out the preceding simulations, it is necessary to have a propeller model, allowing the calculation of its thrust T (in N, newton) and the mechanical power at the shaft P (in W, watt) required for its drive.

The fundamental equations are as follows:

$$T = \rho.C_t.Dia^4.N^2$$

$$P = \rho.C_p.Dia^5.N^3$$

With :

ρ = air density
Ct = propeller traction coefficient
Cp = propeller power coefficient
Dia = diameter of the helix
N = propeller speed

Ct and Cp are not constants but vary with flight speed. They are given in the form of 2D polars measured in a wind tunnel (fig. 69).

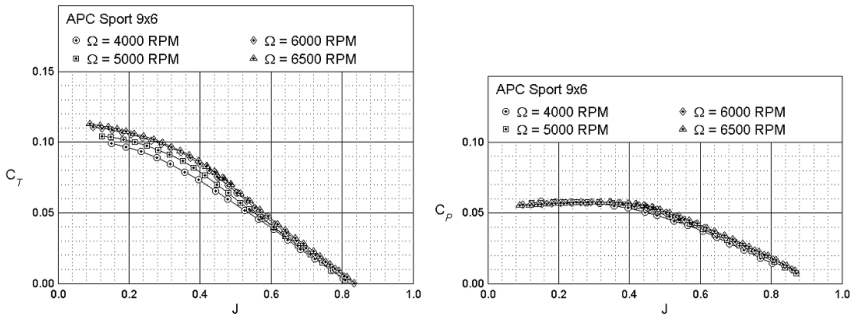

Fig. 69, source: http://m-selig.ae.illinois.edu/props/propDB.html

The x-coordinate of these polar curves is not directly the flight speed, but the propeller's forward speed:

$$J = V/(N.Dia)$$

J is a dimensionless coefficient, making it possible to compare propellers regardless of their size. It represents the angle of attack of the propeller airfoil, that is, the angle (Fig. 70) between its chord and the relative velocity vector at that point (obtained by combining the flight speed and the peripheral velocity). This angle is generally considered to be 70% of the propeller radius.

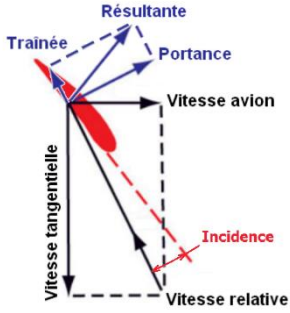

Fig. 70

J is therefore the equivalent of Cl at the propeller level. And, as with a wing, this results in lift and drag which, projected into the aircraft's frame of reference, give the propeller thrust and the resisting torque (which the engine must overcome).

By definition, the maximum value of J is therefore: $J_{\max} = Pas / Dia$

J = 0 represents the static condition (zero velocity), i.e., at ground level. If we take the polar curves Ct and Cp with J = 0, the corresponding coefficients Ct0 and Cp0 allow us to directly determine the static traction and power.

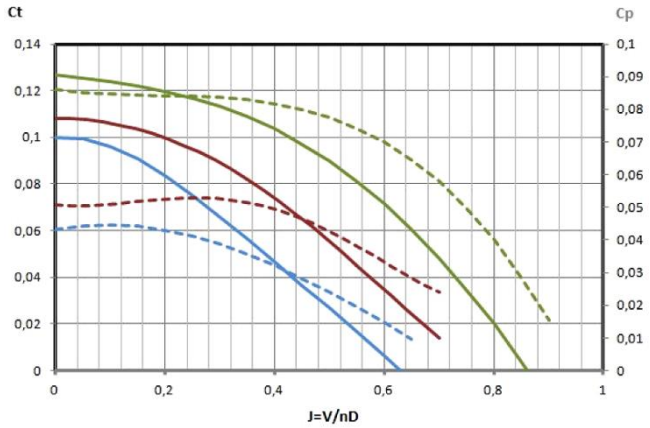

Fig. 71 , traction coefficients (solid lines) and power coefficients (dotted lines) of various propellers (in blue APC 8x4E, in red APC 9x6S and in green APC 7x6E).

For our scale models, the polars of Ct and Cp can be found on Michael Selig's website mentioned earlier or on Guillaume Rouby's excellent website (http://aerotrash.over-blog.com/).

It is also possible to estimate these coefficients satisfactorily using the following correlations (work by Guillaume Rouby based on APC helices):

$$C_t = -0{,}082.(J - J_{\max})^3 - 0{,}25.(J - J_{\max})^2 - 0{,}264.(J - J_{\max}) + 0{,}02$$

$$C_{p0} = k.(0{,}197.J_{\max}{}^3 - 0{,}298.J_{\max}{}^2 + 0{,}225.J_{\max} - 0{,}02)$$

Cp = Cp0 up to Jmaxreal/2 then decreasing linearly up to approximately Cp0/3 at Jmaxreal (its calculation is defined below).

With: k = 0.8, 1 and 1.3 depending on the blade width (narrow, normal, wide type "SF").

We will note on the polars of Ct and on the associated correlation that the real step (corresponding to Ct = 0) is greater than the step (probably purely geometric) given by the manufacturers.

On average, we have:

$$Pas_{réel} = 0{,}85.Pas + 0{,}2.Dia$$

Hence: $$J_{\max\,réel} = 0{,}85.Pas / Dia + 0{,}2$$

The zero traction speed (T0), commonly referred to by the English term "Vpitch" (step speed), is then:

$$V_{T0} = Pas_{réel} . N_{T0}$$

NOTE
Propeller operation is optimal when the air being moved is "clean" and when good continuity is ensured between the spinner and the fuselage. Consequently, the result will be less good than estimated here in the case of an installation with a large open engine cowling, Baron type, or behind a wing (hence the characteristic noise of some "pusher" aircraft, the propeller blades crossing the wing's trailing edge wake with each revolution).

4.9.4 Focus on propeller efficiency

Propeller efficiency (fig. 72) is the ratio between its power transmitted to the aircraft and the mechanical power required by the shaft to drive it into rotation (that is to say, to overcome its drag, we come back to that again!).

Either : $$\eta = Ph / P_{mot} = J.C_t / C_p$$

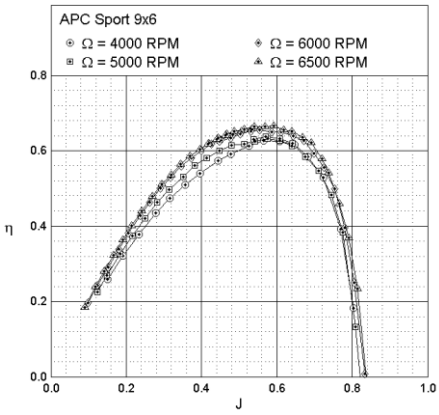

Fig. 72

Note that the efficiency is zero at rest and Jmax (therefore at Vpitch), which is logical since in the first case there is a force but no displacement (therefore no work done) while it is the opposite in the second case (zero traction).

With the propeller model above, it becomes easy to study the influence of the different propeller parameters on its efficiency.

Let's start with the step, at the same diameter:

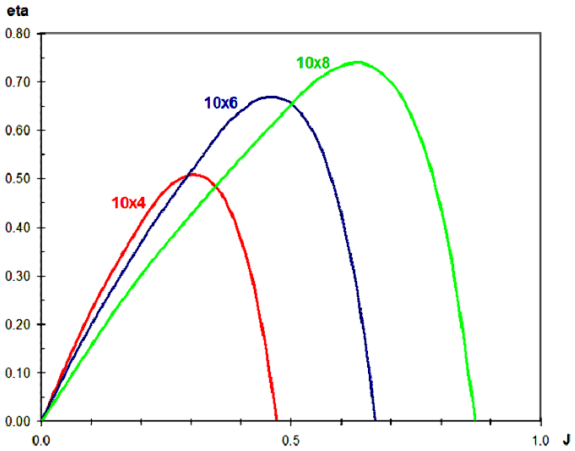

Fig. 73

This influence, which confirms the observation made in §4.9.1, proves to be significant both on the maximum efficiency value and on the corresponding J value. This is naturally explained by the increase in traction at higher speeds, and therefore in power Ph, when the pitch increases.

This same analysis can be performed at the aircraft level, using Vx instead of J (see §4.9.1), and it will then be observed that maximum power is transmitted by the propeller at a certain flight speed that depends on the pitch, generally at 60% of Vpitch. If the propeller pitch is too small, the maximum propulsive efficiency may be located too low in the aircraft's flight envelope. At nominal speeds, the propeller then operates at poor efficiency and wastes engine power.

The influence of the aerodynamic quality of the propeller can also be significant; there can be up to a 10% difference in efficiency between a roughly hewn wooden propeller and a modern cast propeller.

In comparison, and contrary to popular belief, the influence of propeller diameter is negligible, since a good full-size propeller several meters in diameter offers a maximum efficiency only 5 to 10% higher than that (approximately 75%) of a good racing propeller of just 5 inches in diameter. It's also worth noting, to further illustrate the point, that a tiny GWS 3x3 (not even 8 cm in diameter…) offers a maximum efficiency of almost 70%! Consequently, the argument justifying the use of a reduction gear with a large propeller is weak, as the efficiency loss due to the reduction gear is generally of the same order as the gains from the propeller diameter effect (very small, therefore) and from increasing the motor's KV rating (see below). Not to mention the cost and complexity of this solution.

NOTE

- If there's only one thing to remember when choosing a propeller, it's that its diameter is not at all a determining factor in its efficiency. Conversely, a poorly matched pitch, typically undersized relative to the aircraft's flight speed, is a real source of wasted energy. This affects both the propeller's intrinsic efficiency and its propulsive efficiency if the propeller's maximum efficiency is poorly positioned within the flight envelope.
- The sole criterion for choosing the diameter is the propeller's mechanical resistance to centrifugal force. Since centrifugal force is proportional to the radius and the square of the rotational speed, it is clear that increasing power requires indefinitely increasing the rotational speed and necessitating an increase in propeller diameter. This logic also applies to both internal combustion and electric motors; in most cases, it is possible (and generally more advantageous) to maintain direct drive.

4.9.5 Number of blades and diameter equivalence

Since Cp0 depends mainly on Jmax (the terms in Jmax ^{3} and Jmax ^{2} canceling out at the first order), therefore on Pas/Dia, we deduce that the power at the shaft required to drive a propeller at a given speed is a function of Pas.Dia ^{4}.

Consequently, the power equivalence [at the same operating conditions] between two n-bladed propellers can be written as follows:

$$n_1.Pas_1.Dia_1^4 = n_2.Pas_2.Dia_2^4$$

Contrary to popular belief (that the more blades there are, the more each one sees the wake of the previous one), the impact of the number of blades on the actual pitch is minor, on the order of 1 to 5% when going from a two-bladed to a three-bladed design. The effect is slightly more noticeable on the ground, where the airspeed is zero, but the ground is not the same as flight…

4.9.6 Electric motor model

An electric motor and controller assembly can be considered (fig. 74) as a resistance (R) in series with an inductance (generating a back electromotive force, FCE):

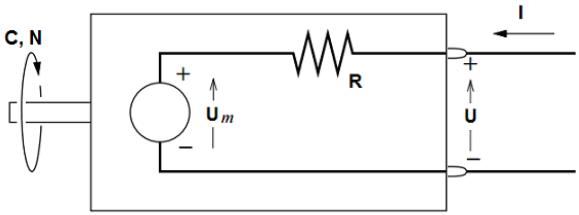

Fig. 74

We have:

$$P_{meca} = U.I.\eta_{mot} = C.N$$

With :

Electrical input: I is the current (in A), U is the voltage (in V)
Output (mechanical): C is the torque (in Nm), N is the speed (in $^{rad.s^{-1}}$)

The fundamental equations are as follows:

$$C = \frac{I - I_0}{KQ}$$

$$U = U_m + R.I$$

$$U_m = (1 + k_C.N).\frac{N}{KV}$$

$$R = R_0.(1 + k_T.\Delta T) = R_0 + R_0.k_T.\frac{\Delta T_{\max}}{I^2_{\max}}.I^2$$

With :

R: internal resistance of the motor (R0 when cold)
I0: motor no-load current
KV: operating constant
KQ: torque constant
kT.ΔT: internal resistance correction as a function of temperature rise (kt = 0.0042 °C $^{-1}$ for copper)
kC.N: torque correction as a function of engine speed

These two corrections are generally neglected, while KQ can be approximated to KV, hence the system of equations:

$$N \cong (U - R_0.I).KV$$

$$C \cong \frac{(U - R_0.I).(I - I_0)}{N}$$

All that remains is to find the constants R0, I0, and KV (knowing that, in the case of brushless motors, these are apparent constants that incorporate both the

characteristics of the motor and those of the controller). However, apart from KV, the other constants are poorly documented or not documented at all by manufacturers. It is generally necessary to resort to bench testing or rely on data from software such as DriveCalc.

As with propellers using Cp and Ct, an efficient approach is to model these constants based on accessible parameters, thus avoiding the need for intimate knowledge of each engine. Guillaume Rouby (him again!) had the idea of using the engine mass (denoted m), based on two obvious facts (though they still needed to be properly applied…): the larger an engine is or the faster it rotates, the more powerful it is and the better its efficiency.

The correlations are as relevant as they are surprisingly simple:

Iso-KV

Moteur	KV	Masse	Imax	I0	Ri
Turnigy AX-2203C	1400	20	7	0.2	0.5
Turnigy 2205C	1400	28	9.5	?	?
Turnigy D2826-10	1400	50	21	?	?
NTM 2836	1400	86	45	?	?
NTM 3536A	1400	117	55	?	?

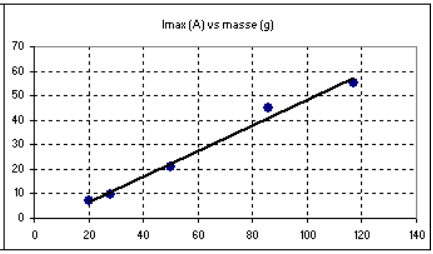

Iso-masse

Moteur	KV	Masse	Imax	I0	Ri
NTM 2836	750	87	17	?	?
NTM 2836	1000	89	30	?	?
NTM 2836	1200	85	36	?	?
NTM 2836	1400	86	45	?	?
NTM 2836	1700	87	50	?	?

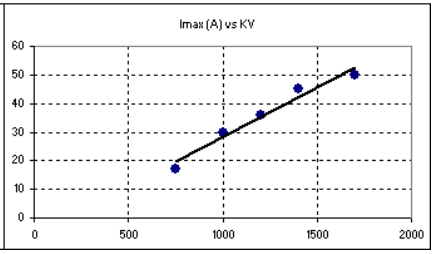

Fig. 75

From this, we can deduce a performance criterion (ranging from approximately 2, mediocre, to 3, excellent) classifying electric motors (m in kg) in the first order:

$$Q_{mot} = \frac{P_{\max}}{KV.m}$$

One final point concerns the effect of KV on torque and efficiency, easily identifiable on a motor available in two very different windings:

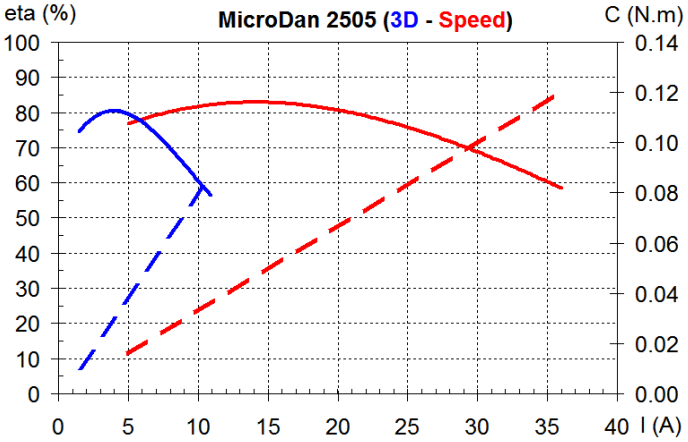

Fig. 76, measurements on the test bench (KV 1160 and 2840) .

Like a conventional brushed motor, the torque of a brushless motor is directly proportional to the current drawn. The maximum torque of a high KV motor is significantly greater than that of a low KV motor, which is often mistakenly associated with "more torque." This is true, but only at the same operating speed. In terms of efficiency, there is an improvement and a wider operating range with higher KV.

NOTE
These findings show that, given the small impact of propeller diameter on its efficiency, using a propeller "not too large" with an engine with a KV "not too low", rather than the other way around, can be beneficial for both the mass of the powertrain and for propulsive efficiency.

The models derived from these correlations are as follows:

$$R_0 = 0.005 + 31.\frac{k}{m^{1.6}.KV^{1.4}}$$

$$I_0 = \frac{KV}{1+\delta KV}.(8.10^{-6}.m + 6.10^{-9}.(\frac{N}{m})^{1.5})$$

With :

k = engine quality coefficient (good 0.75, average 1, poor 1.25)

KV correction if > 1000: $\delta KV = 6.10^{-6}.(KV - 1000)^{1.7}$

I_0 is corrected here according to the actual engine speed (second term of the equation), which allows the implicit integration of the corrections kT.ΔT and kC.N identified above.

One final relationship completes this structure:

$$I = \frac{U - N / KV}{R.(1 + 0{,}07.N / KV)}$$

N is the static regime (on the ground), which can be fixed a priori by considering the engine loading case:

$\frac{N}{KV.U}$ = 65% (very charged), 75% (normal), 85% (lightly charged)

Similarly, the following battery voltage values can be used, which are generic in the case of "normal" use (current between approximately 1/2 and 2/3 of continuous Imax): U /cell = 2.8 V (LiFe), 3.5 V (LiPo – Li-Ion)

NOTE

Note that everything above implicitly assumes full throttle operation at ground level, the only perfectly characterized operating point of the engine. Under engine speed regulation, we obtain this type of result:

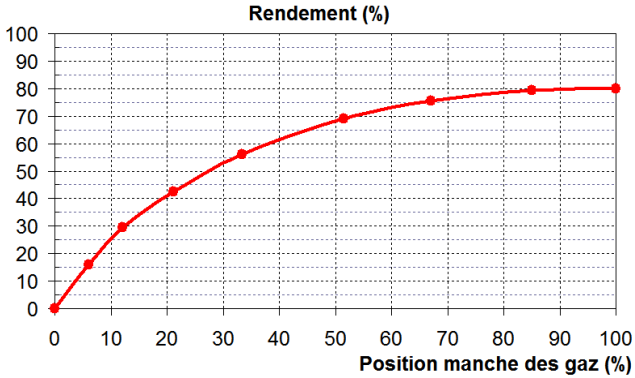

Fig. 77, measurements on the test bench with variable setpoint.

We can de facto conclude that an engine that is too powerful for the need, and therefore constantly working at partial speed, is largely detrimental to efficiency and therefore to range.

4.9.7 Model assembly strategy

The time comes to assemble these models to determine a GMP. To do this, it is first necessary to determine a solution strategy, choosing from all the manipulated data those that will be the outputs of the calculations, the others being the imposed input data.

Generally, choosing the motor specifications beforehand proves quite tricky, whereas selecting the electrical power is more straightforward (thanks to well-known guidelines such as: 100 W/kg for a relaxed flight, 200 W/kg for more dynamic flight, and 400 W/kg for climbing). Similarly, choosing the propeller is fairly simple once the importance of pitch is understood. Ultimately, it makes sense to specify the electrical power (i.e., the battery voltage and a preliminary current) and the propeller, then determine the engine speed and ground traction (control values), and consequently, the motor's characteristics (m, KV, I0, R0) to meet the required workload.

Of course, if the motor is known, it is also possible to use its characteristics by imposing the propeller and battery voltage to observe the result (I, N, Tstat, then Tvol).

In flight simulation, it is also important to consider the evolution of engine speed as a function of flight speed. The calculation of the maximum level flight speed is then much more accurate (sometimes surprisingly, it may even exceed the ground speed…), and it also becomes possible to calculate the intensity of flight, and therefore the range.

4.10 Clarification

Calculating the center of gravity (CG) and engine settings provides a solid foundation for a smooth first flight. However, it's crucial to remember that approximations will always exist, regardless of the precision or power of the calculations or software used. Therefore, the initial flights should be conducted with the usual precautions and primarily focused on finalizing the settings, especially the trims, center of gravity, and engine angles.

Since these settings are interdependent, the order of adjustment and the associated methodology are essential to avoid the common pitfall of correcting one defect with another, such as trying to compensate for a tendency to climb by moving the center of gravity forward. While this might work, it comes at the cost of unnatural behavior at certain flight speeds.

4.10.1 Workshop adjustments

The first step is to mark the fuselage's centerline (Fig. 78), for example, by using a line stretched along the fuselage between two pieces of masking tape. This centerline will serve as a reference point for incidence settings and for horizontal alignment. Generally, this centerline passes through the propeller spinner, or the nose for a glider, and half the height of the tail boom just before the fin.

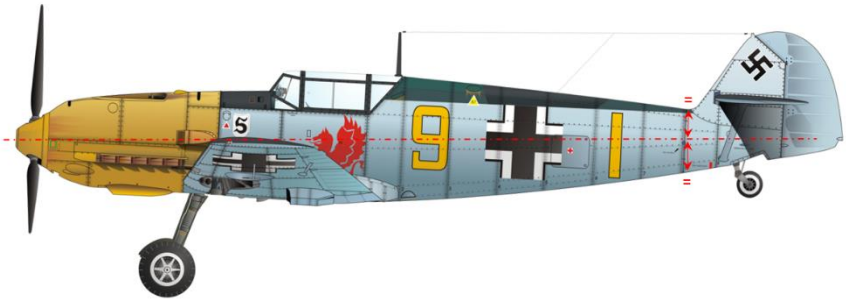

Fig. 78, materialization (red line) of the median axis of the fuselage.

Several techniques exist for measuring the center of gravity (CG) and therefore adjusting it. The most common involves balancing the model on a support (or even using your fingers, although this is significantly less precise) at the calculated position: if the model leans forward, its center of gravity is further forward, and the weights must therefore be moved back; conversely, if the center of gravity is too far forward, the goal being for the fuselage's centerline to be perfectly horizontal. In the case of a low-wing aircraft, it is generally preferable to

position it inverted so that the balance on the support is stable (with the vertical CG lower than the point of contact).

Another technique, known as weighing (Fig. 79) and originating from full-size aviation, proves more precise and very practical to implement. The principle consists of placing the aircraft on scales, one at the level of the main landing gear (one scale under each wheel or one scale under the middle of a beam on which the wheels rest) and one under the tail skid or the third wheel. This also works with a glider, which is placed on two scales using two cradles. In both cases, the aircraft must be as level as possible, as it would be in normal flight.

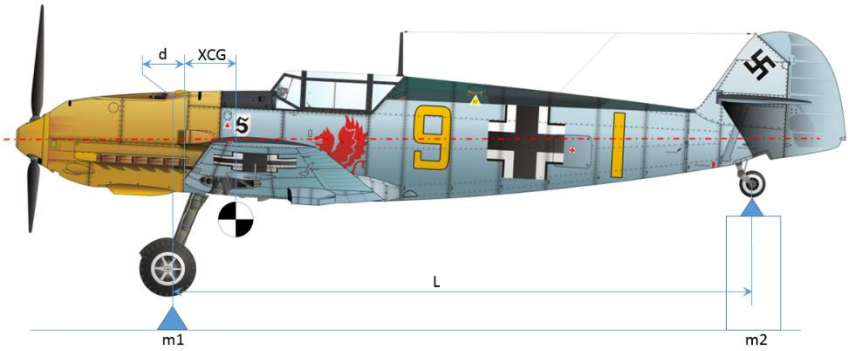

Fig. 79, measurement of the position of the CG by weighing.

From this diagram, a simple leverage calculation, easily automated on an Excel spreadsheet (available on the author's website, with automatic calculation of the centering lead), allows the position of the CG to be determined:

$$X_{CG} = \frac{m2}{m1+m2}.L - d$$

With: L, d and XCG positive when the associated points are found behind the vertical of the main wheels, otherwise negative.

With respect to the fuselage's median axis, the angle of attack is calculated by trigonometry (fig. 80):

$$\alpha = \arcsin(\frac{H1-H2}{C})$$

With: H1-H2 = height of the leading edge relative to the trailing edge.
C = chord.

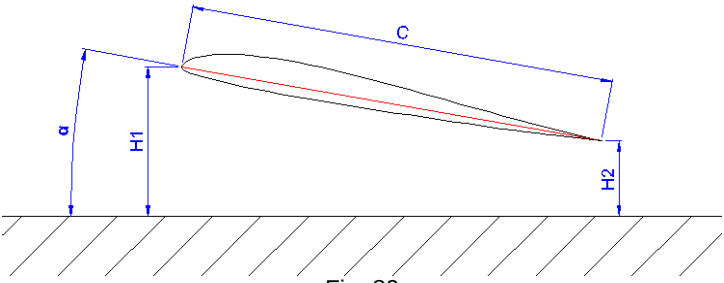

Fig. 80

Since these are generally small angles, the relationship between angle (in degrees) and measured dimensions (in mm) can be simplified as follows:

$$\alpha \approx 57.\frac{H1 - H2}{C}$$

4.10.2 Trim adjustment

The exercise may seem trivial, yet it's undeniable that many pilots use the control sticks to compensate for a tendency for a model to pitch down, pitch up, or bank, simply to keep the control surfaces aligned with the wings on the ground. Admittedly, it looks better, but what discomfort! Similarly, it's common to try to compensate for a tendency to pitch or roll by adding lead, which is a mistake because, in the first case, it affects longitudinal stability, and in the second, it adds inertia in roll.

However, there's nothing unusual about trimming a control surface to compensate for an inevitable imperfection, as no aircraft is built perfectly straight or symmetrically, or is simply poorly designed. Therefore, the primary objective is to achieve straight flight, and there's only one way to do this: completely release the control sticks (strictly speaking, by removing your fingers from the transmitter), observe the model's trajectory, and then trim accordingly until you obtain a perfectly straight path, without any further input from the sticks. In the case of a motorized model, given the potential interaction with engine angles, it's advisable to adjust the trims at low power, say at one-third throttle. This will allow you to subsequently analyze how its behavior changes at full throttle and fine-tune the settings (see below).

4.10.3 Centering check

The principle involves setting the aircraft to a flight condition (angle of attack, lift coefficient, or airspeed) as far removed as possible from the equilibrium condition for which the model is designed, then observing how it returns to equilibrium and adjusting the center of gravity accordingly. This aspect is fundamental because, by definition, without significant imbalance, the effect of stability cannot be demonstrated.

The prerequisite for any centering test is therefore to carefully achieve the equilibrium condition, by adjusting the engine power and the pitch trim (stick released, pull-back) until the model naturally holds a level without any correction to the sticks and at an appropriate speed.

Several methods adhere to this principle:

- Dive test: the most universal and particularly used in gliders, it is based on a change in angle of attack resulting in a significant change in flight speed.
- Pitch-up test: the opposite of the pitch-down test, it requires a motor, otherwise the rapid loss of speed ends in a stall before the effect of stability can be interpreted.
- Inverted roll: This test relies on a radical change of balance at constant speed and can only be applied to an aircraft with at least some capability for inverted flight. The principle is simple: the more forward the center of gravity, the more compensation is required in the nose to maintain level flight in inverted flight, whereas a neutral center of gravity requires no correction once the flight path is established (the transitional changes during the inverted flight phase are not significant). This method is particularly useful for jets, for which the dive test is inapplicable, or for aerobatic aircraft where minimal control input is desired regardless of the flight attitude. This test can also be a good complement to the dive test. For example, the need for significant compensation in the nose during inverted flight contradicts a neutral dive test and should prompt the aircraft developer to reconsider how the latter was conducted.

The accuracy of the nose-up test can be compromised by an improperly adjusted engine down-pitch, as the engine thrust then generates a parasitic pitching moment. Since the thrust varies with airspeed, this moment is also not constant. As the nose-down pitch can only be finalized once the center of gravity is perfectly aligned, this test requires a certain level of expertise to determine—without undue difficulty—whether the center of gravity or the engine trim is responsible for the observed behavior.

The same applies to the inverted flight test for an airplane. This test also suffers from a second flaw in the case of a biplane: the interaction between the two wings is not the same in inverted flight as in normal flight (airfoils and axial offset of the wings are reversed), so the balance between these two phases of flight is not necessarily identical even though the center of gravity may be neutral.

For these reasons, the sharpness test is preferable, when available, as it allows for a clear separation of the different settings. To perform it correctly and obtain a truly usable result, it is also essential to follow a precise methodology:

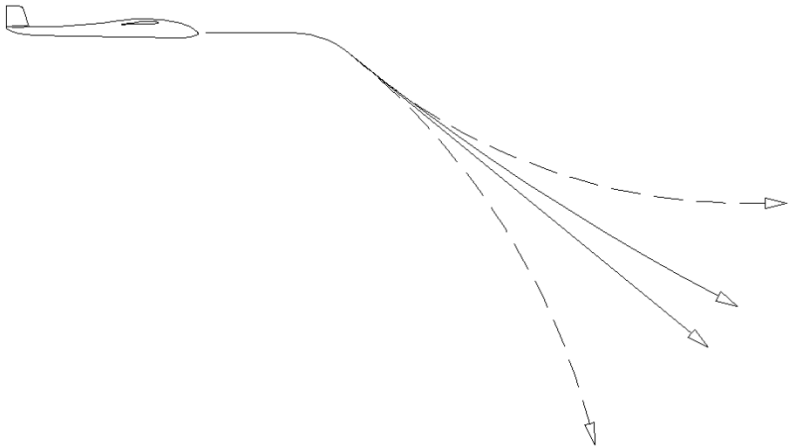

Fig. 81

- Position the model facing the wind and at a sufficient altitude, approximately 50 to 100 m depending on the scale.
- In the case of a motorized model, choose the lowest possible engine speed, just enough to stay in the air.
- Adjust the depth trim (= balance the aircraft longitudinally) to naturally maintain the level flight at a low speed.
- Suddenly put the model into a dive at about 30-45° of slope, and immediately release (as for adjusting the trims) the elevator stick.
- Observe the model's reactions: if it recovers too quickly, the center of gravity (CG) is too far forward (high stability); if it steepens the dive, the CG is aft (increased initial disturbance); if it maintains the descent angle, the CG is neutral. Generally, we always aim for a neutral CG (aerobatics) to slightly forward CG (general case), meaning a very gentle leveling during the dive test.
- Position the aircraft and then move the center of gravity (CG) forward or backward accordingly by shifting or adding weight (battery, lead). Proceed gradually and avoid drastic changes; it's better to perform several flights to reach the desired result rather than trying to adjust everything on the first flight. A good compromise is to adjust the CG in increments of 2% of the average center of gravity.
- Note that each movement of the CG will then require adjusting the pitch trim to return to the initial equilibrium condition: nose down if the CG is moved back, nose up if it is moved forward.

4.10.4 Finalizing the tail adjustment

Once the center of gravity (CG) is set, regardless of the method used, observe the elevator position. To correct a nose-up bias, you must either increase the wing trim (but this alters the flight path) or decrease the horizontal tail trim (ideally), which in both cases amounts to increasing the longitudinal dihedral. The opposite is true, of course, if the elevator is trimmed for nose-down. Here too, proceed gradually until the horizontal tail is perfectly neutral. Note that, unless there is a major flaw, this adjustment is entirely optional as it is purely aesthetic and does not affect flight characteristics.

4.10.5 Engine angles

In the case of a powered model, the tuning process continues with engine trim adjustment, which is broken down into two angles: tail rotor (yaw axis) and down-pitch (longitudinal axis). From level flight at one-third throttle, with trims set, full throttle should not alter the flight path; the model should continue to fly straight. If this is not the case, the two angles are adjusted accordingly. For tail rotor, it is helpful to fine-tune this setting by performing full-throttle climbs as vertically as possible, as this makes it easier to visualize any yaw deviation.

The principle of anti-torque is developed in paragraph §5.16.

Engine pitch control is a bit more complex than it seems. Its principle is to use engine thrust to balance the aircraft's longitudinal moments in all phases of flight while maintaining constant wing lift, all with the aim of minimizing the engine's influence on the flight path. To achieve this, three successive flight phases must be distinguished during a variation in engine power:

- Instantaneous effect: if the engine thrust axis does not pass through the center of gravity (CG), a change in thrust will cause a change in pitching moment, and therefore ultimately in the aircraft's angle of attack. This change in angle of attack will be more or less resisted by pitch stability (forward CG) or less (neutral CG). Therefore, for an aircraft to be "neutral" to changes in engine power, the alignment of the engine axis with the CG must be more precise the more aerodynamically neutral the aircraft is.
- Transition: A change in engine power leads to a change in airspeed. To maintain the flight path, this must be accompanied by an inverse change in the lift coefficient (Cl), and therefore the angle of attack. While it is possible to control the wing with the elevator, this adjustment of the angle of attack is more often achieved by using a pitching moment generated by engine thrust, thus adding a certain pitching angle relative to the theoretical engine axis passing through the center of gravity (CG). Since the aerodynamic moment restoring the aircraft to equilibrium is greater when the static margin is large, this pitching correction will therefore be more significant when the aircraft is forward-centered.

- New equilibrium situation: the aircraft is now stabilized at a constant speed, the need for engine downthrust is less important than during the transition phase, since only the balance of longitudinal moments needs to be achieved.

Ideally, each phase would therefore require a specific pitch angle. A compromise must be found between these three conflicting needs, primarily between the "automatic" adaptation of the wing's angle of attack according to engine power and the balance of moments at steady speed. In practice, a relatively "neutral" engine behavior can be achieved fairly easily across the entire flight envelope of a low-wing or, especially, mid-wing aircraft, particularly if it is centered and relatively neutral. Things are a bit more complicated for a parasol-wing aircraft where the engine is positioned much lower than the aircraft's center of gravity (CG), or, conversely, for a pylon-mounted engine. It should be noted that the term "pitch-down" for the engine's longitudinal angle is sometimes misleading, since an engine positioned high above and in front of the CG will be set up with a "pitch-up" angle. Similarly, the angle to be used is reversed compared to usual practice in the case of a pusher-mounted engine.

As a first step to roughly adjust the settings in the workshop, one can simply, in longitudinal view, align the engine thrust axis with the estimated center of gravity. Flight testing will then be used to fine-tune the downthrust correction. For ease of adjustment, if the correction required is small, it is also possible to use a throttle/pitch control mix to correct the parasitic moment generated by the engine thrust.

4.10.6 Fine-tuning the suspension travel

The final adjustments will be made by fine-tuning the control surface deflections to obtain precise and linear responses (perfectly proportional to the stick input) on each axis, as well as consistent responses across all axes. This often-overlooked step makes all the difference between two identical aircraft, one of which clearly flies better than the other. While the pilot's skill certainly plays a role, this overlooks the even more crucial skill of the aircraft's tuner. Achieving perfect results can be quite tedious, but can be significantly simplified by using the in-flight adjustment functions offered by some programmable radio transmitters.

These adjustments primarily concern the travel of the elevator (pitch), aileron (roll), and rudder (yaw) functions, via stick formatting (generally called "dual-rate," a somewhat inaccurate term from early radio transmitters), aileron differential, elevator-flap-aileron coupling, and wing camber. Exponential control should be used with caution, as its main purpose is not to smooth out overly sharp reactions (that's the goal of "dual-rate") but to linearize the response throughout the entire travel. In some cases, this is achieved through an inverse exponential function.

Once the radio settings are adjusted, these settings must be transferred to the mechanical settings, particularly regarding neutral positions and, above all, servo

travel. Aside from the aesthetic appeal, this has very practical consequences, specifically on flight time and even flight safety. Indeed, a servo's power consumption is directly related to the torque it must deliver to actuate the control surface, which itself depends on the reduction ratio between the servo and the control surface. Therefore, it's highly advantageous to maximize the servo's travel by adjusting the servo arm lever to reduce the torque required for a given control surface deflection, rather than using an excessively long lever arm and electronically limiting the travel. This reduces power consumption, resulting in better flight time, slower servo wear, and a lower risk of voltage drop or a BEC system failure (which can lead to a loss of control). The precision of the piloting also benefits, the angular play of the control surfaces (for given clearances in the control chain) being minimized while the resolution (512 steps, 1024 steps, etc.) of the electronic control chain of the servo is fully exploited.

5. To go further

This final section will allow us to delve deeper into certain aspects raised throughout this series. Here too, rather than aiming for exhaustiveness, we will address practical points that are relevant to both competition and everyday model building.

5.1 Influence of wing loading

Consider a high-performance glider with a wingspan of 2m, aspect ratio 10, airfoil SB96, wing loadings of 20 g/dm² (empty) and 40 g/dm² (ballasted).

Let us first study the polar curves of the speeds and lift-to-drag ratio in level flight (fig. 82):

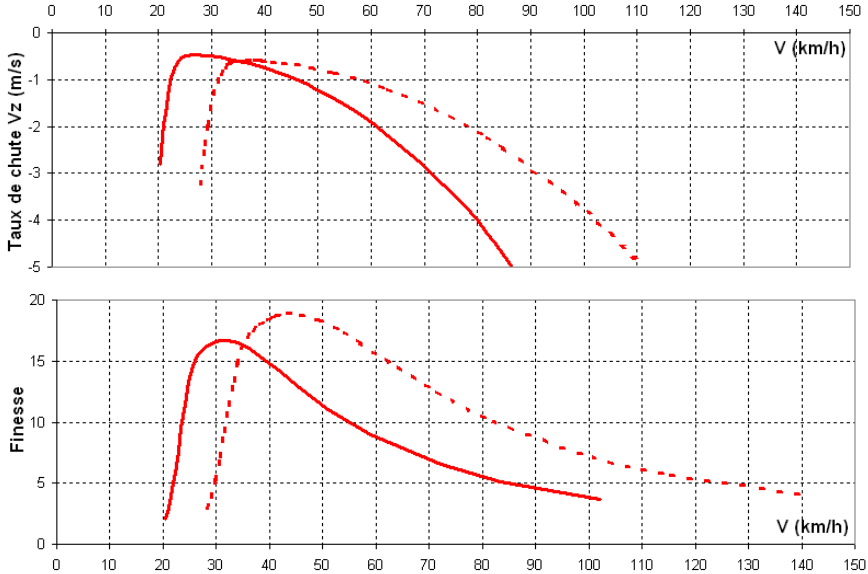

Fig. 82

We can therefore deduce that:

- When thermalling (searching for the minimum sink rate), it's best to fly only slightly faster than the minimum sink rate speed (here, around 25 km/h). Performance is almost identical, whereas below this speed, it deteriorates very quickly (a typical scenario in gliders where, in an aerodynamically unfavorable area, a novice pilot might overuse elevator input, believing this will increase their climb rate, when in fact they are worsening the sink rate). A second benefit is that this also allows you to fly at a glide ratio close to your maximum.

- Wing loading significantly impacts maximum glide ratio and high-speed performance. For the same sink rate of 3 m/s, doubling the wing loading allows this aircraft to fly at 90 km/h instead of 70 km/h. That's almost 30% faster…
- The same polars with a really different airfoil (for example, a simple ClarkY) would show that wing loading, just like aspect ratio, has a significantly greater impact on performance than the airfoil.

NOTE
This improvement in maximum lift-to-drag ratio with wing loading is typical of small-scale aircraft due to the influence of the Reynolds number on airfoil performance. Conversely, the drag coefficient (Cd) of very large models and full-size aircraft is almost constant, and the maximum lift-to-drag ratio is relatively unaffected by wing loading. However, the same performance shift is observed at higher speeds.

5.2 Comparison of aerodynamic configurations

Here is a comparison of sink rate and glide ratio in level flight (Fig. 83) for two masses (0.8 kg and 1.6 kg) between standard (red), flying wing (green), and canard (blue) models with identical configurations: same wing geometry (wingspan 2 m, surface area 40 dm², zero mean sweep, Eff=0.6), as well as the same Vs (= 0.5) and airfoil airfoil between the standard and canard (SB96). The airfoil chosen for the flying wing is specific (Cm0≥0) but with performance equivalent to that of the SB96.

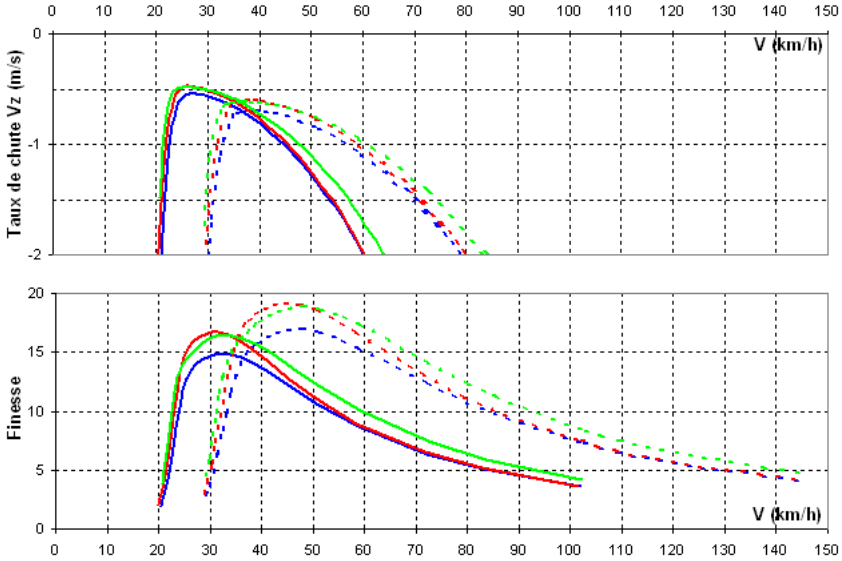

Fig. 83

The performance differences are undeniable: regardless of wing loading, the duck's performance is significantly lower.

This is mainly due to the tail Cl (fig. 84).

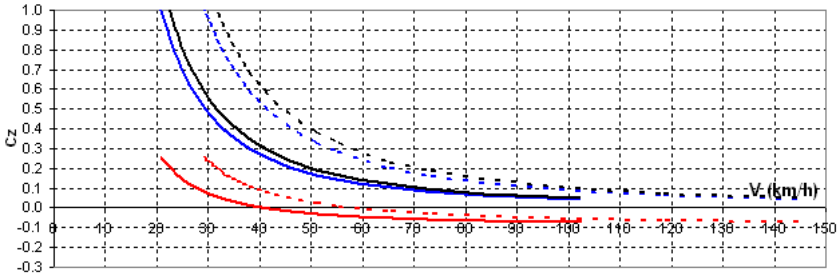

Fig. 84

In the case of the canard, the horizontal tail lift coefficient (blue curves) is indeed very high (due to the center of gravity being very far forward relative to the wing's aerodynamic center). It is at the same level as the wing lift coefficient (black curves), compared to 3 to 6 times lower for a normal model (red curves), which results in high horizontal tail drag (airfoil + induced drag) that impairs performance (despite the additional lift provided by the horizontal tail).

The duck formula has three other major drawbacks:

- The wing's behavior varies and is uneven depending on the flight phase because it is affected by the wake of the horizontal tail, whose wingspan is smaller than that of the wing. Similarly, the horizontal tail's wingtip vortex locally impacts the wing's performance.
- The use of camber flaps is problematic: the overall center of pressure is located very far forward from the wing control surfaces. This generates a significant pitching moment, which will require a substantial increase in the horizontal tail lift coefficient (Cl) to counteract it. However, the horizontal tail lift coefficient is already very high on this type of model; increasing it will further worsen its drag (induced and airfoil) while risking reaching the horizontal tail's maximum lift coefficient.
- Since the horizontal tail is naturally very loaded at low speed, the margin for maneuver to pitch up in this phase is particularly reduced.

Conversely, the flying wing offers good results in rapid level flight, the drag in this context being reduced, the larger rudder surface to maintain correct yaw stability being compensated by the absence of a horizontal tail and the compactness of the fuselage, when there is one.

Things reverse at high lift coefficients (Cl), as the flying wing airfoil (by nature at $Cm0 \geq 0$) cannot offer as high a maximum lift coefficient (and therefore as low drag at high Cl) as that of a standard airfoil. This is even more pronounced in maneuvers at constant Reynolds numbers, such as pylon racing (Fig. 85); the

slight superiority of the flying wing at low Cl is thus reversed at high Cl (here at 50 km/h and 100 km/h). That said, it should be noted that the results are essentially equivalent.

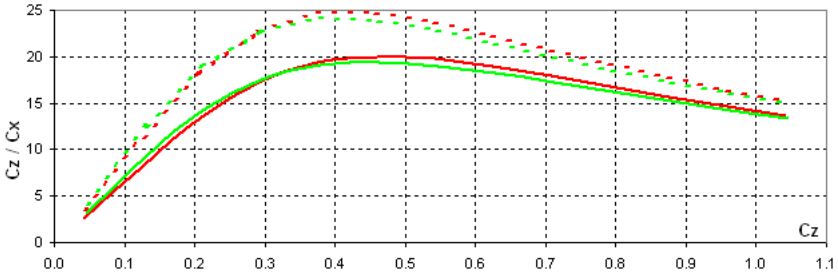

Fig. 85

The flying wing design allows little to no use of camber flaps (with significant sweep), since the camber is used for pitch control. In the case of a swept wing, only areas of the wing near the root could potentially accommodate a change in camber without significantly impacting the pitch moment, as the distance between the local apex of the chords and the global apex of the wing is then very small.

Furthermore, using camber to control the pitch axis is contradictory (unfortunately!) to the performance requirements at high lift coefficients (increasing lift coefficient => increasing center of gravity => raising the trailing edge => reducing maximum lift coefficient and increasing drag coefficient). It's the same polar envelope principle, but inverted, as detailed in §5.3 for camber flaps. If these elements are factored into the performance comparison, the flying wing is inevitably inferior to a standard model in tight turns. Some experimenters have attempted to mitigate these drawbacks by controlling the elevator through variations in the center of gravity position, but this comes at the cost of a loss of stability that can only be limited, even with electronic assistance such as a gyroscope or an angle-of-attack sensor.

NOTE
This mechanism of degradation of the Cl_max of the flying wing also explains the narrowness of its center of gravity range, at the forward limit as soon as the Cl_max (reduced by the raising of the BF) corresponds to the equilibrium Cl: having no more margin to pitch up, the wing "porpoises" at the slightest input of the elevator.

5.3 Bending flaps, snap-flap

Who hasn't heard: "Lower the flaps to increase lift"? This trivial and universally accepted statement is, however, completely false!

This misinterpretation stems from a common pitch-related side effect when flaps are extended, generally a tendency to pitch up, hence the confusion. However, on some aircraft (typically those with a large horizontal tail volume), the effect is sometimes reversed, which seems quite paradoxical. In both cases, this side effect can be canceled out by simple elevator compensation (via mixing, for example), which already provides some food for thought. Furthermore, in level flight, taking a step back to consider the aircraft as a whole and over time, we observe that while there is indeed a change in lift at the moment of flap deflection (albeit a transient one), a new equilibrium situation then results, with mechanically the same lift as before the deflection (= mg). Once again, the airfoil does not determine lift; it is influenced by it.

The curvature flaps actually have two functions:

- Delaying stall by increasing the maximum lift coefficient (Cl max) of the airfoil (by lowering the flaps) is far from systematic at low Reynolds numbers. Especially on a small scale, using flaps does not necessarily delay stall and can even make pitch behavior tricky by introducing changes in lift coefficient (Cm) and non-linearities in lift coefficient/alpha. For this reason, Fowler-type flaps (increasing wing area) or leading-edge slats (which promote flow at high angles of attack) are much more effective.
- Modulating the airfoil drag in each phase of flight to optimize the machine's efficiency. This is actually the most interesting function, because it is the most significant, at our scale.

Regarding this last point, two contradictory needs exist, the principle of which we will modify later, is briefly outlined below:

- Increased drag (landing):
    - raised, at high Cl: braking on final approach
    - lowered, low Cl: high-speed braking
    - significantly lowered, regardless of the Cl: braking
- Drag reduction (performance):
    - lowered, at high lift coefficient: tight turns, loops, thermalling, and searching for maximum glide ratio
    - raise, at low Cl: transition, maximum speed

The flaps can be controlled statically via a switch (directly or via flight phases) or dynamically via a slider, a control stick (4-axis control), or a mixing system. The latter is managed by the snap-flap function, which links the camber flaps to the elevator. Their use is closely linked to the airfoil, particularly the control surface deflections. Typically, a very cambered airfoil will respond well to raised flaps (reducing camber) and less well to lowered flaps (increasing camber), while a relatively flat airfoil will respond well in both directions.

Here is an example of a study with the TP74 airfoil, one of the current references in 60" glider competition and also perfectly suited to electric racers.

Let us apply a flap deflection of +5° and +10 (fig. 86).

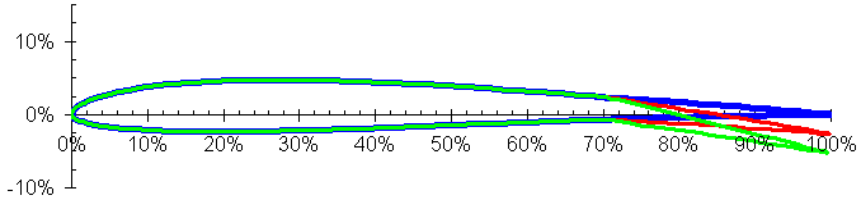

Fig. 86

Let us now observe the polars Cd / Cl at Re = 200k (fig. 87).

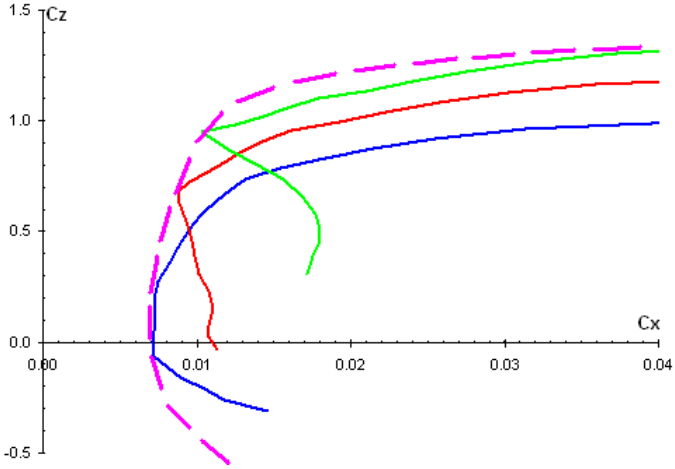

Fig. 87

At high lift coefficients (Cl): increasing the camber significantly reduces drag compared to a smooth airfoil. The envelope of the different polars for a given lift coefficient (Re) constitutes a virtual polar (here in dashed magenta): when used judiciously, varying the camber in flight makes the airfoil considerably more versatile and efficient (= lower drag, higher maximum lift coefficient).
At low lift coefficients (Cl): drag is significantly increased.

This adaptation of the camber to the Cl allows us to raise two important points:

- If incorrectly adjusted, the curvature setting can produce the opposite of the expected result.
- The change in curvature can be used to intentionally generate drag, for example during landing phases.

Let us now turn to the polars Cl/α and Cm/Cl (fig. 88).

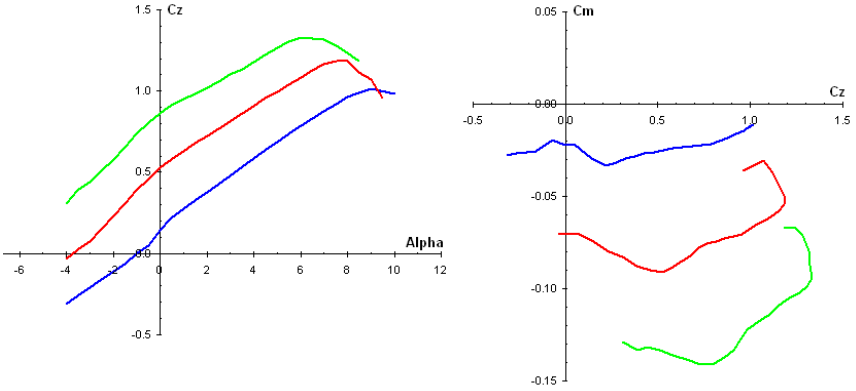

Fig. 88

The slope of the Cl/α curve remains unchanged, but α0 and Cm0 increase in absolute value with increasing curvature:

- The airfoil alignment is increased by the deflection of the camber flaps, therefore the longitudinal V.
- During a change in camber, the increase (in absolute value) of Cm0 opposes the moment generated by the transient change in lift due to the variation of Alpha0. If the horizontal tail volume is small, the effect of Cm0 dominates (e.g., if the flaps are lowered, the overall result is a pitching moment; this is, in fact, the principle of piloting a flying wing), and conversely if the horizontal tail volume is large (because the distance between the center of gravity and the wing aerodynamic center is significant). Between these two extremes, flap deflection may not generate any moment.
- Knowing the Cm0 and α0 of the airfoil with curvature at the same time as the wing Cl corresponding to the phase to be optimized allows us to calculate the horizontal tail Cl (see above), and therefore ultimately the elevator deflection adapted to compensate for the resulting moment.
- This compensation should be adjusted as needed. It will generally be minimal during the landing phase (flaps braking) since the typically nose-up moment at flap extension is in the correct direction (it replaces a nose-up input from the pilot). For a racing aircraft in tight turns (seeking better performance), this implies reducing the elevator deflection compared to a streamlined configuration. The fuselage angle of attack at high lift coefficients is therefore reduced, and consequently, the fuselage experiences less drag thanks to the camber flaps.

5.4 High-lift devices

It is common to find this type of publication, a summary of NACA work from the 1930s, in various forum discussions:

Designation	Diagram	$C_{L_{max}}$	α at $C_{L_{max}}$ (degrees)	L/D at $C_{L_{max}}$	$C_{m_{ac}}$	Reference NACA
Basic airfoil Clark Y		1.29	15	7.5	−.085	TN 459
.30c Plain flap deflected 45°	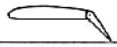	1.95	12	4.0	—	TR 427
.30c Slotted flap deflected 45°		1.98	12	4.0	—	TR 427
.30c Split flap deflected 45°		2.16	14	4.3	−.250	TN 422
.30c hinged at .80c Split flap (Zap) deflected 45°	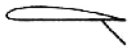	2.26	13	4.43	−.300	TN 422
.30c hinged at .90c Split flap (Zap) deflected 45°	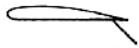	2.32	12.5	4.45	−.385	TN 422
.30c Fowler flap deflected 40°		2.82	13	4.55	−.660	TR 534
.40c Fowler flap deflected 40°		3.09	14	4.1	−.860	TR 534
Fixed slot		1.77	24	5.35	—	TR 427
Handley Page automatic slot		1.84	28	4.1	—	TN 459
Fixed slot and .30c plain flap deflected 45°	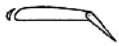	2.18	19	3.7	—	TR 427
Fixed slot and .30c slotted flap deflected 45°		2.26	18	3.77	—	TR 427
Handley Page slot and .40c Fowler flap deflected 40°		3.36	16	3.7	−.740	TN 459

Fig. 89

While some experiments appear positive, generally on "smaller" models, others, on the contrary, are based on autosuggestion. The reason is quite simple: these results are valid for full-size aircraft at high Reynolds numbers (around 600 k here), potentially very different from those of a scale model. As we have seen, high lift coefficients (Cl) and low Reynolds numbers don't mix well. Consequently, before accepting any spectacular gains in maximum lift coefficient (Clmax) at face value, it's wise to verify their range of validity. In addition, verification in a digital wind tunnel, or failing that, searching for work carried out at our scale (e.g., on Michael Selig's website), is essential to further confirm the results.

Furthermore, any potential gains in lift coefficient (Cl) must be weighed against the associated increase in drag: if the latter is too significant, it can completely negate the gain in maximum lift coefficient (remember, it's drag that causes the lift to drop...). This is typically the case with slotted systems, which remain relatively efficient on a small scale thanks to the boundary layer dynamization caused by the flow through the slot, but generally at the cost of significant drag.

The choice of such a device has consequences for the horizontal tail load, as the airfoil's lift coefficient (Cm0) can be significantly altered, requiring at least elevator compensation. The lift coefficient (Cl) and lift distributions (see §5.6) are also affected: for example, lowering the flaps increases the local angle of attack of the airfoil, thus loading the wing root. The root will then stall well before the wingtip, which is the desired effect to ensure a safe stall (in addition to delaying it). Hence the fact that high-lift devices, like braking devices, are always located at the wing root, never at the wingtip.

To complete this overview, there are some very interesting recent studies on the internet which show that, at our scale, the airflow from a propeller on a wing can significantly improve its performance, as well as, if not better than, a conventional high-lift flap:

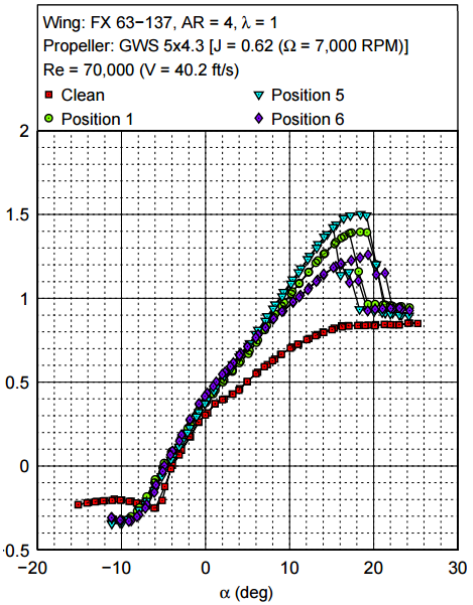

Fig. 90, excerpt from “Propeller Induced Flow Effects on Wings at Low Reynolds Numbers”, University of Illinois

5.5 Effects and usefulness of a turbulator

A turbulator (Fig. 91) generally consists of a positive step (zigzap strip, glued wire, studs, rough band, etc.) positioned at a precise point on the airfoil. Its principle is to generate small turbulences in the boundary layer (see §2.5), the role of which is to energize this boundary layer and prevent separation. This separation occurs when the air can no longer follow the airfoil (low Reynolds numbers or high angle of attack), which generates a turbulent zone (called a recirculation zone or laminar bubble) that severely impairs the airfoil's performance.

To be effective, a turbulator should be positioned ahead of, typically 5% of the chord, the laminar-turbulent transition point. Positioning it further forward is unnecessary and can degrade the airfoil's performance at the Reynolds numbers at which it functions correctly.

Similarly, its thickness must be consistent with that of the boundary layer (generally 0.1 to 1% of the chord at our scales), which is thicker the lower the Reynolds number. One-third of this thickness gives a satisfactory result, or as a first approximation if the turbulator is not placed too far back on the airfoil (C being its chord):

$$h_{turbu} \approx 0{,}3.C.\mathrm{Re}^{-1/2}$$

Fig. 91: Example of a zigzag turbulator on a DG1000 wing

Here are the polar curves (fig. 92) of a high-performance airfoil for a large glider (FAD18-13/3.0) at Re = 50 000 and 200 000, in smooth (blue polar) and equipped with an extrados turbulator at 25% of the chord (red polar):

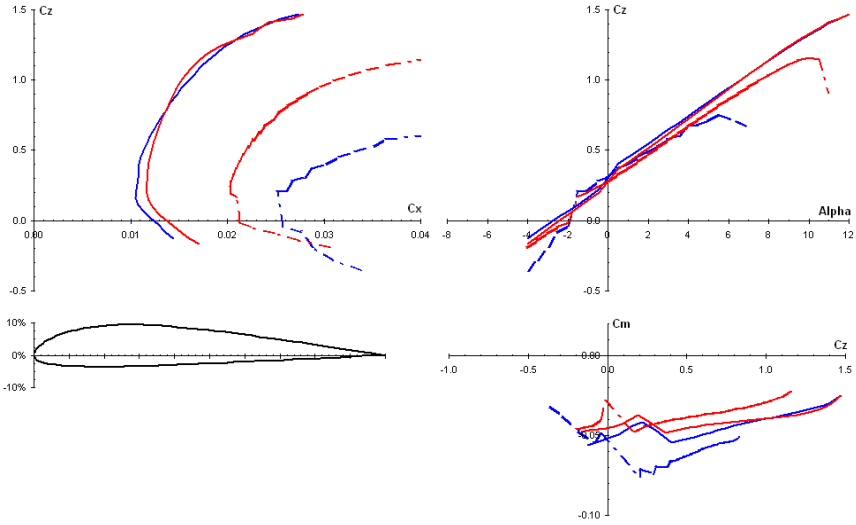

Fig. 92

The gain at Re = 50 000 is particularly significant, both in terms of performance (reduced drag coefficient, improved maximum lift coefficient) and behavior: constant maximum lift coefficient and linear lift coefficient with respect to the angle of attack. Conversely, this airfoil naturally functions well at Re = 200 At 000, no improvement in behavior appears while performance is slightly altered at low Cl, while a slight drag gain appears at high Cl.

Depending on the airfoil airfoil, the benefit of a turbulator is clear at low Reynolds numbers or high lift coefficients (Cl), but it increases drag at high Reynolds numbers or low Cl. This technique can also be used to improve the efficiency/reduce the drag of camber flaps (or other control surfaces). Within this performance optimization framework, the main challenge is therefore to find the position along the chord that offers the best compromise. The design point is a good starting point, based on the x/c polars (position of the laminar-turbulent transition as a percentage of the chord) provided by Xfoil. The method, with a very practical thickness chart, is illustrated here: http://www.mh-aerotools.de/airfoils/turbulat.htm

Conversely, if the sole objective is to achieve healthy behavior, without performance constraints, the turbulator's position is not critical. Placing it sufficiently forward on the chord (e.g., 10% of the chord length before the maximum thickness) will be enough to obtain the desired result.

NOTE
In the specific case of micro-models operating at very low Reynolds numbers, the use of a plank airfoil with a sharp leading edge for the horizontal tail has been suggested. This leading edge shape actually acts as a turbulator and significantly improves the performance and handling of the horizontal tail airfoil. The same applies to a slightly rough surface finish on the wing, which explains why Crobe micro-gliders finished with Japanese paper are noticeably more pleasant at low speeds than the same gliders finished with heat-shrink film. This should not be overlooked, as the differences in performance and handling can be significant.

5.6 Approximate lift and lift coefficient (Cl) distributions

NACA report no. 948 (fig. 93) provides an affordable alternative to VLM-type numerical methods for calculating the lift distribution of a trapezoidal wing, provided its sweep is moderate. The semi-empirical principle, known as the Schrenk method, is based on the strong similarity between the wing's lift distribution curve and the average of two purely geometric curves: one describing the evolution of the wing's chords, and the other describing the evolution of the chords of an elliptical wing of the same surface area and wingspan.

Actual wing chord: $$C1(y) = CE(1 - \frac{2.y}{E/2}.(1 - eff))$$

Elliptical wing chord: $$C2(y) = \frac{4.S}{\pi.E/2}.\sqrt{1-(\frac{2.y}{E/2})^2}$$

Equivalent chord representing the lift distribution:

$$C(y) = \frac{C1(y)+C2(y)}{2}$$

Local lift: $$Fz(y) = \frac{Fz_{voilure}}{nbCordes}.\frac{C(y).E}{S}$$

With nbCordes being the number of chords used to discretize the wing

By applying this equation to a number of chords along the span, a dozen (y = 0, y = 10%E, etc.) is quite sufficient, we obtain a perfectly suitable lift distribution curve.

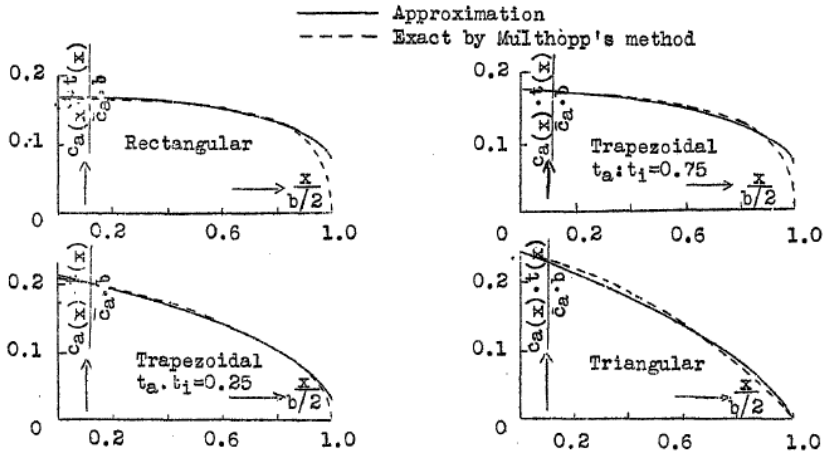

Fig. 93, extract from NACA report no. 948

We can also extract the Cl distribution curve:

$$Cz(y) = Cz_{voilure} \cdot \frac{C(y)}{.C1(y)}$$

This lift coefficient (Cl) distribution curve can be further modified by introducing twist and/or a difference in Alpha0 in the case of a multi-airfoil wing, ultimately allowing the lift distribution curve to be recalculated with these two factors. In the case of a canard configuration, it is essential to subtract the local angle of attack reduction corresponding to the wake deflection of the leading edge.

Finally, knowing the distribution of Cl, it becomes possible to estimate the Oswald coefficient by quantifying the ratio between the average lift and its local maximum:

$$e = \frac{\sum Cz(y).C1(y)}{\max(Cz(y)).\sum C(y)}$$

An approximate solution can be written as follows:

$$e \approx \frac{1}{1 + \frac{Cz_{\max} - Cz_{moy}}{Cz_{moy}}}$$

Apart from calculating the Oswald coefficient, the practical applications of these curves are as follows:

- Lift distribution: study of wing loading and its mechanical resistance in bending and torsion (see link given in § 3.2), study of wing efficiency relative to the elliptical (via the Oswald coefficient, see below)

- Cl distribution: analysis of stall (search for the maximum Cl zone), analysis of Cl constancy (performance).

In both cases, the levers to use to improve one or the other of the distributions, or even both, are simply the input data of these calculations, that is to say the planar geometry of the wing and its evolution of aerodynamic twist.

Depending on the need, the results and solutions implemented can differ completely. A performance glider geometry, with a constant lift coefficient over the entire wingspan and an elliptical lift distribution, is for example not at all suitable for a beginner model where a decreasing lift coefficient evolution from the wing root to the wingtip is preferable to guarantee a safe stall (no wing engagement and retention of roll control as long as the wingtip is not stalled) and a preventative stall (the aircraft sinks instead of pitching down if only part of the wing stalls).

Example of a Cl distribution study on a Baron-type aircraft:

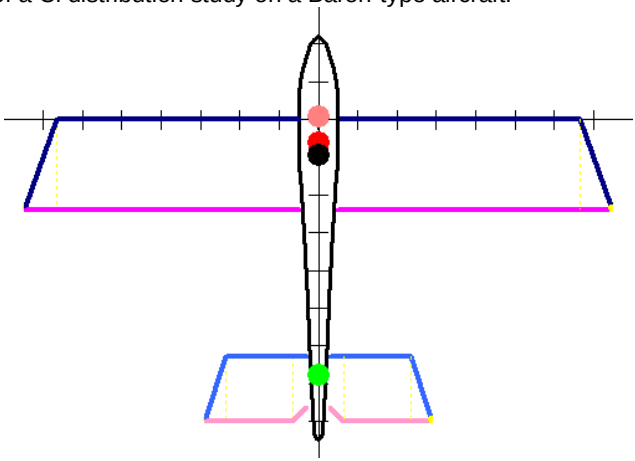

Fig. 94

Note the wingtip-shaped structure, which has a rather unusual effect on the distribution of Cl and is far from negligible:

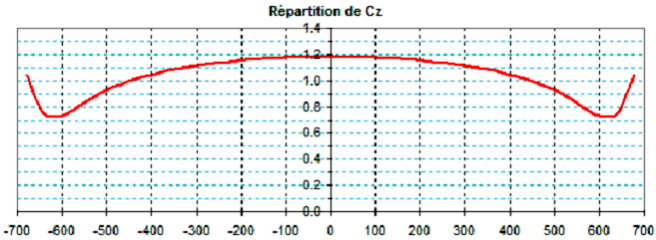

Fig. 95

The wingtip is heavily loaded, almost as much as the wing root, with fortunately a sufficiently pronounced Cl dip with the rest of the wing, thus limiting the propagation of the stall.

Now, let's apply a strong twist to the wingtip from the terminal rib, which is equivalent to creating a Dornier-type wingtip imitation:

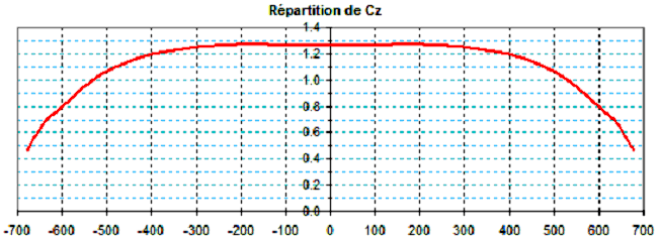

Fig. 96

Despite the unchanged, rudimentary geometry, the situation is noticeably improved, with more consistent wing performance over half the wingspan and a decreasing lift coefficient (Cl) towards the wingtip, thus ensuring a gentle stall, ideal for a beginner's aircraft. Incidentally [for an aircraft with significant drag like this one], the wing geometry efficiency also improves slightly at high lift coefficients (but is compromised at low lift coefficients).

5.7 Final calculation of the CG

Thierry Platon has developed all of these calculations in his publications, so I will only give a summary and the main lines of his approach, as well as a small personal contribution.

This time, the fuselage is formally taken into account in the variation of moments around the center of gravity (Fig. 97). Contrary to what is often found in some full-scale aerodynamics books, the entire fuselage is considered, not just the forward section. Calculating the relative fuselage efficiency becomes more complex, but the result is also more precise.

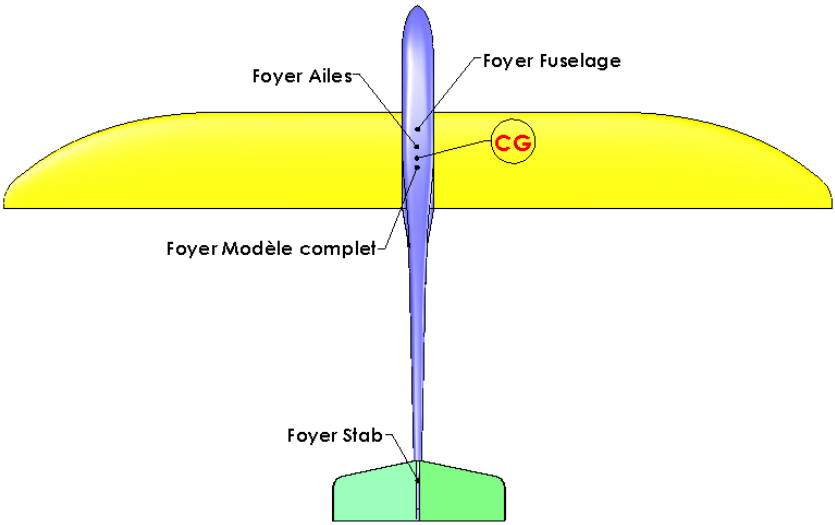

Fig. 97

Assuming the system is linear with respect to the angle of attack (therefore neglecting any possible variation in the moment of the airfoil), the problem of the global neutral point can be summarized solely by the variations in the lifting moments (= lift * lever arm) of each element around this neutral point (fig. 98):

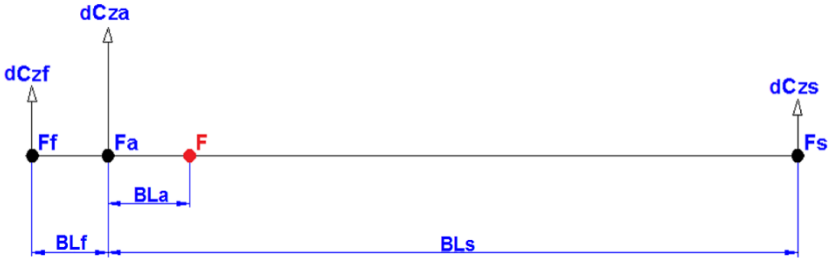

Fig. 98

By omitting the term $\rho.V^2/2$ that appears in the expression for each lift, we can write, for a change in angle of attack d α:

$$(BL_f + BL_a).S_f.dCz_f + BL_a.S_a.dCz_a = (BL_s - BL_a).S_s.dCz_s$$

As :

$$dCz_f = 0{,}11.A_f.d\alpha$$
$$dCz_a = 0{,}11.A_a.d\alpha$$
$$dCz_s = 0{,}11.A_s.(1-\varepsilon').d\alpha$$

We obtain:

$$(BL_f + BL_a).S_f.A_f + BL_a.S_a.A_a = (BL_s - BL_a).S_s.A_s.(1-\varepsilon')$$

Either :

$$BL_a = \frac{BL_s.S_s.A_s.(1-\varepsilon') - BL_f.S_f.A_f}{S_a.A_a + S_f.A_f + S_s.A_s.(1-\varepsilon')}$$

By relating the distance BLa to the mean chord relative to the wing neutral point:

$$xF = xF_a + \frac{BL_a}{CMA_a}$$

The final result is:

$$xF = xF_a + \frac{BL_s.S_s.A_s.(1-\varepsilon') - BL_f.S_f.A_f}{CMA_a.(S_a.A_a + S_f.A_f + S_s.A_s.(1-\varepsilon'))}$$

The Af coefficient is homogeneous with the lift efficiency coefficients As and Aa, but its calculation differs. Thierry proposes a fixed coefficient of approximately 0.7, derived from the analysis of several gliders. This coefficient is well-suited in the general case, but it can range from approximately 0.4 to 1 with other models if considered as an adjustment variable to perfectly match the calculated aerodynamic center to the actual aerodynamic center. By manipulating this coefficient, I realized that it is very strongly correlated with the wing's lift efficiency and the ratio between the wing's mean chord and the fuselage's width. The origin of this correlation remains to be precisely determined, although a wing/fuselage interaction seems a priori to be a very good candidate (the wing pressure field generating an additional moment downstream to the fuselage's lift moment). This hypothesis is further confirmed by canard configuration models, for which the formula below applies not to the wing but to the horizontal tail. The results are very convincing, so it would be a shame not to take advantage of them.

$$A_f \approx 0{,}2.A_x.(1+\frac{CMA_x}{l_f})$$

This empirical relationship is defined by:

With: lf the width of the fuselage.

For a flying wing with a fuselage, we directly use Af = 0.1.

Finally, the lifting surface and the position of the fuselage's center of gravity can be calculated in a simplified manner, from the top view dimensions and a qualitative determination of the shape of the tail beam (fig. 99):

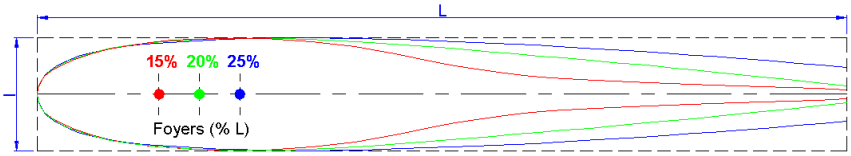

Fig. 99

- As a first approximation, the center of gravity can be positioned along the length of the fuselage (denoted Lf), from the forward tip, depending on the shape of the tail boom. For a conventional aircraft: 15% (thin boom), 20% (normal boom), or 25% (wide boom). For a canard, with its inverted fuselage shape: 45%, 35%, and 25% L, respectively.
- In both cases, the lifting surface Sf can be approximated from the area of the rectangle circumscribed around the fuselage: 55%, 70% or 85% l*L.
- The case of jets is more complex, due to the airflow within the fuselage, from the air intakes to the nozzles. A focal point at 45% L and a lift area of l*L (l being the width before the air intakes) gives a satisfactory result.

BLf is easy to determine if we introduce the distance between the leading edge of the fuselage and the leading edge at the wing root (denoted Xav). Knowing the respective positions of the wing and fuselage apogees (see above, denoted xFf), the calculation of BLf then boils down to the difference between these two distances:

$$BL_f = Xav_f + FL_{CMA\,a} + xF_a.CMA_a - xF_f.L_f$$

NOTE
A similar approach, derived from the NACA TR711 and delivering equivalent results (from a fuselage position chart), is given here:
http://adg.stanford.edu/aa241/stability/staticstability.html
See also the calculation method developed by Multhopp.

5.8 Influence of the fuselage on the horizontal tail's position

If the neutral line of the fuselage is not aligned with the trajectory for the Cl setting, it is necessary to correct the angle of attack of the horizontal tail to compensate for the moment induced by the lift of the fuselage.

We assume that the fuselage lift is linear. It is related to the wing's angle of attack by the wing/fuselage angle (αK):

$$Cz_f = 0.11.A_f.(\alpha_a - \alpha\kappa_a)$$

As a reminder, at the adjustment coefficient (Cl), we have:

$$\alpha_a = \frac{9.1}{A_a}.Cz_{a\ reg} + \alpha 0_a$$

Referring back to the diagram in fig. 96 and still omitting the term $\frac{\rho.V^2}{2}$ that appears at each lift phase, we can write the equilibrium equation of the longitudinal moments around the CG :

$$\begin{aligned}&(BL_f + CMA_a.(xCG - xF_a)).S_f.Cz_f \\ &+ CMA_a.(xCG - xF_a).S_a.Cz_a + Cm0.CMA_a.S_a \\ &= (BL_s - CMA_a.(xCG - xF_a)).S_s.Cz_s\end{aligned}$$

Which gives:

$$Cz_s = \frac{S_a.(CMA_a.Cm0 + Cz_a.BL_{CG}) + S_f.(BL_f + BL_{CG}).Cz_f}{S_s.(BL_s - BL_{CG})}$$

With :

$BL_{CG} = CMA_a.(xCG - xF_a)$ = distance CG / wing neutral point

If the distance CG / wing center (BLCG) is sufficiently small compared to the horizontal tail lever arm (BLs), the equation becomes:

$$Cz_s \approx \frac{Cm0 + Cz_a.(xCG - xF_a)}{V_s} + \frac{BL_f + BL_{CG}}{BL_s}.\frac{S_f}{S_s}.Cz_f$$

We can then determine the horizontal tail's position relative to the fuselage:

$$\alpha\kappa_s = 9{,}1.(\frac{Cz_s}{A_s} + \varepsilon'.\frac{Cz_{a\ reg}}{A_a}) + \alpha 0_s + \alpha\kappa_a - \alpha_a$$

Either : $\alpha\kappa_s = 9{,}1.(\frac{Cz_s}{A_s} - (1-\varepsilon').\frac{Cz_{a\ reg}}{A_a}) + \alpha 0_s + \alpha\kappa_a - \alpha 0_a$

Thierry Platon proposes an alternative arrangement of the longitudinal V-equation, highlighting the contribution of the various elements involved in the equilibrium of moments. It also explicitly demonstrates that the V-equation becomes independent of the Cla when the static margin is zero.

Here is the final result, the demonstration being described in the publication "Study of the V" mentioned in §3.2:

$$V_{longi} = k.\frac{ms}{V_{CG}.0{,}11.A_s}.Cz_a - \frac{Cm0}{V_{CG}.0{,}11.A_s} + k'.(\alpha\kappa_a - \alpha 0_a) + \alpha 0_a - \alpha 0_s$$

With :

$$k = 1 + \frac{(xF - xF_a).CMA_a}{BL_s - (xF - xF_a)} + (1 + \frac{(xF - xF_f).CMA_a}{BL_s - (xF - xF_a)}).\frac{A_f.S_f}{A_a.S_a}$$

$$k' = \frac{xCG - xF_f}{V_{CG}}.\frac{A_f.S_f}{A_a.S_a}$$

$$V_{CG} = V_s.(1 - \frac{(xCG - xF_a).CMA_a}{BL_s})$$

And :

xFf the position of the fuselage center relative to the leading edge of the mean chord and relative to the latter.
VCG is the volume of the horizontal tail relative to the CG (and no longer to the wing focal point).

We can therefore consider that the longitudinal V-shape required for the aircraft's equilibrium in horizontal flight comprises five components depending respectively on:

- of the center of gravity associated with the flight coefficient (Cl): $k.\frac{ms}{V_{CG}.0{,}11.A_s}.Cz_a$

- of the sail area (cm): $-\frac{Cm0}{V_{CG}.0{,}11.A_s}$
- of the fuselage's lift: $k'.(\alpha\kappa_a - \alpha 0_a)$
- zero-lift angles of attack of the wing and horizontal tail: $\alpha 0_a$ and $\alpha 0_s$

The first component depends on the center of gravity and the trim angle (Cla), unless the static margin is zero (neutral CG). The others depend only on the wing airfoil and the glider geometry.

5.9 Twist of a single-trapezoidal flying wing

Using a zero or even positive lift coefficient (Cm0) airfoil on a flying wing is tempting for improving performance, particularly sink rate and maximum lift-to-drag ratio, thanks to a better maximum lift coefficient (Clmax) and, above all, reduced drag at high lift coefficients (compared to a self-stabilizing airfoil). To get the most out of this approach, it generally goes hand in hand with the use of different airfoils between the wingtip and the root, as well as a fairly high aspect ratio and sweep: typically, an airfoil with a Cm0 < 0 at the root, evolving into an airfoil with a Cm0 ≥ 0 at the wingtip, with a sweep of around 15° to 20°.

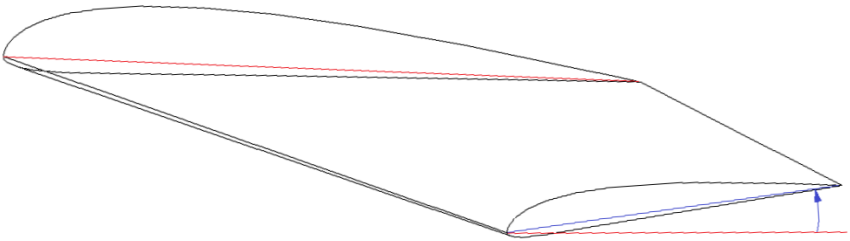

Fig. 100, negative twist of a wing

Thanks to the significant sweep, a considerable portion of the wing root has a near-zero leverage with the center of gravity, allowing the use of camber-changing flaps without any induced effect on the pitching moment. The benefit is twofold: increased glider performance and the possibility of implementing crocodile airbrakes with minimal constraints.

Optimizing this type of wing for performance requires the use of powerful software such as XFLR5, but the calculation of the wingtip twist (fig. 98) - to ensure the balance of longitudinal moments - can be done using an analytical formula, that of Panknin:

$$\alpha_{geo} = \frac{k.Cm0_{emp} + (1-k).Cm0_{saum} - ms.Cz_{a\ reg}}{1{,}4.10^{-5}.\lambda^{1,43}.\Lambda_{C/4}} - (\alpha 0_{emp} - \alpha 0_{saum})$$

With :

$$k = \frac{3 + 2.Eff + Eff^2}{4(1 + Eff + Eff^2)}$$

And :

Eff = taper ratio
$\Lambda_{C/4}$ = angle of the sweep at 1/4 of the chord
$\alpha 0_{empl}$ = zero lift angle for the root airfoil
$\alpha 0_{saum}$ = zero lift angle for the tip airfoil
$Cm0_{empl}$ = moment coefficient for the root airfoil
$Cm0_{saum}$ = moment coefficient for the tip airfoil
Cla_{reg} = lift coefficient for level flight adjustment (reminder: generally 0.3)
ms = static margin (reminder: usually 5%)

5.10 Better understanding the dive test

In his study of the generalized longitudinal V, Thierry Platon proposes a formula giving the radius (in m) of the trajectory in the dive test of a stabilized aircraft:

$$R \approx \frac{2\pi.A_s.V_s.BL_s}{ms.(Cz_{trim} - Cz_a)}$$

With: Cltrim = wing Cl corresponding to the longitudinal V setting either by construction (generic value = 0.3, see above) or after setting the depth trim, ms = static margin and Cla = wing Cl.

This formula is particularly instructive, as it allows, among other things, the highlighting of the functioning of the equilibrium in leveling as well as the coupling of centering / incidence settings:

- CG before (ms > 0): the level flight lift coefficient (Cl) (and therefore the corresponding airspeed) always tends to return to the trim airspeed. Indeed, if we apply a pitch-down disturbance (like the dive test) from level flight at trim airspeed: Cl decreases => R exists and is positive => the trajectory bends to a pitch-up => the model levels out and resumes its flight at trim airspeed. It's exactly the same with a pitch-up disturbance; R will be negative,

which corresponds to a pitch-down trajectory that will counteract the disturbance.

- CG neutral (ms = 0): the radius is infinite (= straight line) so the sharpness test is neutral.
- Rear center of gravity (ms < 0): the sign of the radius of curvature is the same as that of the disturbance, the system is divergent. However, since the radius of the trajectory is proportional to the static margin, this formula shows that the machine remains controllable with a slightly negative static margin.
- Regardless of the center of gravity (CG), as long as it's forward, the elevator trim allows you to adjust the natural flight speed. This is particularly useful for models experiencing very large speed variations, such as F3K and F3B gliders: launch or winch launch, endurance trials, speed trials. Each phase corresponds to a specific elevator trim setting to maintain a straight trajectory.
- Combining a high static margin (> 5%) and a high lift coefficient (Cl) results in a small radius, and therefore a rapid leveling during the dive test. Except for very specific flying conditions (pure thermalling or free flight), this combination is undesirable because it leads to an uncomfortable flight due to the significant elevator corrections required to maintain the trajectory during airspeed adjustments and the possible occurrence of annoying self-sustaining oscillations, such as the infamous roller coaster effect.
- If we expand the horizontal tail volume, the BLs term appears squared, clearly demonstrating the importance of the horizontal tail lever in maintaining the correct pitch trajectory. This should be considered in light of the increased fuselage drag along the lever arm.

NOTE
This formula, which neglects the variation of the wing's lift moment relative to that of the horizontal tail, is therefore obviously not applicable to a flying wing. That said, since it shows that the trajectory radius is smaller the smaller the horizontal tail volume, it effectively explains the high sensitivity of a flying wing to its center of gravity and the need for a small elevator deflection. This is further compounded, as we will see below, by a very short pitch response period (easily observed with a center of gravity that is too far forward) due to its inertia and very low damping on the longitudinal axis.

5.11 Refine the choice of the tail lever arm

Besides its role in the aircraft's balance, the tail assembly generally has two other important functions:

- A damping function (more details below) of pitch and yaw movements: it is said that the damping is greater the shorter the time taken by the glider to

return to its equilibrium position after having undergone a disturbance (crossing a turbulence or action on a control surface).
- A function for controlling pitch and yaw movements (pitch control and rudder control).

The length of the lever arm influences both of these functions; to make the right choice, here are some points to remember:

- The damping provided by a tail element of surface area S is proportional to the product $S.L^2.V$ where V is the airspeed and L is the length of the lever arm between the CG and the neutral point of the surface considered.
- The damping time constant is much more important in yaw than in pitch. Therefore, it is most often the yaw behavior that determines the choice of lever arm, unless the fin and horizontal tail are separated in such a way as to increase the fin's lever arm without affecting that of the horizontal tail.
- Consequently, a glider intended to fly slowly needs a priori a tail assembly with a product $S.L^2$ greater than a speed glider, particularly for the rudder.
- Since the leverage is squared, it is more efficient to lengthen the lever arm than to increase the tail surface area. Hence the long lever arms observed on F3K and F3J gliders.
- But the lever arm must not be too long because the fuselage drag in turns then increases significantly and the dimensions of the horizontal tail may become too small with a risk of operation below the critical Reynolds number.
- The control surface deflections required to control a given trajectory of curvature (elevator and rudder deflections) are greater the longer the rear lever arm (steering is roughly proportional to the lever arm).

To simplify things during the preliminary design of a glider that must meet these criteria, we can, as a first approximation, replace MAX with E/λ and use Ss = 10% Sa.

This gives: $$BL_s = 10.\frac{E_a}{\lambda_a}.V_s$$

5.12 Dynamic operation

The sustained undulating trajectory that can be observed under certain conditions (the famous roller coaster effect) leads us to consider the dynamic behavior of the aircraft. The principle is identical to the operation of a car shock absorber (or, in electronics, a resistance/inductance/capacitance circuit).

The same components are found in both: inertia (the vehicle's mass or the aircraft's pitch inertia), stiffness (the spring or the static center of gravity margin), perturbation (deviation from equilibrium: spring compression or the difference between the flight lift coefficient and the set lift coefficient), and damping (a force proportional to the speed of movement, which opposes the motion). In the case

of a hydraulic damper, the movement of a piston in oil provides this braking force. In the case of an aircraft, it is the rotational speed around the center of gravity that gives each element an additional angle of attack, and therefore additional lift. Depending on the position of each element's center of gravity relative to the center of gravity, this additional lift either opposes the rotation (horizontal tail downstream of the wing, wing in the case of a flying wing or canard) or exacerbates it (the general case of the wing and fuselage for an aircraft with a horizontal tail).

The system's response frequencies are related to the inertia-to-stiffness ratio, while the return-to-equilibrium time is determined by the damping. Typically, the oscillation frequency of the stable system (center of gravity forward) will be lower when the inertia is high and/or the static margin is low, while convergence will be faster when the damping is high. Note that the study of these phenomena is accessible using AVL, XFLR5, and PredimRC software.

On a healthy aircraft, the longitudinal dynamics are characterized by two types of oscillations, called natural modes (fig. 101 and 102):

- A first one, of short period (a few tenths of a second), concerns the transient movement towards the equilibrium angle of attack (Cltrim) after each action at depth or each turbulence traversed.
- The second type, with a long period (on the order of a few seconds at our scales), is called the phugoid. It results from the exchange between the aircraft's kinetic energy and its potential energy (gravity) during alternating climbs and descents at a nearly constant angle of attack. This oscillation is almost undetectable in model aircraft due to the short durations of level, stabilized flight. To a first approximation (Lancaster approximation), it is independent of the aircraft's characteristics and is a function only of the flight speed (see equation below).

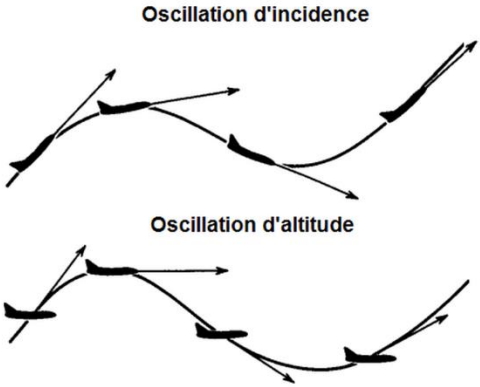

Fig. 101, attitudes of the aircraft in oscillation

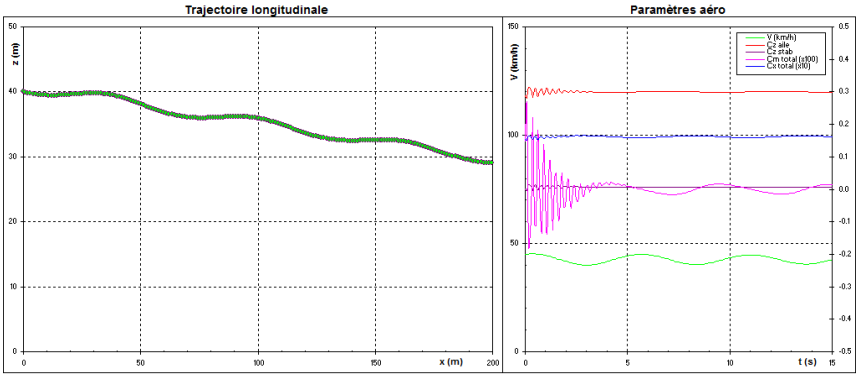

Fig. 102, response of a glider after perturbation (short mode then phugoid)

The first mode is studied in pitch response after a disturbance, a response which can take four different forms (in a vertical plane, but it works the same way for yaw in a horizontal plane):

- Answer 1: oscillatory motion maintained around equilibrium (excessive stiffness and/or insufficient damping).
- Answer 2: Damped oscillatory with return to equilibrium (correct stiffness and damping).
- Answer 3: aperiodic (without oscillation) with return to equilibrium (strong damping).
- Answer 4: aperiodic (without oscillation) divergent (backward CG: ms < 0).

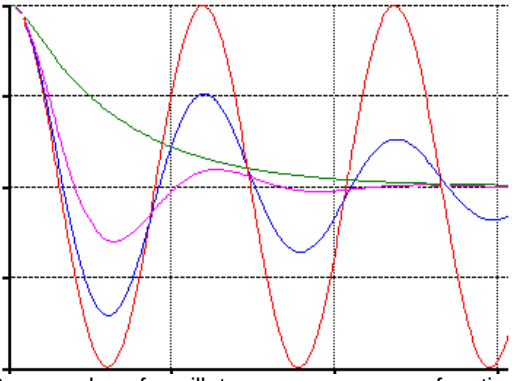
Fig. 103, examples of oscillatory responses as a function of time

The ideal case is the pink curve (Fig. 103), with a return to equilibrium in just a few oscillations, which is easily achieved by adhering to the design rules proposed here. Apart from the specific case of a center of gravity that is too far aft, a truly significant error is required to encounter any noticeable oscillatory behavior. For example, consider a flying wing with a center of gravity too far forward, consequently requiring a strong pitch correction to maintain level flight. Since this

type of model is generally poorly damped in pitch, the resulting oscillations are easily detectable.

It will also be necessary to avoid off-center masses as much as possible. Not only will this improve the aircraft's dynamic behavior (shorter reaction time and a lighter feel at the controls), but it will also reduce drag during a change of course or when passing through a disturbance. Indeed, less inertia means less effort is required to maintain the same rate of rotation (around the controlled/stabilized axis).

The following equations, which very approximately quantify the two principal modes for an aircraft with a horizontal tail, can be found in the aerodynamic literature:

Short-period mode (angle of attack oscillation):

Clean pulse:

$$\omega_s \approx \sqrt{\frac{Cm_\alpha . q . S_a . CMA_a}{I_{yy}}}$$

Depreciation rate:

$$\tau_s \approx \frac{q.(S_s . BL_s . \omega_s + S_a . CMA_a . Cm_\alpha) + g . Cx / Cz}{2 . \omega_s . V}$$

With :

$$Cm_\alpha = -dCm / d\alpha = -0{,}11 . A_a . ms$$

q the dynamic pressure (= $\rho V^2/2$)

Iyy is the longitudinal moment of inertia of the aircraft, to be calculated based on the aircraft's mass distribution. As a first approximation, it can be considered equivalent to $m.CMAa^2$.

Long-period mode (phugoid):

Clean pulse:

$$\omega_{ph} \approx \sqrt{2} . \frac{g}{V}$$

Depreciation rate:

$$\tau_{ph} \approx \frac{2 - \delta}{2 . \sqrt{2}} . \frac{Cx}{Cz}$$

With: δ = -1 for a glider or propeller plane and 0 for a jet engine.

As a reminder, the frequency of an oscillation is:

$$f = \frac{\omega}{2 . \pi}$$

Another way to approach dynamic stability is through an iterative calculation (Fig. 104). The principle consists of calculating the aircraft's aerodynamic coefficients at time t as a function of its trajectory to determine, via the fundamental principle of dynamics with an Euler-type integration, its new trajectory at time t+1. These

results are then fed into the calculation input, and so on, with a small time increment (between 0.01 and 0.1s at our scales).

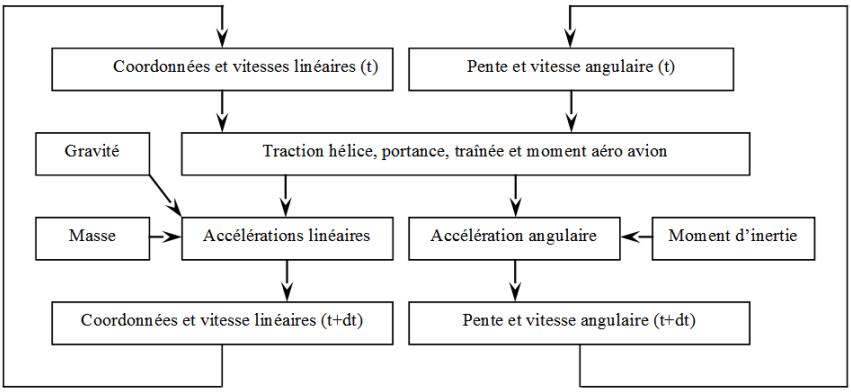

Fig. 104

The implementation, which is quite complex, is described in detail in the PredimRC user manual, so there is no need to reproduce it here.

Provided the aircraft model is sufficiently detailed and precise (particularly regarding the operation of the horizontal tail, but also the fuselage), this approach is especially valuable because it allows for the analysis of the influence of the model's characteristics and settings on the trajectory (Fig. 105), flight speed (Fig. 106), the evolution of aerodynamic coefficients (Fig. 102), takeoff time, etc. It is even possible to identify dynamic instability linked to excessive inertia, even when static stability is positive.

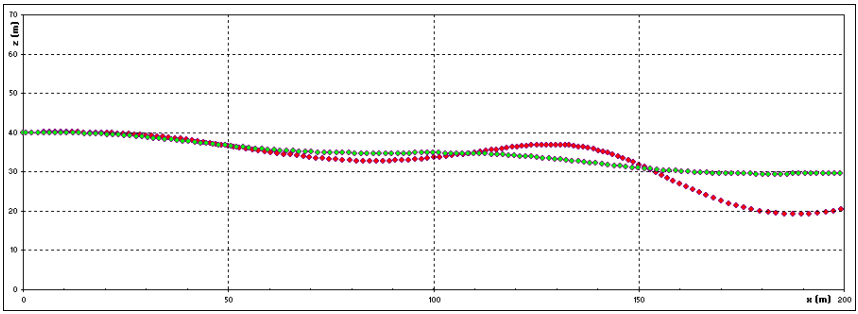

Fig. 105, study of the influence of inertia on the stability of the phugoid

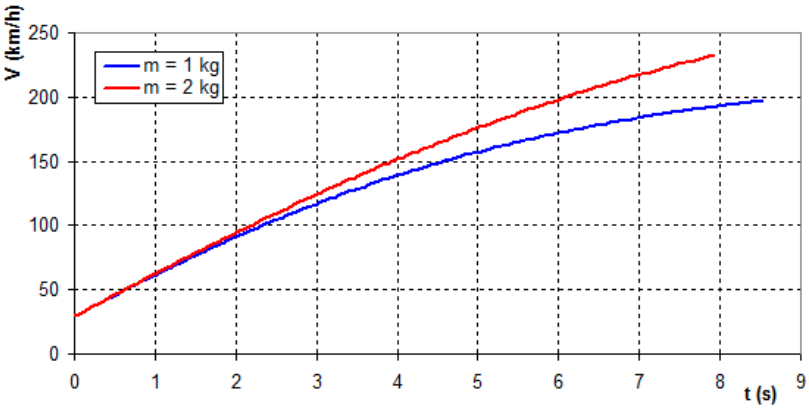

Fig. 106, study of the influence of mass on the increase in speed during a dive.

5.13 The flutter

This aeroelastic resonance phenomenon primarily affects wings and control surfaces, sometimes dramatically and potentially leading to their destruction. It results from the interaction between the mechanical properties of the wing or control surface (specifically its torsional and bending stiffness, as well as its mass and inertia) and an aerodynamic load (Fig. 107) that excites its structure. Generally, the mechanical response—in bending and torsion—dampens the load, but sometimes it is in phase with it: the phenomenon then becomes self-sustaining and amplifies, only stopping if the flight regime is significantly altered or by the destruction of the component. In the case of negative-sweep wings, the bending response is exacerbated by the torsional response, making them more susceptible to this phenomenon.

In all cases, the only simple solution to get out of this resonance is to reduce the flight speed, which changes the excitation but also reduces the energy to be dissipated.

The excitation that causes flutter is of two types:

- External, that is to say, when crossing a layer of turbulent air.
- Intrinsic to the aerodynamics of the aircraft, due to the turbulent wake, called Von Karman aisles, downstream of a airfoil or appendage.

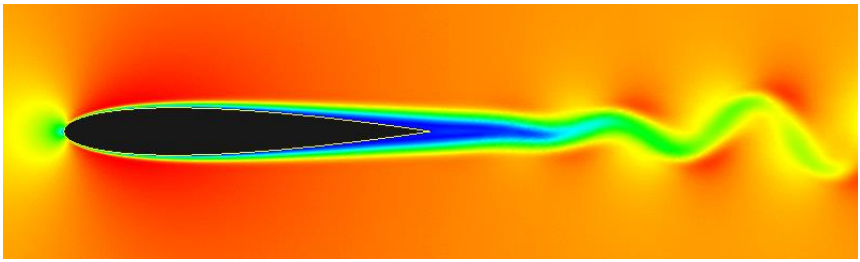

Fig. 107, numerical simulation of Von Karman avenues

The frequency of Von Karman alleys can be approximated by the following formula, valid up to Re = 10k:

$$\frac{f.C}{V} \approx 0{,}2.(1-\frac{11}{\mathrm{Re}})$$

With: f the frequency, C the chord or diameter, Re the Reynolds number

The fC/V ratio is called the Strouhal number. For higher Reynolds numbers, this type of chart is sufficient (Fig. 108):

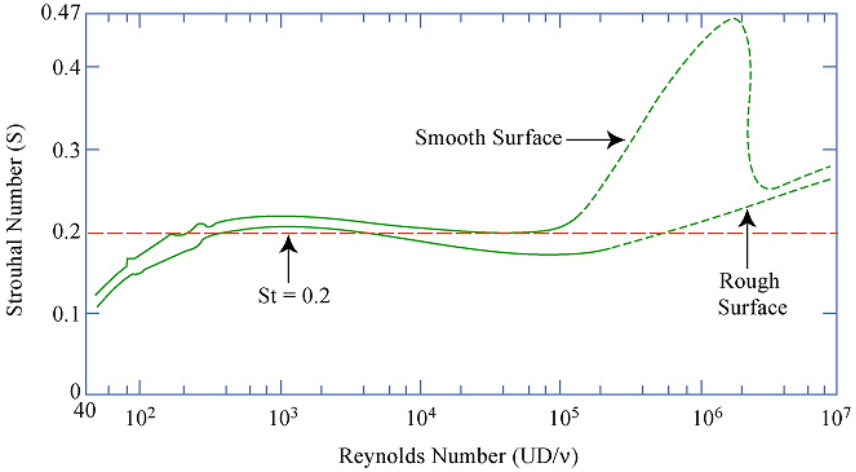

Fig. 108, source MIT OpenCourseWare

It now remains to calculate the stiffness, mass, and inertia of the wings to determine their natural modes and verify at what flight speed they can be excited by the Von Kármán vortices. For this, mechanical simulation software will be invaluable. These mechanical calculations are not detailed here, as they do not fall directly under the aircraft's aerodynamics and would require almost as much development as the rest of this work.

Nevertheless, it is worth recalling the main solution used to avoid the occurrence of this phenomenon, which consists of changing the rotational inertia of the rudder by adding a mass cantilevered from its leading edge.

Fig. 109, anti-flutter mass (elevator rudder, Lockheed P38).

5.14 Variable pitch propeller, a panacea?

We saw in §4.9.4 that an unsuitable propeller pitch can be extremely detrimental to propulsion efficiency. Rather than testing several propellers, it is tempting to consider using a variable-pitch propeller, such as the VarioPROP, which allows for optimal positioning of the maximum efficiency point.

However, everything is not perfect:

- The shape of the blades, that is to say the distribution of chords, airfoils and twists, is only optimal for a given pitch. Even if this pitch is judiciously chosen, e.g. in the center of the usable range, other pitches are inevitably unsuitable and the maximum efficiency is lower than that of a fixed-pitch propeller [designed for that pitch].
- The diameter is not modifiable, therefore it is not possible to convert between diameter and pitch to maintain a constant motor load.

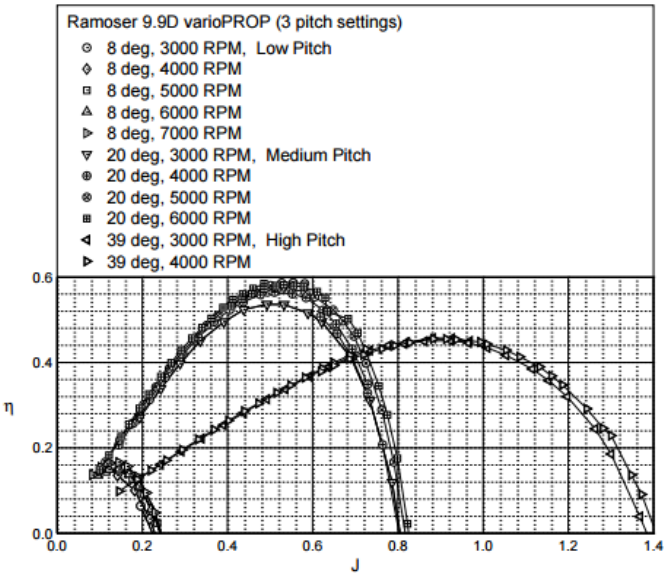

Fig. 110, efficiency curves of a variable-pitch propeller

5.15 Is the propeller blocked or free-spinning?

Which one creates more drag? It's a question everyone thinks they have an obvious answer to. Some will say it's the propeller spinning freely under the influence of the relative wind that creates less drag, others will argue the opposite… and they're probably all right, depending on the model they're referring to. The issue is twofold: a propeller can be an advantageous brake for landing or, conversely, a hindrance during the glide phase.

If you search a little on the internet, using the keyword "windmilling drag", you quickly come across this type of graph:

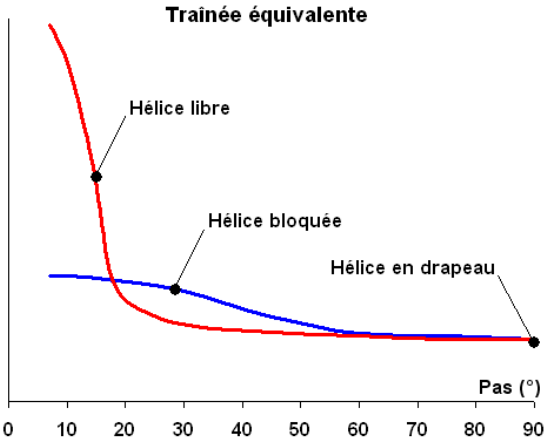

Fig. 111

The decoding is relatively simple: for each pitch studied (specifically, a geometric angle of attack of the propeller airfoil), there is a corresponding drag for a locked propeller and an equivalent drag (specifically, a rearward force) for a propeller rotating under the action of the wind (windmilling). Comparing these two configurations shows that the freely rotating propeller generates significantly more drag than the locked propeller if its pitch is small, and the opposite is true beyond a certain pitch.

The transition point is located at approximately twenty degrees, which allows us to determine (knowing that the geometric pitch is considered to be 70% of the propeller diameter) an empirical law of drag with the engine off:

- If not geo. < 70% diameter: free propeller slows down more than the blocked propeller.
- If not geo. > 70% diameter: free propeller slows less than the blocked propeller.

But where does this come from? A simple sketch decomposing the velocities and then the forces makes things clear for powered flight:

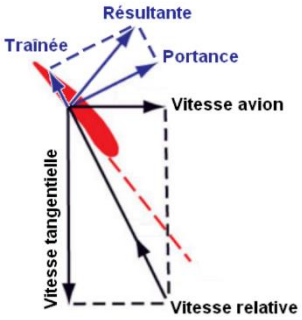

Fig. 112

It's all a matter of the local angle of attack of the propeller airfoil, just like with an airplane wing. Projecting the aerodynamic resultant onto the propeller's plane of rotation gives the torque that the engine must provide, while projecting it onto the axis of rotation gives the propeller thrust.

Let's apply the same formalism to the free helix:

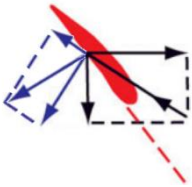

Fig. 113

The resulting force is directed rearward and can be considered drag once integrated over the entire propeller. It should be noted that the often-mentioned concept of "disk swept" drag by the propeller does not exist; the forces are exerted only on the surface of the propeller, exactly as on a wing.

5.16 Helical propeller blast, myth or reality?

A geometric study similar to that of the forces acting on the propeller allows us to estimate the gyration (commonly called helical slipstream) of the air downstream of the propeller. This slipstream is often attributed significant effects on yaw and roll, due to a misinterpretation of photographs of vortices visible at the propeller tip on some full-size aircraft. The shape of this vortex is indeed particularly helical. However, this trace in the air mass does not directly reflect the shape of the propeller slipstream but merely represents the propeller pitch. In the aircraft's

frame of reference, the value of the gyration is actually only a few degrees, and its influence is generally quite insignificant. This is also illustrated in other photos, easily found online (for example, on the website interaction.free.fr), by woolen threads attached to the fuselage, threads desperately aligned with the aircraft's axis instead of being bent by the propeller's slipstream. To completely dispel this myth, it's also important to remember that propeller rotation decreases proportionally to airspeed and the distance from the propeller at which it is measured, just like wake deflection. Propeller rotation is, in fact, the deflection of the propeller's wake measured in the aircraft's fixed frame of reference.

That said, the fact that the effects at play are generally weak does not negate the need to decipher them. They exist primarily in the following forms:

- Roll axis: the action of rotation on all surfaces of the aircraft, through local changes in angle of attack, produces a moment around the aircraft's flight axis, in the same direction as the propeller's rotation. However, since this moment is in the opposite direction to the engine torque, it tends to (slightly) counteract the latter, which is generally then fully countered by aileron trim.
- Pitch axis: the few degrees of rotation that locally combine with the wing's angle of attack can promote an asymmetric stall when the aircraft is powered at a high angle of attack. This phenomenon is particularly noticeable on certain warbirds equipped with propellers that are sometimes enormous in proportion to the wing size.
- Yaw axis (aerodynamics): Since the rudders of our aircraft are rarely symmetrical with respect to the horizontal plane, the action of rotation on the rudder will generate a force in the direction of rotation, hence a yaw moment. On a model aircraft, typically equipped with a propeller rotating clockwise when viewed from the rear, this moment tends to rotate the aircraft to the left. This tendency is most noticeable on the ground or at the end of a vertical climb (this facilitates a rollover… in one direction only) and can, if necessary, be compensated for by a rudder correction or, more conventionally, by the engine's anti-torque angle. Note that this term is rather inaccurate, but it is now so widely used that it is difficult to redefine it.
- Yaw axis (mechanics): Depending on the aircraft's angle of attack, the propeller's axis of rotation makes a non-zero angle with the relative speed, causing a thrust shift and requiring a drift correction. At a high angle of attack, the down blade has a greater angle of attack than the up blade, so the thrust is shifted towards the down blade. Conversely, at a high negative angle of attack, the thrust is shifted towards the down blade. This is also true for the pitch axis if the yaw angle is not zero.

Highlighting the nature of the effects and the means of countering them confirms their minor importance. Indeed, on the majority of well-built and normally powered aircraft, engine stall is generally symmetrical, while engine anti-torque and aileron trim corrections are of little consequence.

To learn more, reading NACA Technical Note No. 1146 is very helpful. In my opinion, the most informative graphs are Figures 14, 15, and 16 ("concluded"), which summarize the results as curves showing the rudder angle of attack in the

relative wind for various yaw slip angles imposed on the aircraft. This is done for three propeller pitches and three tail surfaces positioned at varying distances from the propeller. The rudder angle of attack measured at zero yaw slip thus provides a good indication of the local gyro value at the rudder.

Here is a quick summary:

- A yaw angle of 0° corresponds to a vertical angle of attack of 0° to approximately 2° for the most extreme case (35° propeller pitch and tail assembly closest to the propeller).
- Propeller rotation introduces a very pronounced non-linearity in the yaw response around neutral, with a shallow curve over approximately +/-10° (0.25° of vertical tail angle of attack for every 1° of yaw, while the rest of the curve is closer to 1° for every 1°). This non-linearity likely reflects the effect of the air flowing around the fuselage when it is sideslipped in the relative wind.

This excellent photo of a KR2 (manufacturer's photo) clearly shows, thanks to the wool threads, the almost complete lack of vorticity in the airflow along the engine cowling. A marked separation is also visible downstream of the engine's cooling air outlet.

5.17 Representativeness of the calculations

Having addressed this issue by highlighting the need for accurate representation of the calculations involved, it's worth concluding by returning to this essential point. Indeed, what could be more legitimate than thinking that all this is pointless

squeezing lemons, yielding little more than an excessive intake of aspirin? Most modelers manage quite well without calculations… So, what's the point?

5.17.1 CG, incidence settings and performances

First and foremost, the essentials—the calculation of the center of gravity (CG)—cover a large portion of the calculation assumptions presented in this guide. Backed by extensive experience gained through their implementation on PredimRC, the calculations presented here have proven remarkably robust and reliable across all models, from micro-gliders to large-scale aircraft, not forgetting airplanes of all types. The differences between the calculated and actual CG rarely exceed a few percent of the mean aerodynamic chord, and as a general rule, most pilots leave the calculated setting as is. The benefit for the average modeler is twofold: firstly, a properly adjusted CG in the workshop prevents any unpleasant surprises on the first flight. Let he who has never experienced a wild rodeo or, worse, a crash due to an incorrectly adjusted CG cast the first stone… Secondly, accurately calculating the CG position allows for optimizing weight distribution from the design stage or, failing that, during radio installation, resulting in a clear weight saving. Simply observing the amount of lead needed to center certain models is enough to grasp the full value of this approach.

The calculations for the foil settings, which are directly derived from the CG calculation, also prove to be very predictive, provided that reliable Alpha0 and Cm0 values are available. For this, XFoil is a valuable tool that has also proven its worth. This digital wind tunnel is sometimes criticized for its representativeness at very low Reynolds numbers (< 100 000), with the main criticism being a tendency to exaggerate the non-linearities of Cl and Cm. In other words, XFoil is supposedly more pessimistic than reality, almost the opposite of what "calculation skeptics" believe calculations are always too optimistic. My experiments in the field of very low Reynolds numbers lead me to believe that XFoil performs rather well, at least with certain precautions (see below). Among other things, an unfortunate experience reinforces this position, concerning the Mini-Discus developed for the company CCM. While the first version with sheeted wings flew superbly, its all-fiberglass variant was, let's be frank, a resounding failure. The only difference: the surface finish, which was relatively uneven on the sheeted wings, became perfectly smooth on the fiberglass wings, thus eliminating the small imperfections that actually acted as turbulators and played a very active role in the airfoil's performance. Out of curiosity, I ran this airfoil (developed at the time using Eppler code that didn't handle critical lift) through XFoil, and the conclusions were clear: no hope without turbulators. Go figure…

Similarly, the engine simulations were compared to real-world conditions, particularly regarding key operating points such as maximum level speed and maximum rate of climb. Here too, the results are very convincing and effectively validate the drag calculations. Furthermore, propeller optimizations on existing airframes were highly successful, not only from a measurement perspective but

also in terms of pilot feedback, with some pleasantly surprised to discover new potential in their favorite aircraft.

Two fine examples of atypical models (Elektro Retro by Vincent Besançon and SlowWing by Lionel Bernardin) validating the CG calculations discussed here: the first is centered at more than 50% of the mean chord, while the very low aspect ratio and the strong sag of the second are not common.

5.17.2 XFoil and nCrit

XFoil takes into account the surface finish effects of the airfoil via the nCrit parameter, which models the average level of turbulence of the air flowing around the airfoil. This parameter depends primarily on the actual surface finish of the airfoil being studied and significantly influences the laminar/turbulent transition, just like a turbulator, with the same effects: improved results (better drag

coefficient, reduced non-linearities in lift coefficient and lift coefficient) at low Reynolds numbers and degraded drag coefficient at high Reynolds numbers. The generic value of 9 is well-suited to models with a very smooth surface finish, such as those made entirely of plastic using a machined mold. However, the more imperfections the wing surface has, even small ones (roughness, facets, steps, etc.), the more this parameter should be reduced to avoid erroneous conclusions. For example, the representative nCrit of a micro-glider finished with Japanese paper (slightly rough) like the Crobe, or of a wing with a structural frame, is typically 3. For most other constructions (sheeted wings), an nCrit of 6 seems appropriate to avoid overestimating performance at high Reynolds numbers and misinterpreting behavior at low Reynolds numbers. It's worth noting that many publications from laboratories and test centers support this view (easily found online) and confirm the effectiveness of XFoil with a correctly set nCrit.

5.17.3 Linear vs. non-linear

The linear theory [of thin airfoils] presented throughout this work is a simplification of reality, which assumes that the relationship between lift and angle of attack is independent of the airfoil (up to its Alpha0) and that the moment is constant. This theory is reliable and predictive in most cases, except near the stall point and when the airfoil is poorly suited to the flight Reynolds numbers (i.e., used below its critical Reynolds number).

Conversely, the non-linear approach is more representative of reality (Fig. 114), but is very sensitive to Reynolds number effects, particularly depending on the modeling conditions (nCrit, turbulator). Therefore, care must be taken to choose these carefully according to the flight envelope and the design of the aircraft being studied (see the previous chapter, "xFoil and nCrit").

Nonlinear phenomena cannot be understood through simple calculations and require the use of numerical simulations. To date, among software accessible to the general public, only Gemini Aero Designer offers this type of solution, combining two approaches simultaneously: a 1.5D lifting surface solver and a 3D VLM solver coupled with a nonlinear xFoil interpolator, whose data is partially reduced via thin airfoil theory for the linear case.

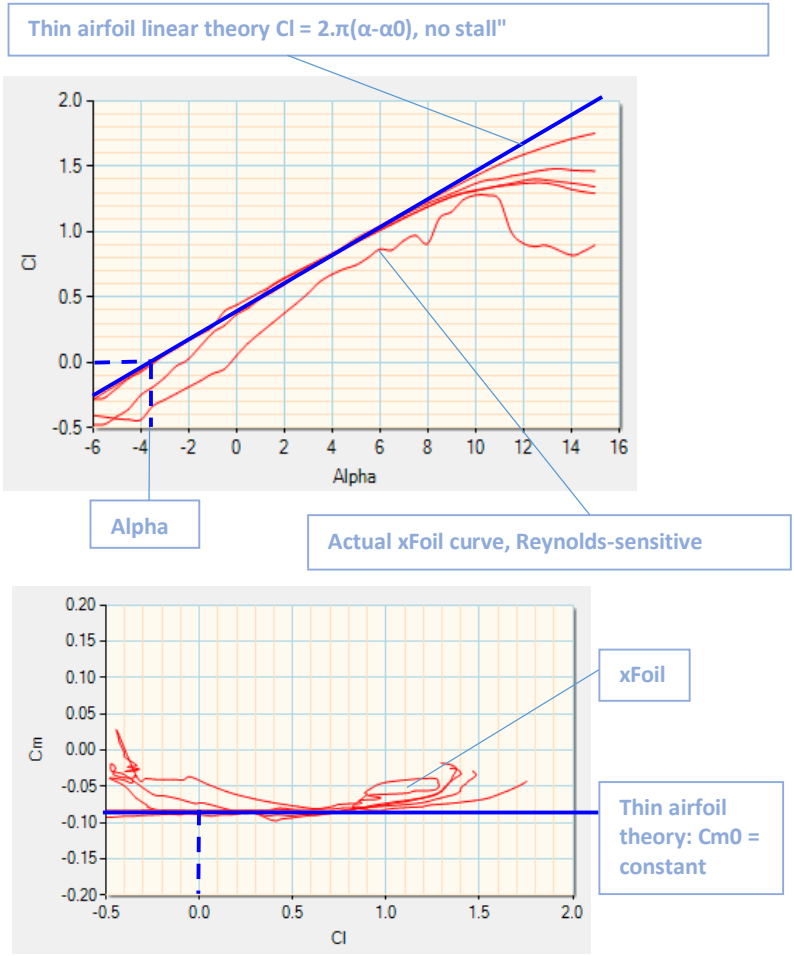

Fig. 114

At the level of the complete aircraft (Fig. 115), the difference between linear and non-linear dynamics is generally relatively small in terms of performance. This is not always the case with regard to stability and balance; the difference can be significant at low Reynolds numbers and can reveal instabilities at certain operating points. This type of analysis is therefore a valuable asset for making informed adjustments to the choice of airfoils, surface finish, or turbulator.

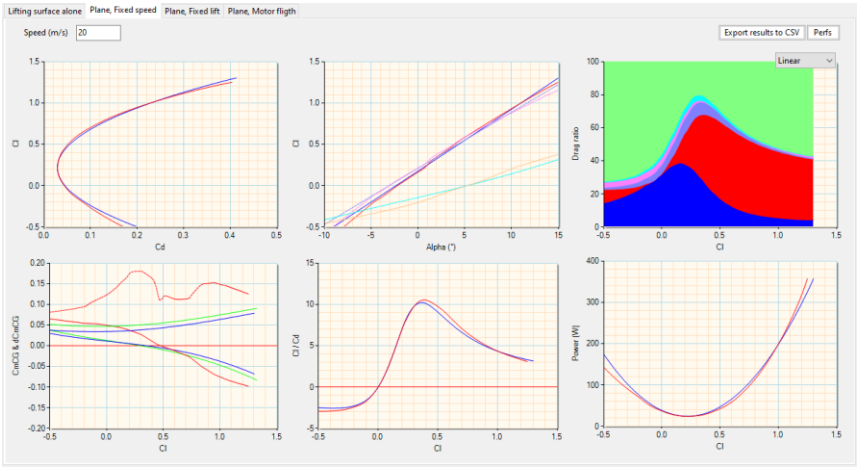

Fig. 115, linear (blue curves) vs non-linear (red curves)

5.17.4 A little common sense

The precautions [related to non-linear effects] to be taken when simulating airfoils naturally lead us to discuss the impact of construction defects on the flight performance of the complete model. And, consequently, are the calculations of this performance reliable? The answer is… it all depends, particularly on the precautions taken by the user.

On the one hand, the input data for the calculation must accurately describe reality (model dimensions, airfoils, flight conditions, etc.), and the calculations performed must be consistent with the study being conducted. This is obvious, but… For example, it's pointless to expect miracles from a model that omits certain significant elements, such as a large landing gear, struts, or particularly prominent control surfaces. Aside from this obvious point, it's not necessary to model every last detail to obtain a robust simulation; the important thing is to consider the main elements. Similarly, minor defects in shape or appearance generally have a negligible impact on the overall result. For example, a sheeted polystyrene wing cut by CNC, properly constructed (no twisting, minimum airfoil respected, trailing edge not too thick, clean finish) will offer performance very close to that of the same wing molded in fiberglass using a machined mold. Even if its performance were slightly reduced, the impact on the overall model wouldn't necessarily be significant because the wing isn't the only part that flies. For example, a 10% increase in drag on the airfoil (which only represents on average 30% to 50% of the total drag) only penalizes the aircraft's overall performance by 3% to 5%. Proof

of this lies in the fact that it's not uncommon for home-built models constructed simply (but cleanly) to excel in glider and racing competitions, always raising numerous questions about the comparison between all-fiberglass construction and "traditional" construction. Conversely, it's clear that a wing cut from open-cell foam with a completely unfinished surface is very likely to generate significantly more drag than expected. A poorly tensioned fabric covering can also significantly alter the performance of a wing by deforming the airfoil, just as the presence of marked discontinuities on a fuselage will obviously result in greater drag than that of a fuselage of the same dimensions but correctly airfoild.

On the other hand, in addition to the representativeness of a digital wind tunnel like XFoil for airfoil airfoils, which is quite good provided the nCrit value is chosen judiciously, we must also mention the representativeness of the calculations for the complete model, induced drag, wetted surface area, interaction, etc., which are found in tools like Gemini Aero Designer, PredimRC, and XFLR5. The publications—and therefore the numerical experiments—on this subject are countless and date back to the very beginnings of aerodynamics, so it is quite rational to trust them. Especially since the theoretical approaches used are derived from experimentation, it would be absurd if their results were completely off the mark.

5.17.5 Experiment

At our level, it's also possible to conduct some experimentation to compare calculations with physical reality. Electric propulsion is a real boon for this, as it allows us to easily determine the aerodynamic power consumed by the model, thanks to a datalogger, onboard airspeed measurements (pitot tube, GPS) or ground-based measurements (radar, for example), and a characterization of the propeller's propulsive efficiency (UIUC measurements, for example). Several measurement points in level flight at various engine power levels are then sufficient to reconstruct the lift-to-drag and sink-rate polars. However, careful attention must be paid to measurement accuracy and test conditions (it must be conducted on flat terrain, in neutral weather, and without wind); a certain rigor is essential to obtain reliable measurements—at least as reliable as the calculations we want to verify!

In a different vein, Matthieu Scherrer installed a Jibe F5D directly in a wind tunnel. Everything is detailed on Matthieu's blog and is well worth a look, with particularly interesting results:
http://sailplane-matscherrer.blogspot.com/search/label/Aerodynamics

The rapid evolution of competition aircraft based on minimizing drag across a wide lift range (racers, gliders) is also an excellent indicator of the relevance of simulation tools, XFoil chief among them. In particular, while the absolute accuracy of these tools cannot be guaranteed—mainly due to the difficulty of accounting for all the details of physical reality—their use in relative (comparison)

applications has been extremely fruitful in recent years. This is evidenced by all the modern airfoils (TP, AG, etc.) that have repeatedly proven themselves in competition and which simply would not exist without XFoil. Food for thought…

More accessible, comparing the results of a model with the actual settings of a model, particularly the neutral centering (the only unambiguously definable center of gravity position) and its associated calibrations, is always very instructive. Performing this exercise on various typical cases, without preconceived notions, is also beneficial for definitively eliminating any remaining false cognates that may have persisted after reading this document.

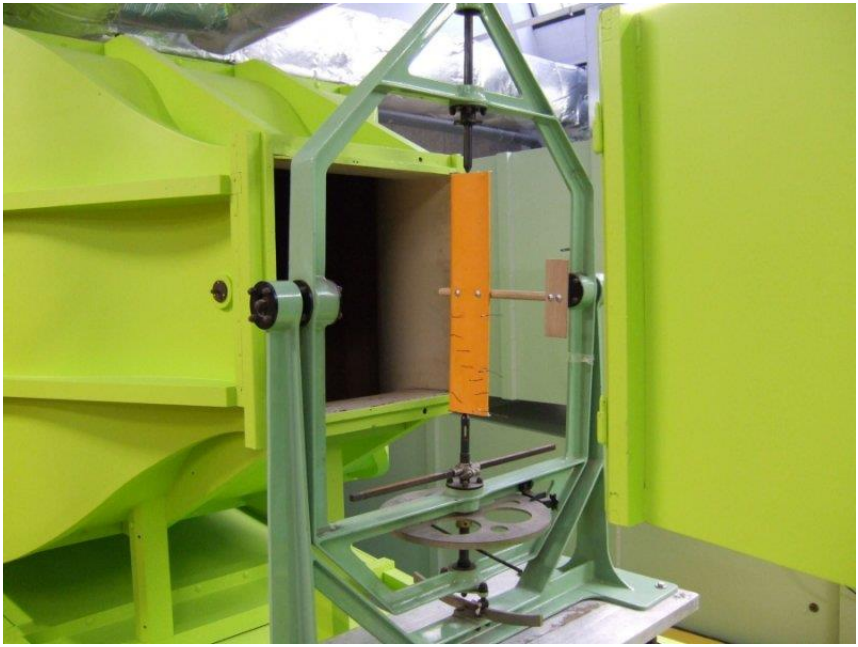

These wind tunnel tests, conducted at the IUT of Ville d'Avray (JL. Bolteau), validated the aerodynamic center position of a simple configuration at low Reynolds numbers. To consider only the wing/horizontal tail couple, the fuselage has a constant cross-section, and its aerodynamic center is positioned at the overall aerodynamic center of the wing and horizontal tail (without the fuselage). The results perfectly match the calculations... or perhaps the opposite!

5.18 Some practical applications

5.18.1 60" Glider

The overall wingspan is fixed by the regulations: 1.52 m. The fuselage will be narrow, say 40 mm, giving an aerodynamic wingspan of 1480 mm.

- ⇨ Aspect ratio: λa = 11.4
- ⇨ Given that $\lambda = Envˆ2 / Sa$, we have : Sa = 19.2 dm²
- ⇨ Wing loading empty: 27 g/dm²
- ⇨ Empty mass: 520 g

To stay within the scope of this discussion, the wing is a simple trapeze. Given that the wingtip chord is 60% of the root chord, we have:

- ⇨ Cemp = 162 mm
- ⇨ Csaum = 97 mm
- ⇨ MAC = 132 mm
- ⇨ Characteristic speeds (Cl = 0.05 / 0.3 / 0.8) = 26 / 43 / 106 km/h
- ⇨ Re corresponding to the MAC = 81000 / 132000 / 325000
- ⇨ Re corresponding to tip chord = 49000 / 79000 / 194000

The airfoil chosen is the TP74 (thickness 7%, Cm0 = -0.029, Alpha0 = -1.3°), perfectly suited to the flight domain of this 60", i.e. the characteristic (Cl, Re) pairs encountered here.

To simplify construction, the BFs of the two wings are aligned:

- ⇨ Fl = 65 mm
- ⇨ Fl_MAC = 46 mm

The chosen horizontal tail is a V-shaped one with an opening of 110°, with an equivalent surface area of 8% of that of the wing, an equivalent aspect ratio of 5 and a wingtip chord of 60% of that of the wing root:

- ⇨ Vs = 0.35
- ⇨ Ss = 1.9 dm²
- ⇨ BLs = 578 mm
- ⇨ Equivalent wingspan: 308 mm
- ⇨ Equivalent chords: 77 mm / 46 mm
- ⇨ Actual dimensions: chords 94 mm / 56 mm / length 188 mm

Fuselage length = BLs + 0.4 * BLs + 40mm horizontal tail mounting = 849 mm

Calculation of the CG:

- ⇨ Aa = 0.85
- ⇨ As = 0.71
- ⇨ Hs = 43
- ⇨ ε ' = 0.26
- ⇨ Ceffs = 0.62

- ⇨ Position of the global neutral point on the mean chord: xF = 37%
- ⇨ Position of the overall focal point at the root / BA: XF = 95 mm
- ⇨ Position of the CG on the first flight on the middle chord: xCG = 32%
- ⇨ Position of the CG on first flight at the wing root / BA: XCG = 88 mm

Calculation of the adjustments for Cla = 0.3:

- ⇨ α a = +1.9°
- ⇨ Cls = -0.02
- ⇨ α s = +0.5°
- ⇨ Longitudinal velocity = +1.4°

5.18.2 K-Nar by Patrice Pons (MMag n°704)

Simplified dimensions taken from the plan:

- ⇨ Wing: chords = 110 / 81 mm, sweep = 15 mm, wingspan = 910 mm
- ⇨ Sa = 8.7 dm², λa = 9.5
- ⇨ Wing loading = 34.5 g/dm²
- ⇨ MAC = 96 mm
- ⇨ Fl_MAC = 7.1 mm
- ⇨ Plano-convex airfoil, 8% thickness: Cmo ≈ -0.05, Alpha0 ≈ -3°
- ⇨ Horizontal tail: chord = 70 mm, wingspan = 300 mm, BLs = -410 mm
- ⇨ Thin plano-convex airfoil: Alpha0 ≈ -1.5°
- ⇨ Ss = 2.1 dm², λs = 4.3
- ⇨ Vs = -1.03

Calculation of the CG:

- ⇨ Aa = 0.83
- ⇨ As = 0.68
- ⇨ ε ' = 0
- ⇨ Ceffs = 0.82
- ⇨ Position of the global neutral point on the middle chord: xF = -70%
- ⇨ Position of the CG at ms = 5% on the middle chord: xF = -75%
- ⇨ CG position at ms = 5% at the root / BA: XF = -65 mm

Calculation of the adjustments for Cla = 0.3:

- ⇨ α a = +0.3°
- ⇨ Cls = +0.44
- ⇨ α s = +4.4°

Note that the stab Cl calculation was carried out using the complete formula, given that the CG is relatively far from the wing aerodynamic center.

The plan indicates a center of gravity (CG) 67mm ahead of the leading edge root, a difference of barely 2mm compared to the simplified calculations presented here. With its complete formulation, the CG calculated with a 3% static margin perfectly matches the actual CG. Similarly, the wing and horizontal tail angles correspond quite well to reality (approximately 0° and 5° on the plan).

6. Form

6.1 Flight reference

x : flight direction
z: normal to the direction of flight in the vertical plane
y: normal to the direction of flight in the horizontal plane (depending on the wingspan)
h: horizontal axis (ground)
v: vertical axis (ground)

6.2 Main designations

E : wingspan
C[i] : chord no. i
CE: root chord
CS: tip chord
CMA : mean aerodynamic chord
S : lifting surface of a wing
Sm : wetted area
λ : aspect ratio
Eff : wing taper ratio
FL : sweep of leading edge
Λ : sweep angle of a wing (leading edge, chord /4 or /2)
m : mass
CHA : wing loading
BL : horizontal distance (lever arm) between two foci
H : vertical distance between two foci
β : opening angle of a V-tail
L, l, h : main dimensions of the fuselage

Re: Reynolds number
Cl : lift coefficient
Cd : drag coefficient (Cx in french original book)
Cm : moment coefficient
Fz : lift force
Fx : drag force
M : moment
Vx (or V) : flight speed
Vz (or Vv) : sink rate
Vh: horizontal speed
f : finesse

α : aerodynamic angle of attack (angle between the airfoil and the x-axis)
α0 : zero lift angle of attack
Cm0 : moment coefficient at zero lift
αK : angle of attack of a wing

A : lift efficiency coefficient
F : neutral point (point where the moment is independent of the angle of attack)
Vs: tail volume
ms : static margin
Kf : fuselage center correction coefficient
kf : fuselage shape coefficient
e : Oswald coefficient of wing

6.3 Prefixes

x: relative axial position (of a neutral point or the CG) to the mean chord of the wing
X: absolute axial position (of a neutral point or of the CG) at the leading edge of the wing at the root
d: small variation of a parameter

6.4 Suffixes

a : wing
s : horizontal tail
f : fuselage
u : accessory
i : induces
p or ∝: airfoil
min : minimum of a variable
max : maximum of a variable
avg : average of a variable